FIBROUS MINERALS IN THE WABUSH IRON ORE DISTRICT, LABRADOR, NEWFOUNDLAND, CANADA

by

© RAYMOND K. MARTTILA

A Thesis

Submitted to the School of Graduate Studies

in Partial Fulfilment of the Requirements

for the Degree

Master of Science

McMaster University

December, 1979

FIBROUS MINERALS IN THE WABUSH IRON ORE DISTRICT, LABRADOR, NEWFOUNDLAND, CANADA

MASTER OF SCIENCE (1979)
(Geology)

McMASTER UNIVERSITY
Hamilton, Ontario

TITLE: FIBROUS MINERALS IN THE WABUSH IRON ORE DISTRICT, LABRADOR, NEWFOUNDLAND CANADA

AUTHOR: RAYMOND K. MARTTILA, B.Sc. (McMaster)

SUPERVISORS: JAMES R. KRAMER
H. DOUGLAS GRUNDY

NUMBER OF PAGES: xiv, 128 + Appendices

ABSTRACT

Fibrous minerals are common in the highgrade, metamorphic, Precambrian Wabush Iron Formation, Labrador, Newfoundland, Canada. The most abundant fibres are amphiboles of the cummingtonite-grunerite series; mineralogical studies support the work of Klein (1960, 1964, 1966) and Chakraborty (1966). Iron ore mining and pelleting operations in the Labrador City area yield tailings containing many fibres (amphibole; iron and iron-manganese compounds) which find their way into the natural waterways. Water samples in Wabush Lake have fibre concentrations greater than 2×10^9 per litre. Analysis of concentration and/or chemical composition of water, tailings, rock, bottom sediment, and soil samples identifies mine waste deposits as the major source of fibres. Comparisons between sediment inputs (and inputs of mineral fibres) from mining operations and natural weathering processes indicate the major impact of mine wastes. Calculations applying Stokes' Law of Settling to the fibrous minerals illustrate how the fibres settle out in Wabush Lake.

ACKNOWLEDGEMENTS

Funding for this study of the Fate of Asbestiform Particles was through a grant from the Office of Research Subventions, Inland Waters Directorate, Environment Canada. I am deeply indebted to Drs. J. R. Kramer and H. D. Grundy for their guidance and supervision in this investigation. Many thanks are also due to Mr. O. Mudroch for his transmission electron microscopy and X-ray fluorescence analyses, Mrs Lynn Falkiner for typing, Mr. Len Falkiner for his help in the drafting, and my field assistants Mr. W. Kramer and Mr. M. Burley. I would also like to acknowledge the co-operation of the Iron Ore Company of Canada and Wabush Mines in allowing the collection of samples, Dr. J. C. Rucklidge of the Geology Department, University of Toronto, for the use of the electron microprobe, and Mr. N. W. Massey for the samples collected during the summer of 1978. Finally, I would like to thank every member of the Geology Department who encouraged and advised me during the course of this study.

TABLE OF CONTENTS

LIST OF TABLES

LIST OF FIGURES

APPENDIX

CHAPTER ONE

INTRODUCTION

1.1 STATEMENT OF PROBLEM

Fibrous minerals, some of which pose a health hazard, are considered to be a major environmental contaminant. They are ubiquitous, being found in air, lakes, rivers, drinking water, beverages, and building materials. In most cases, their presence appears to be a direct or indirect product of our industrialized society. Fibres can be generated by human activities such as the mining and processing of ore, construction, blasting, drilling, and by natural processes such as weathering and erosion.

Precambrian metamorphosed iron formations often contain many fibrous amphiboles; the mining and processing of these ore bodies can result in the addition of many more fibres to the environment than would normally be present from natural weathering processes. Reserve Mining Company which mines taconite ore in the Mesabi Iron Range of Minnesota has dumped tailings which contain more than 10^{24} fibres of cummingtonite into Lake Superior since 1955 (Kramer, 1976). The mining operations have also increased the concentration of fibres in the surrounding air and run-off waters

(Ashbrook, 1978).

Fibrous amphiboles are also found in the Wabush Iron Formation near Labrador City, Newfoundland (Fig. 1). Their mineralogy is well documented (Klein, 1960, 1964, 1965, 1966; Chakraborty, 1966) and the cummingtonite from this locality has been used as a reference sample for cummingtonite (Deer et al. 1966). The Iron Ore Company of Canada is presently mining an area west of Wabush Lake where many of these fibrous amphiboles are found. Tailings from their pelleting plant are dumped into the south end of Wabush Lake, giving a situation similar to the Reserve Mining Operation near Lake Superior but on a smaller and far more restricted scale (Figs. 2, 3, & 4). Tailings from the Wabush Mines pelleting plant (south of Wabush Lake) are deposited into Flora Lake (Fig. 2).

The purpose of this work is to carry out a study of the Wabush Lake area to:

1. Characterize the mineralogy of fibres present in the iron formation, surrounding rocks, soil, water (lake and run-off), tailings, and lake and stream sediments.
2. Determine the concentrations of fibres present in the waters, sediments, and tailings.

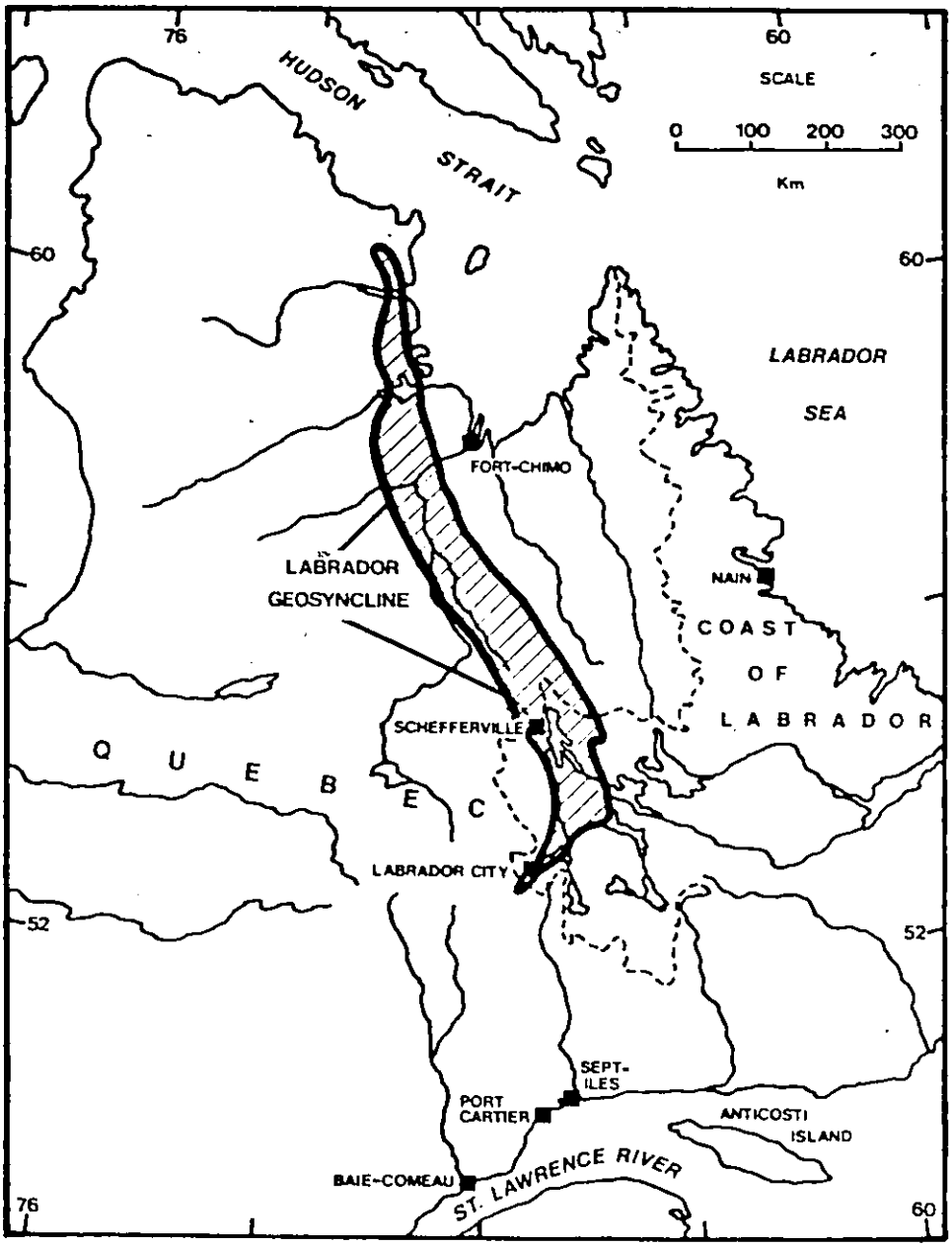

Figure 1: Location map showing Labrador City and the Labrador Geosyncline (Trough)

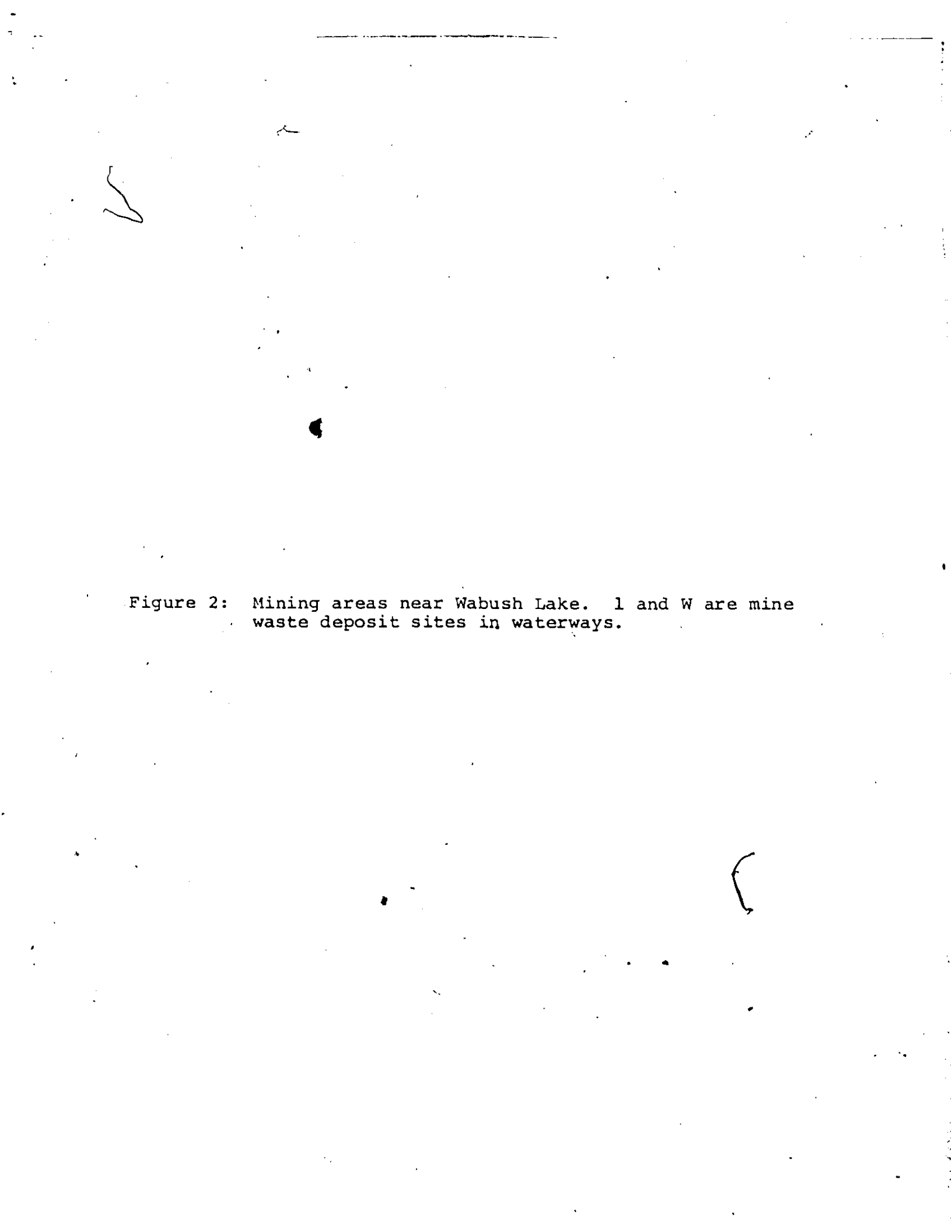

Figure 2: Mining areas near Wabush Lake. 1 and W are mine waste deposit sites in waterways.

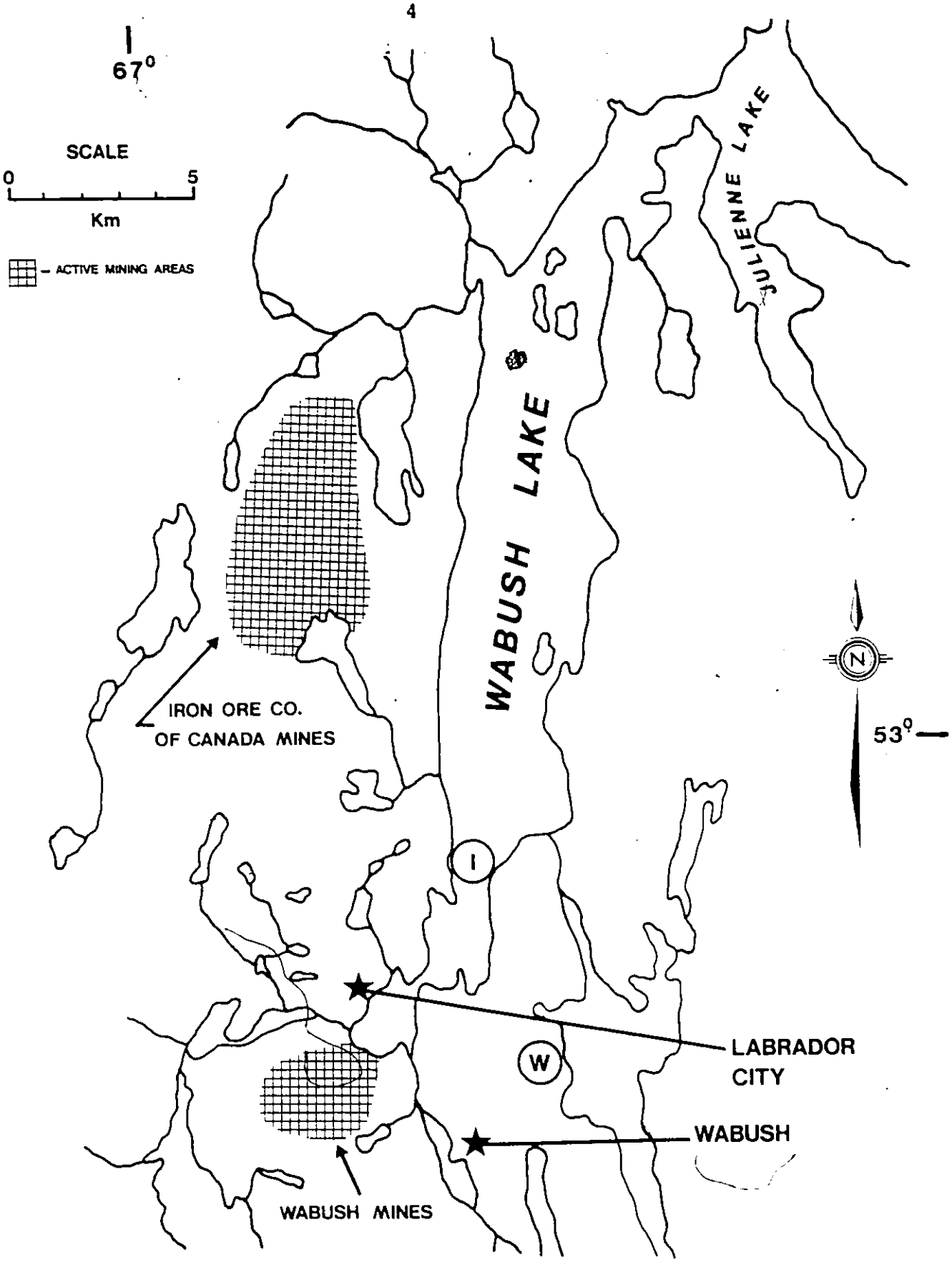
67°
SCALE
0
5
Km
– ACTIVE MINING AREAS
JULIENNE LAKE
WABUSH LAKE
N
53°
IRON ORE CO.
OF CANADA MINES
I
W
LABRADOR
CITY
WABUSH
WABUSH MINES

Figure 3: Iron Ore Company of Canada mine waste deposit at southend of Wabush Lake.

Figure 4: Smallwood Mine, Iron Ore Company of Canada

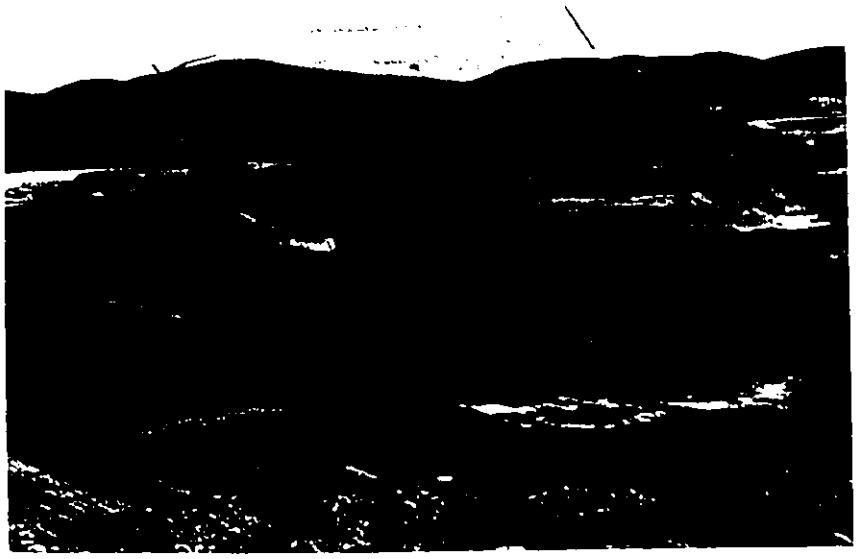

3. Study the effect that weathering and erosion have on the distribution of fibres so that the impact of the mining operations can be assessed.
4. Define the ultimate fate of these fibres in the Wabush Lake area.

1.2 GEOLOGY OF THE WABUSH IRON ORE DISTRICT

Location and Regional Geologic Setting

The Wabush Iron Formation outcrops near Labrador City, Newfoundland, Canada between 52°54' and 53°06' north latitude and 66°52' and 67°00' west longitude and covers an area of approximately 65 square miles. The iron formation of the Wabush Iron Ore District and surrounding areas forms the southern part of the metamorphosed Precambrian (Proterozoic) ferruginous sedimentary series of the Labrador trough (Fig. 1). It is situated at the junction of the Superior, Churchill, and Grenville structural provinces. The Archean Ashuanipi complex, last intensely deformed during the Kenoran orogeny, lies to the north. The Lower Proterozoic rocks, which contain the Wabush Iron Formation, lie to the south of the area and rest unconformably on the Archean. Altered Middle Proterozoic sediments and volcanics, last deformed during the Hudsonian orogeny lie to the east.

The deposits of the iron formation which are mined by the Iron Ore Company of Canada and Wabush Mines generally

occur in the centre of synclines where they are protected from erosion. In the northern part of the area, north of the Grenville Front, they are unmetamorphosed. South of the Front, they are metamorphosed with the metamorphic grade increasing in a southerly direction from greenschist facies near the Front to upper epidote-amphibolite in the Wabush area to pyroxenite facies in the Mount Wright area to the southwest.

The biotite isograd shown on Figure 5 (Fahrig, 1960) separates amphiboles and pyroxenes from sheet silicates. The iron formation north of this isograd consists of carbonates, hematite, magnetite, chert, and minor minnesotaite and stilpnomelane. South of this isograd, carbonates, magnetite, specularite, amphiboles, pyroxenes, and quartz are present. Amphiboles are more abundant in the Wabush Lake area whereas pyroxenes predominate in areas to the southwest (Kranck, 1961). The metamorphism and increased structural complexity are attributed to the Hudsonian and Grenville orogenies (Knowles and Gastil, 1959; Jackson, 1962; Klein, 1966; Rivers, 1978a). Gabbros and associated basic rocks intrude the Archean gneisses and trough rocks and have also been deformed by the Grenville orogeny and possibly by the Hudsonian orogeny (Rivers, 1978a). The recrystallization of the iron formation to coarse grained quartz-specularite schists renders the iron formation amenable to profitable

Figure 5: Geologic map of the Wabush Lake District. The biotite isograd is after Fahrig (1960)

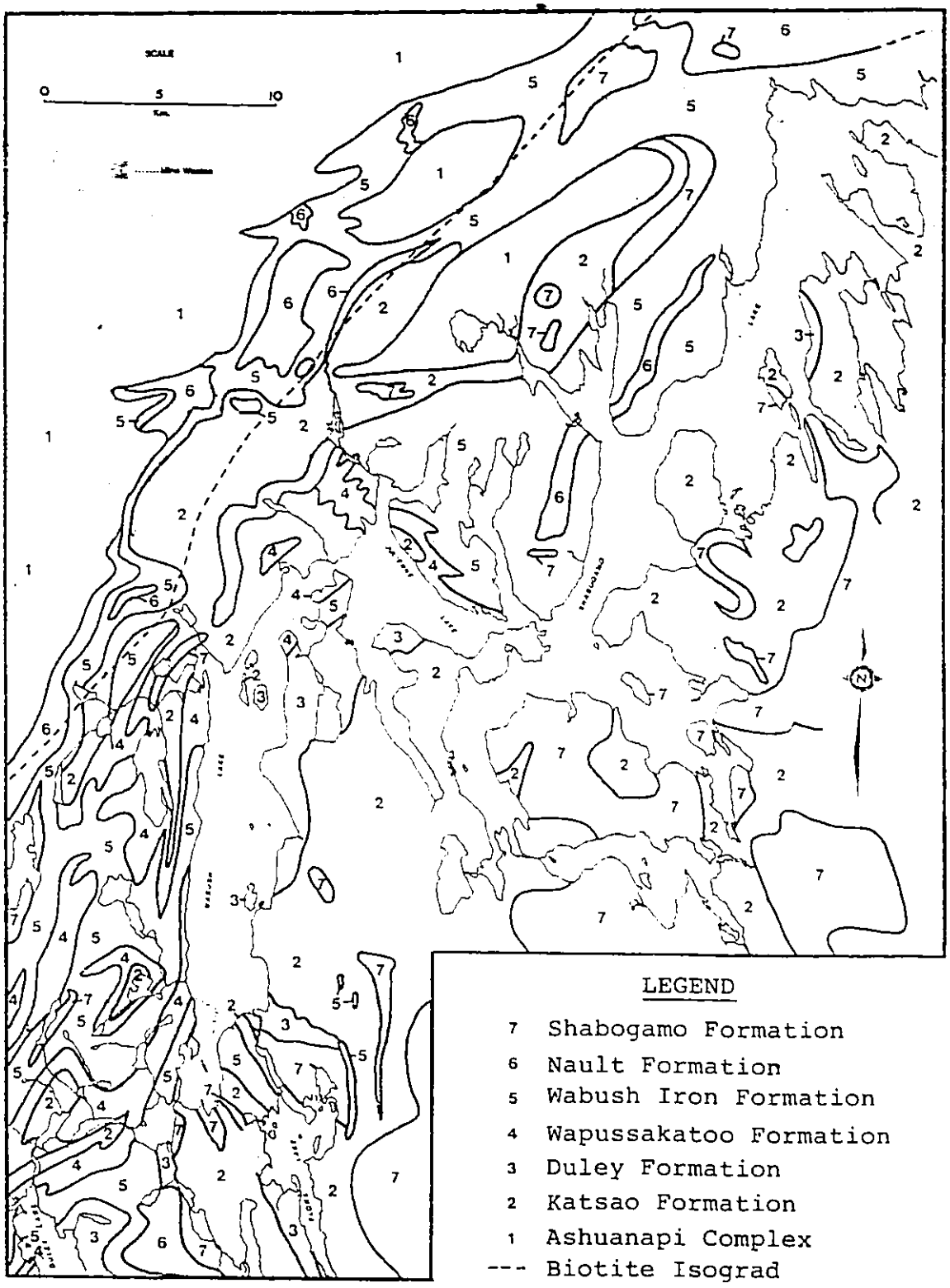
SCALE
0
5
10
km
LEGEND
7 Shabogamo Formation
6 Nault Formation
5 Wabush Iron Formation
4 Wapussakatoo Formation
3 Duley Formation
2 Katsao Formation
1 Ashuanapi Complex
--- Biotite Isograd

mining by concentration methods (O'Leary et al., 1972).

North of Julienne Lake and in Wabush Mines at the south end of Wabush Lake, the iron formation has been extensively leached and secondary iron has been deposited obscuring the original iron formation types. Some leaching, but not as extensive, has occurred in the iron deposits west of Wabush Lake (O'Leary, et al., 1972; Rivers, 1978a).

Previous Geologic Work

A. P. Low (1895) of the Geological Survey of Canada was the first geologist to study the Labrador Trough iron formations. Gill and James (1929) discovered the iron deposits in the Wabush Lake area. The first description of the rock types was done by Gill, Bannerman, and Tolman (1937). Mumtazzudin (1958) conducted a reconnaissance survey of the area; Gastil and Knowles (1960) presented a description of the stratigraphy and structure; Fahrig (1960) mapped the Shabogamo Lake area adjacent to Wabush Lake. Klein (1964) and Chakraborty (1966) studied the amphiboles and associated ferromagnesian silicate minerals in the iron formation and Klein (1966) studied its mineralogy and petrology. Knowles (1967) conducted a detailed structural survey with the assistance of the Iron Ore Company of Canada, Labrador Mining and Exploration Company, and Canadian Javelin Limited.

The first published maps of the iron deposits

and associated rock formations in the Wabush Lake area were compiled by Fahrig (1960); Gastil and Knowles (1960) and Gross (1968). Many other studies (including mapping and drilling projects, magnetic surveys, etc.), most of which are unpublished, were undertaken by mining and exploration companies prior to, and after, the commencement of mining in 1962 by the Iron Ore Company of Canada and 1964 by Wabush Mines. At the present time, the Newfoundland Department of Energy and Mines is mapping in detail the Wabush Iron Ore District. One map (Rivers, 1978b) of the Flora Lake - Wabush Lake areas has been published. A preliminary map of the Wabush Lake - Sawbill Lake area is included in a preliminary project report (Rivers 1978a) and a final copy of the map is being made.

Stratigraphy

Table 1 gives the stratigraphic sequence in the Wabush Iron Ore District as established by Iron Ore Company of Canada geologists with some modifications by the author. In areas other than directly west of Wabush Lake the iron formation can only be divided into a lower silicate carbonate facies and an upper oxide facies (contains the ore body) due to leaching and structural complexity. The areal distribution of the rock types is shown on the geologic map in Figure 5 which is a compilation of a reduced version of the Flora Lake -

TABLE 1: WABUSH LAKE AREA STRATIGRAPHIC COLUMN

AGE	FORMATION	MEMBER	MAJOR LITHOFACIES
APHEBIAN -HELIKIAN?	SHABOGAMO FORMATION		Gabbro Metagabbro Amphibolite: Horneblende-biotite ± garnet schist
	INTRUSIVE CONTACT		
PROTEROZOIC (APHEBIAN)	GAGNON GROUP	NAULT FORMATION	Quartz-graphite-feldspar-(biotite-muscovite) schist
		WABUSH IRON FORMATION — UPPER IRON FORMATION	Quartz-(actinolite-grunerite) schist Quartz-grunerite schist Quartz-(carbonate-grunerite) gneiss Quartz-carbonate gneiss
			Quartz-carbonate-magnetite gneiss Quartz-grunerite-magnetite schist Quartz-magnetite-grunerite gneiss Quartz-magnetite-carbonate gneiss
			Quartz-carbonate gneiss Quartz-(carbonate-grunerite) schist and gneiss
		MIDDLE IRON FORMATION	Quartz-magnetite-specularite schist
			Lean quartz-specularite schist
			Quartz-specularite schist Quartz-specularite-anthophyllite ± talc schist
			Quartz-(magnetite-specularite)rock Quartz-magnetite rock Quartz-magnetite-carbonate gneiss
		LOWER IRON FORMATION	Quartz-carbonate gneiss Quartz-(carbonate-grunerite) gneiss
			Lean quartz-(specularite-magnetite) rock Quartz-magnetite carbonate gneiss Quartz-carbonate-magnetite gneiss
			Quartz-carbonate gneiss Quartz-(carbonate-grunerite) gneiss
	WAPUSAKATOO (CAROL) FORMATION	UPPER MEMBER	Quartzite with accessory amphibole Quartzite with accessory carbonate
		MIDDLE MEMBER	Orthoquartzite Quartzite with accessory muscovite
		LOWER MEMBER	Quartz-muscovite ± garnet schist
	DULEY FORMATION		Calcitic marble ± tremolite Dolomitic marble ± tremolite
	KATSAO FORMATION		Quartz-feldspar-biotite-muscovite schist Quartz-biotite ± muscovite schist
	UNCONFORMITY		
ARCHEAN	ASHUANIPI COMPLEX		Granitic and granodioritic gneisses Granite intrusives

Wabush Lake map sheet found in the 1977 report on activities of the Mineral Development Division, Newfoundland Department of Mines and Energy, the preliminary map in Rivers (1978b) and part of the Shabogamo Lake map sheet by Fahrig (1960).

1.3 AMPHIBOLES AND RELATED MINERALS IN THE WABUSH IRON ORE DISTRICT

Prior to the study by Klein (1960) most of the work done in the Wabush District was on the iron oxides contained within the iron formation. Klein (1960) collected seventeen amphibole bearing specimens in an area west of Wabush Lake, determined the chemical composition of the amphiboles by optical methods, and looked at the associated minerals. Detailed studies (chemical and X-ray) of one grunerite and one manganoan cummingtonite were also carried out. All of these amphiboles were collected from the Wabush Iron Formation. At this time, only the lower quartz-carbonate-amphibole and upper quartz-magnetite-specularite members of the Wabush Iron Formation were recognized in this region. Later work allowed the Iron Ore Company of Canada geologists to recognize three members as shown in Table 1. Table 2 summarizes the mineralogical data from Klein (1960). A classification of the amphiboles (based on their chemical composition) which will be referred to in this study appears in Table 2A. Klein's conclusion regarding the occurrence of amphiboles in the Wabush

TABLE 2: SUMMARY OF MINERALOGY OF THE WABUSH IRON FORMATION (from Klein, 1960)

LOWER WABUSH IRON FORMATION

Member	Major Minerals	Minor Minerals	Description of Amphiboles
Quartz Carbonate (banded)	quartz calcite dolomite ankerite siderite grunerite* goethite*	magnetite penninite pyrite	Grunerite: greenish beige to light beige to dark brown colour, fine to medium grained, acicular, some crystals found up to 5" long, sometimes occurs in clusters, always <10% of rock volume
Quartz Amphibole (banded or schistose)	quartz cummingtonite-grunerite actinolite magnetite calcite	diopside garnet enstatite-orthoferrosilite ankerite penninite anthophyllite	Grunerite: light beige to brown colour, fine to medium grained, acicular (sometimes occurs as well lineated needles or in asbestiform habit), sometimes found as radiating groups of acicular crystals, up to 90% of rock volume. Cummingtonite: light greenish brown to beige to light brown colour, fine to medium grained, acicular, prismatic, asbestiform. Actinolite: light to dark green, fine to medium grained, subhedral, interwoven with cumm.-grun. Anthophyllite: fibrous inclusions in some samples, microscopic.

Table 2: continued

UPPER WABUSH IRON FORMATION

Quartz Magnetite** (massive banded)			Cummingtonite: short fine grained stubby needles, also elongate medium grained needles
Magnetite (massive banded)	Quartz specularite magnetite	hornblende anthophyllite cummingtonite-grunerite Mn cummingtonite phlogopite spessarite pyrolusite garnet epidote calcite limonite	
Specularite Magnetite (schistose)			Anthophyllite: medium to coarse grained, white to yellow brown to light gray acicular, in stellate groups parallel to schistosity (light brown at edges due to limonite stain) or concentrated in thin veneers parallel to schistosity. Mn-Cummingtonite: pale grayish green to green, fine go medium grained, acicular, randomly oriented, can form up to 90% of rock volume.
Specularite (schistose)			

* major constituent in some localities only

** always found at bottom of Upper Wabush Formation may be so rich in cummingtonite-grunerite that contact between Upper and Lower Wabush hard to see.

TABLE 2A CLASSIFICATION OF AMPHIBOLES (from Deer et al, 1966)

	Composition	Cleavage	Crystal System	Notes
Anthophyllite -Gedrite	$(Mg,Fe^{+2})_7(Si_8O_{22})(OH,F)_2$ to $(Mg,Fe^{2+})_5Al_2(Si_6Al_2O_{22})(OH,F)_2$	(210) perfect	orthorhombic	Limit of anthophyllite comp'n is 40% $Fe_7Si_8O_{22}(OH)_2$
Cummingtonite -Grunerite	$(Mg,Fe^{2+})_7(Si_8O_{22})(OH)_2$ to $(Fe^{+2},Mg)_7(Si_8O_{22})(OH)_2$	(110) good (110):(1$\bar{1}$0) $\approx 55^o$	monoclinic	Cummingtonite range from 30-70% and grunerite from 70-100% $Fe_7Si_8O_{22}(OH)_2$ Mn substitution common
Tremolite -Actinolite -Ferroactinolite	$Ca_2Mg_5(Si_8O_{22})(OH)_2$ to $Ca_2Fe_5^{+2}(Si_8O_{22})(OH)_2$	(110) good (110):(1$\bar{1}$0) $\approx 56^o$	monoclinic	Al a common substitute Tremolite range from 0-20%, actinolite from 20-80% and ferroactinolite from 80-100% replacement of Mg by Fe
Hornblende	$(Na,K)_{0-1}\ Ca_2(Mg,Fe^{+2},Fe^{+3},Al)_5(Si_{6-7}Al_{2-1}O_{22})(OH,F)_2$	(110) good (110):(1$\bar{1}$0) $\approx 56^o$	monoclinic	Wide compositional range. Many possible substitutions.
Glaucophane -Riebeckite	$Na_2Mg_3Al_2(Si_8O_{22})(OH)_2$ to $Na_2Fe_3^{+2}Fe_2^{+3}(Si_8O_{22})(OH)_2$	(110) good (110):(1$\bar{1}$0) $\approx 58^o$	monoclinic	Complete range of Fe^{+3}-Al substitution between $Na_2Mg_3Al_2Si_8O_{22}(OH)_2$ and $Na_2Mg_3Fe_2^{+3}Si_8O_{22}(OH)_2$ i.e. from glaucophane through crossite to magnesioriebeckite. Complete solid solution between magnesioriebeckite and riebeckite.

Iron Formation near Wabush Lake are as follows:

1. Megascopically visible needles of anthophyllite are found only in the specularite schists of the Upper Wabush Iron Formation where it occurs in stellate groups or thin veneers parallel to regional foliation. Microscopic fibrous inclusions of anthophyllite in quartz may be observed in quartz-grunerite schists from the quartz-amphibole member of the Lower Wabush Iron Formation.
2. Amphiboles of the cummingtonite-grunerite series are restricted to the Lower Wabush Iron Formation and the contact (transitional) between this formation and the Upper Wabush Iron Formation; however, they are only sparsely distributed through the quartz-carbonate member of the Lower Wabush Iron Formation. In some locations, the major part of the quartz-amphibole member of the Lower Wabush is made up of acicular grunerite. This quartz-grunerite schist may contain two different grunerites with a medium to coarse grained dark brown acicular grunerite randomly cutting across a well lineated fine grained grunerite groundmass. Cummingtonites occur in

the magnetite rich rocks and grunerites are restricted to rocks with ≤ 5 per cent magnetite. Coarse grained grunerite found in the quartz amphibole member of the Lower Wabush Iron Formation is often closely associated with eulite (En_2Fs_8).

3. Manganoan cummingtonites are found only in the specularite schists of the Upper Wabush Iron Formation. Bands of manganoan cummingtonite may be seen to grade into anthophyllite along strike.
4. Green actinolite was observed only in the quartz-amphibole member of the Lower Wabush Iron Formation. In the few outcrops where it was found, it was associated with light brown acicular cummingtonite.
5. Amphiboles of the hornblende group occur in bands along the gradational contact between irregular quartz-biotite bands and the Upper Wabush Iron Formation. These bands represent the metamorphosed equivalents of clay rich bands in the iron formation. They are dark green in colour, fine to coarse grained and subhedral to euhedral.
6. The chemical compositions of thirteen cummingtonite-grunerite samples as determined by optical methods varied between 59 mole per cent iron to almost 100 mole per cent iron. A chemical analysis of one grunerite samples gave a calculated formula of

$(Fe^{+2}_{5.8}, Fe^{+3}_{0.1}, Mg_{0.6}, Ca_{0.1}, Mn_{0.1})(Si_{7.8}, Al_{0.2})$
$O_{22}(OH)_2$

which appears to be deficient in the octahedral site by 0.3. A manganoan cummingtonite (manganoan cummingtonites contain > 10 mole per cent manganese) containing 16.8 weight per cent MnO gave a calculated formula of

$(Mg_{4.1}, Fe^{+2}_{0.4}, Fe^{+3}_{0.2}, Mn_{2.0}, Na_{0.1}, Ca_{0.2})(Si_{7.8}, Al_{0.2})O_{22}(OH)_2$.

The chemical composition of two hornblendes approximated that of hastingsite $NaCa_2Mg_4Al_3Si_6O_{22}(OH)_2$ in which Mg and Al have been replaced by iron. One sample of actinolite gave a composition (determined optically) of 62 per cent tremolite ($Ca_2Mg_5(Si_4O_{11})_2(OH)_2$) and 38 per cent ferrotremolite ($Ca_2Fe_5(Si_4O_{11})_2(OH)_2$).

Klein (1964) presented nine chemical analyses (determined by chemical, optical, and X-ray methods) of members of the cummingtonite-grunerite series from the Wabush Iron Formation. These analyses, along with additional analyses from the literature were calculated in terms of the components $Mg_7Si_8O_{22}(OH)_2$, $Fe_7Si_8O_{22}(OH)_2$, and $Mn_7Si_8O_{22}(OH)_2$. The solid solution within this ternary system was found to contain 35 to 100 mole per cent $Fe_7Si_8O_{22}(OH)_2$ and 0 to 3[illegible] mole per cent

$Mn_7Si_8O_{22}(OH)_2$. The most useful optical properties for determining chemical composition were found to be the γ index and $Z \wedge C$ angle. With respect to unit cell dimensions, the b dimension showed a significant systematic variation with composition, whereas a sin β varied little. The variations in unit cell dimensions with respect to chemical composition can be expressed by the equation b = 0.0055 Fe + 17.895 and a sin β = 0.001 Fe + 9.27 where a and b are unit cell dimensions in Angstroms, β is $a \wedge b$, and Fe is the mole per cent Fe^{2+} assuming a grunerite stoichiometry of $Fe_7Si_8O_{22}(OH)_2$. Finger (1967) obtained the following function: V = 873.41 + 0.53 Fe + 0.58 Mn + 0.97 Ca $\mathring{A}^3$ where V = unit cell volume in $\mathring{A}^3$; Fe, Mn and Ca are the mole per cent of Fe^{+2}, Mn^{+2} and Ca^{+2} respectively for the octahedral site assuming that cummingtonite-grunerite has the stoichiometry $(Mg,Fe)_7Si_8O_{22}(OH)_2$. Kramer (1976) simplified this for Fe-Mg variations to V = 873.41 + 0.53 Fe $\mathring{A}^3$. A similar relationship between cell volume and chemical composition of cummingtonite-grunerite from Klein (1964) can be expressed as V = 877.82 + 0.453 Fe $\mathring{A}^3$ and gives comparable results. Finger (1969) presented a model of the crystal structure and cation distribution of a grunerite from Klein (1964).

A detailed study of the mineralogy and petrology of the Wabush Iron Formation appears in Klein (1966). Thirty-four mineral phases in the iron formation were analyzed by

wet chemical or electron microprobe techniques. In addition, refractive indices, extinction angles, unit cell parameters (from X-ray diffraction), and densities were determined for each mineral. The amphiboles studied by wet chemical, optical and X-ray diffraction methods were a grunerite, an anthophyllite, two antinolites, a riebeckite-tremolite, and a magnesio-riebeckite. The manganoan cummingtonite sample discussed in Klein (1964) was analyzed using an electron probe. The magnesioriebeckite and riebeckite-tremolite were found in the Upper Wabush Iron Formation. They were dark green-dark blue green in colour and occurred as acicular or lath like crystals.

Klein (1966) also noted the occurrence of black manganese oxide stains on the weathered surfaces of the iron formation. This staining was principally attributed to the weathering of manganoan cummingtonite but outcrops of iron formation containing rhodonite ($(Mn,Ca,Fe)(SiO_3)$) were also seen. Other manganese bearing minerals found in the iron formation were rhodochrosite ($MnCO_3$), kutnahorite ($CaMn(CO_3)_2$), calderite ($3MnO.Fe_2O_3.3SiO_2$), and manganoan aegerine ($(Mn,Na,Fe)(Si_2O_6)$). The manganese content of the ore bodies west of Wabush Lake was estimated by Chakraborty (1966) to be less than 1 per cent. South of Wabush Lake it varied locally from 2 to 8 per cent. Massey (1979) reported some sooty black stained outcrops in the iron formation north of Julienne Lake.

Chakraborty (1966) studied the chemical and optical properties and modes of occurrence of anthophyllite, cummingtonite and actinolite from the Wabush Iron Formation of Wabush Lake and adjacent areas. Most of his identifications were confirmed by X-ray diffraction. Chemical analyses and optical properties of three manganoan cummingtonites were presented and he concluded that manganoan cummingtonite has a chemical composition and optical properties more similar to anthophyllite than to members of the cummingtonite-grunerite series. He also verified Klein's (1964) conclusion that the variation in composition of members of the cummingtonite-grunerite series can be related to the iron content of the rock, i.e., the Fe:Mg ratio in cummingtonite-grunerite increases moving from the carbonate facies (Lower Wabush) to the silicate facies (Lower Wabush) to the oxide facies (Upper Wabush) of the Wabush Iron Formation.

The tremolite contained in the Duley Formation, a dolomite-calcite marble is briefly mentioned by several authors. However, no detailed physical description or chemical analyses of this tremolite appear in the literature.

1.4 FIBRE NOMENCLATURE

Some of the amphiboles in the Wabush Lake area occur in a fibrous or asbestiform habit. The use of the electron microscope to identify and enumerate similar "asbestos-like"

particles has presented a major problem in terminology to analysts, health researchers, and mineralogists (Kramer, 1977). This improper application of mineralogical terms was accentuated by the Reserve Mining Company trial in Minnesota where the company was being prosecuted for dumping amphibole "fibres" into Lake Superior. During this trial, the term "asbestiform" in reference to the cummingtonite-grunerite fibres was defined as "any mineral which may crystallize as asbestos and/or has fibrous cleavage fragments, with length:width aspects of 3:1 or higher" (Zoltai and Stout, 1976). These fibres should have been referred to as fibrous cleavage fragments of amphibole according to accepted mineralogical nomenclature.

The Glossary of Geology (American Geological Institute, 1972; second printing, 1973) gives the following definitions:

1. Asbestos:
   a) a commercial term applied to a group of highly fibrous silicate minerals that readily separate into long, thin, strong fibres of sufficient flexibility to be woven, are heat resistant and chemically inert, and possess a high electrical insulation, and therefore are suitable for uses (as in yarn, cloth, paper, paint, brake linings, tiles, insulation cement, fillers and filters), where incombustible, nonconducting, or chemically resistant material is required.
   b) a mineral of the asbestos group, principally chrysotile (best adapted for spinning) and certain fibrous varieties of amphibole (eg. tremolite, actinolite, and crocidolite).
   c) a term strictly applied to the fibrous variety of actinolite.
2. Asbestiform: Said of a mineral that is fibrous, i.e. that is like asbestos.

3. Acicular: (cryst) — Said of a crystal that is needlelike in form.

4. Fibrous: — Said of the habit of a mineral, and of the mineral itself (eg. asbestos), that crystallizes in elongated thin, needle-like grains or fibres.

The Ontario Ministry Committee on Asbestos Analysis report (1977) suggests the following definitions:

1. Asbestos — a generic term for several fibrous silicate minerals of the serpentine or amphibole group. Examples are chrysotile, actinolite, cummingtonite-grunerite, anthophyllite, crocidolite, and tremolite.

2. Fibre — a particle having essentially parallel sides and a length to width ratio of 3:1 or greater. An asbestos fibre may be an individual fibril or a bundle of fibrils.

3. Fibril — a single fibre, which cannot be separated into smaller components without losing its fibrous properties or appearance.

4. Aspect Ratio — the ratio of length to width

5. Amphibole — a double chain silicate consisting of Si_4O_{11} units, laterally linked by various ions such as calcium, magnesium, iron, aluminum, and sodium. Amphiboles may consist of or contain fibres formed through natural growth processes and may also produce fragments that conform to the definition of a fibre as a result of crushing and milling processes.

To avoid any possible ambiguities, the terms fibre and fibrous in this study will mean any particle having apparent crystal continuity, parallel sides, an aspect ratio of 3:1 or greater, and widths in the micrometer or submicrometer range.

1.5 ENUMERATION AND IDENTIFICATION OF FIBRES BY TRANSMISSION ELECTRON MICROSCOPY

Since most fibres contained in water and sediment samples are below the range of optical microscopy, electron microscope methods must be used to enumerate and analyze fibres. Scanning electron microscopes have been employed but most studies indicate that the transmission electron microscope is superior because it allows examination at low (~ 200 x) and high (~20000 x) magnification and gives better contrast and brightness (McCrone and Stewart, 1974; Beaman and File, 1976; Pattniak and Meakin, 1973). Most transmission electron microscopes can also be fitted with instruments to allow selected area electron diffraction (SAED) and energy dispersive X-ray spectroscopy analyses (EDS) to be carried out on individual fibres (Anderson, 1977).

Sample Preparation

The major problem in the preparation of grids for TEM analysis is in the transfer of the sample material to be studied onto the TEM grid with as little loss (quantitatively) and fracturing of fibres as possible. There are many methods currently in use by researchers, all of which involve some fibre loss and splitting. Water samples (normally 1 L) are concentrated by filtering through a Millipore or Nucleopore

filter. Nucleopore filters however are prone to fibre loss during handling whereas Millipore filters retain fibres well but generate a structured background if carbon coated prior to destruction of the filter structure (Beaman and Walker, 1977). Blanks of the filters are usually run since all filters can be considered contaminated with fibres to variable degrees. Sediment samples, unlike water samples, normally require no filtering.

The U.S. Environmental Protection Agency (Anderson, 1977) and the Ontario Ministry of the Environment (MOE report prepared by the Committee on Asbestos Analysis, 1977) suggest interim procedures for the preparation of TEM grids based on the Jaffe-Wick method. This method involves placing sections of the filter (Nucleopore) on top of the TEM grids and dissolving the filter with chloroform, leaving a representative sample on the grids.

Biles and Emerson (1968) and Cunningham and Pontefract (1971) in their examinations of chrysotile fibres in beer, beverages and drinking water, prepared their grids in the following manner: concentrated the fibres by ultracentrifuging, filtered the sample, ashed the filter by low temperature ashing, dispersed the particles in distilled water with an ultrasonic vibrator, then centrifuged the particles directly onto the TEM grids. Kramer (1976) used a similar procedure (except that fibres were removed from the filter by

sonification instead of low temperature ashing) in his study of Lake Superior fibrous cummingtonite:

- Filter water sample through a 0.45 to 0.1 μm Millipore or Nucleopore filter
- Roll filter paper inwards and place in vial with 5-15 ml. of fibre-free water
- Suspend fibres using a high intensity ultrasonifying probe at 30,000 Hz for 1-5 minutes.
- Transfer microlitre aliquots of solution directly to a Cu or Ni Parlodion-coated 200 mesh TEM grid using a micropipette.
- Dry in an upside down position.

The major problem with this method is the breakage and splitting of chrysotile fibres (but not amphiboles) during sonification: Other problems associated with the Jaffe-Wick method and other preparation techniques are discussed in McCrone and Stewart (1974), Beaman and File (1976), Zoltai and Stout (1976), Beaman and Walker (1977), Anderson (1977).

An optimal concentration of fibres on the TEM grid is between 5 and 50 fibres per grid square. These figures represent an average of cited figures found in the literature. Overloading of the grids makes enumeration cumbersome and inaccurate as many fibres may overlap.

Enumeration and Size Analysis of Fibres

Table 3 summarizes four of the many procedures,

TABLE 3: PROCEDURES FOR ENUMERATION AND SIZE ANALYSIS OF FIBRES

	Ontario Ministry of the Environment Interim Method	U. S. Environmental Protection Agency Interim Method	McMaster University	Illinois Institute of Technology
Reference	M.O.E. report from the Committee on Asbestos Analysis, 1978	Anderson, 1977	Kramer, 1976 Zoltai and Stout, 1976	Zoltai and Stout, 1976
T.E.M. grid mesh	normally 200; may use 400 if over-loaded	not specified	200	not specified
Magnification	20,000 x	10,000-20,000	20,000-25,000	20,000
Replicate grids run	Yes	Yes	Yes	not specified
Optimal concentration (# fibres/ grid square)	≥ 5 ≤ 50	≤ 50	≥ 5 ≤ 30	not specified
Lower limit on diameter of fibres counted & sized	not specified	not specified	250 Å (.025μ)	200 Å (.020μ)
Number of grid squares scanned	≥ 4 ≤ 20	≤ 5 on each of 2 grids = ≤ 10 total	≥ 4	
Minimum No. of fibres counted & sized	≥ 100	50 on each of 2 grids = 100 total	≥ 100	100

found in the literature, to enumerate and size fibres. No detailed studies of their reproducibility have been completed but the McMaster University procedure has been estimated to have a reproducibility of ± 10 per cent (Mudroch, 1979). Generally, the McMaster counts are higher due to less fibre loss in sample preparation, less discriminatory acceptance of amphiboles in the count, and possible breakage of fibres in the ultrasonic treatment (Zoltai and Stout, 1976). Discussions on the reliability of measurements of amphibole fibre concentrations in water are found in Brown et al. (1976) and Leineweber (1977).

Most analysts suggest counting and sizing approximately 100 fibres in order to calculate a reasonably precise concentration. Dr. C. Harwood of the Illinois Institute of Technology, believes that counting only 100 fibres per sample is statistically significant (Zoltai and Stout, 1976). Figure 6 compares the variability of total fibre count to fields of view examined. A constancy is achieved at about 60 fibres or more if the grid is optimally loaded.

Identification of Fibres

Some analytical techniques are possible without the use of SEM or TEM if the fibres are large enough and/or constitute a high proportion of the sample. Kramer (1976) used X-ray diffraction to study fibrous amphiboles from the Reserve

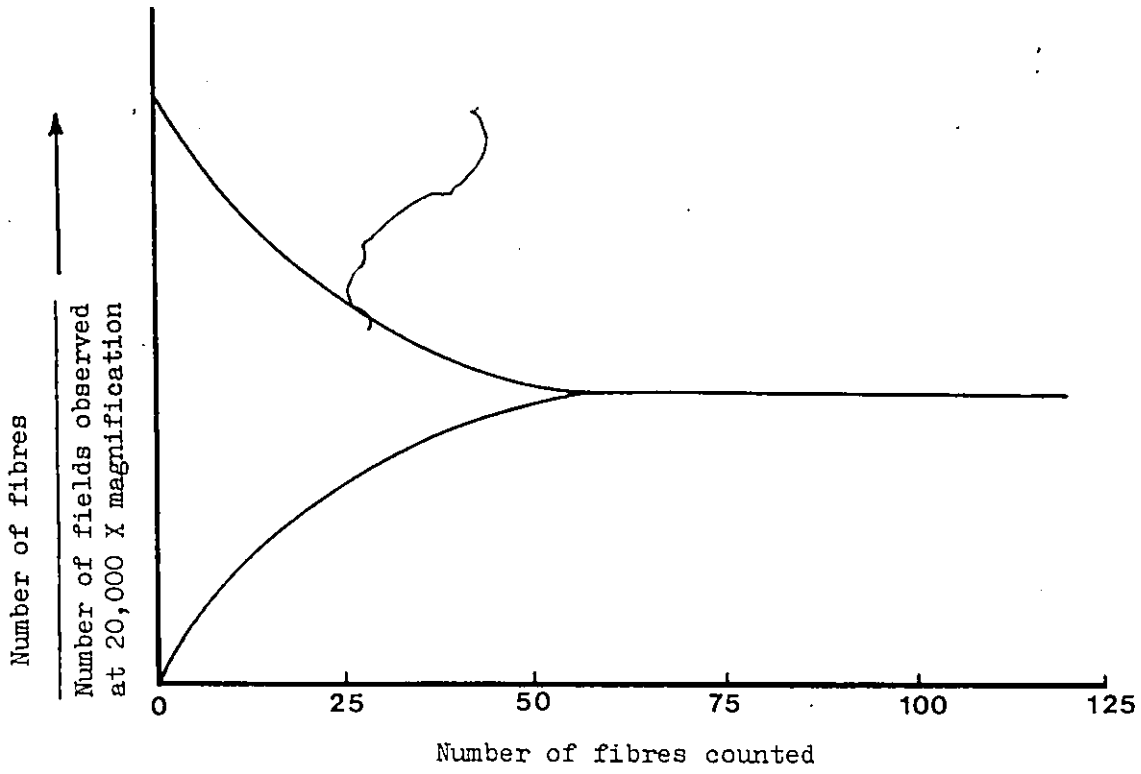

Figure 6: Variability of fibres per area with total fibre count (from Zoltai and Stout, 1976)

Mining Company tailings where approximately 40 wt.% of the tailings were amphibole. The petrographic microscope can be used to determine refractive indices, birefringence, sign of elongation, and extinction angle for fibres (and amphibole cleavage fragments) longer than 1 μm (Klein, 1960, 1964, 1965, 1966; Chakraborty, 1966; Bonnichsen, 1969; McCrone, 1977). These procedures should be used whenever possible since they are usually more mineralogically definitive than analytical electron microscopy.

Submicron size mineral fibres are identified using an analytical transmission electron microscope (ATEM) which consists of a transmission electron microscope equipped with energy dispersive X-ray fluorescence spectroscopy (EDS) and in some cases, scanning electron microscopy capabilities. With this instrument the fibre morphology can be examined, elemental abundances determined using EDS, and the structure of crystalline materials studied using selected area electron diffraction (SAED).

Most researchers agree that in order to positively identify mineral fibres, their morphology, elemental composition, and lattice geometry must be simultaneously determined. Identification by only one or two characteristics can often lead to ambiguous results.

Energy dispersive X-ray spectroscopy data can be converted to elemental abundance using known standards, giving

a relative error normally less than 10% (Anderson, 1977; Beaman and Walker, 1977). This figure is verified by Kramer (1977) in his study of compositional variations along individual fibres. He found that the element/Si ratios varied between 5-10% for individual UICC amosite and crocidolite fibres and were <10% for individual asbestiform cummingtonite-grunerite samples from Labrador. Most of this variation can be accounted for by compositional changes but some must be due to X-ray absorption and secondary radiation from iron in the samples. Therefore, many individual fibres within a specific sample must be analyzed to get a reasonably accurate chemical composition.

Selected area electron diffraction can be carried out completely on a microscope equipped with an accurate goniometer stage so that fibres can be properly oriented. The interpretation of the patterns obtained is extremely time consuming and requires a great deal of expertise. At the present time, most laboratories are in the process of building up a library of standard patterns which can be used to identify fibres on the basis of apparent similarity of diffraction patterns with these standards. However, this short-cut method is very unreliable. Extremely small variations in crystal orientation, substitutions, defects, etc. can result in apparent anomalous diffraction patterns. In addition, different minerals may give similar patterns if their interplanar distances are

similar, as is common to many silicates (Zoltai and Stout, 1976).

Discussions of analytical transmission electron microscopy techniques and the reproducibility of results can be found in Hirsch et al. (1965), McConnell, in Zussman (1967), Andrews, et al. (1971), Beeston et al. (1973), Rudd et al. (1976), Wenk (1976), Chopra (1977), and Nord (1977).

CHAPTER TWO

SAMPLING TECHNIQUES AND LOCATIONS

Water, mineral, sediment, and soil samples from the Wabush Lake district were collected by the author during the summers of 1976 and 1977. In addition, some mineral specimens from the Wabush Iron Formation north of Julienne Lake were received from N. Massey, employed during the summer of 1978 by the Newfoundland Department of Mines and Energy.

2.1 WATER SAMPLES

In August 1976, water samples were collected from 51 locations in and around Wabush Lake (Fig. 7); during June, 1977, 111 locations were sampled (Fig. 8). At least one litre of water was taken at each sampling point and all of the samples were of surface waters except for some locations in Wabush, Julienne, and Shabogamo Lakes where samples at various depths were taken using a van Dorn bottle. The lake depth was noted in some cases when sounding by line was possible (Table 4 & Fig. 10). Two samples (1976 numbers 7 & 8) were drinking water samples from the Sir Wilfred Grenfell Hotel in Wabush. Six samples, one each day over a period of six days (numbers CL-1 to CL-6) were taken from the Carol Lodge

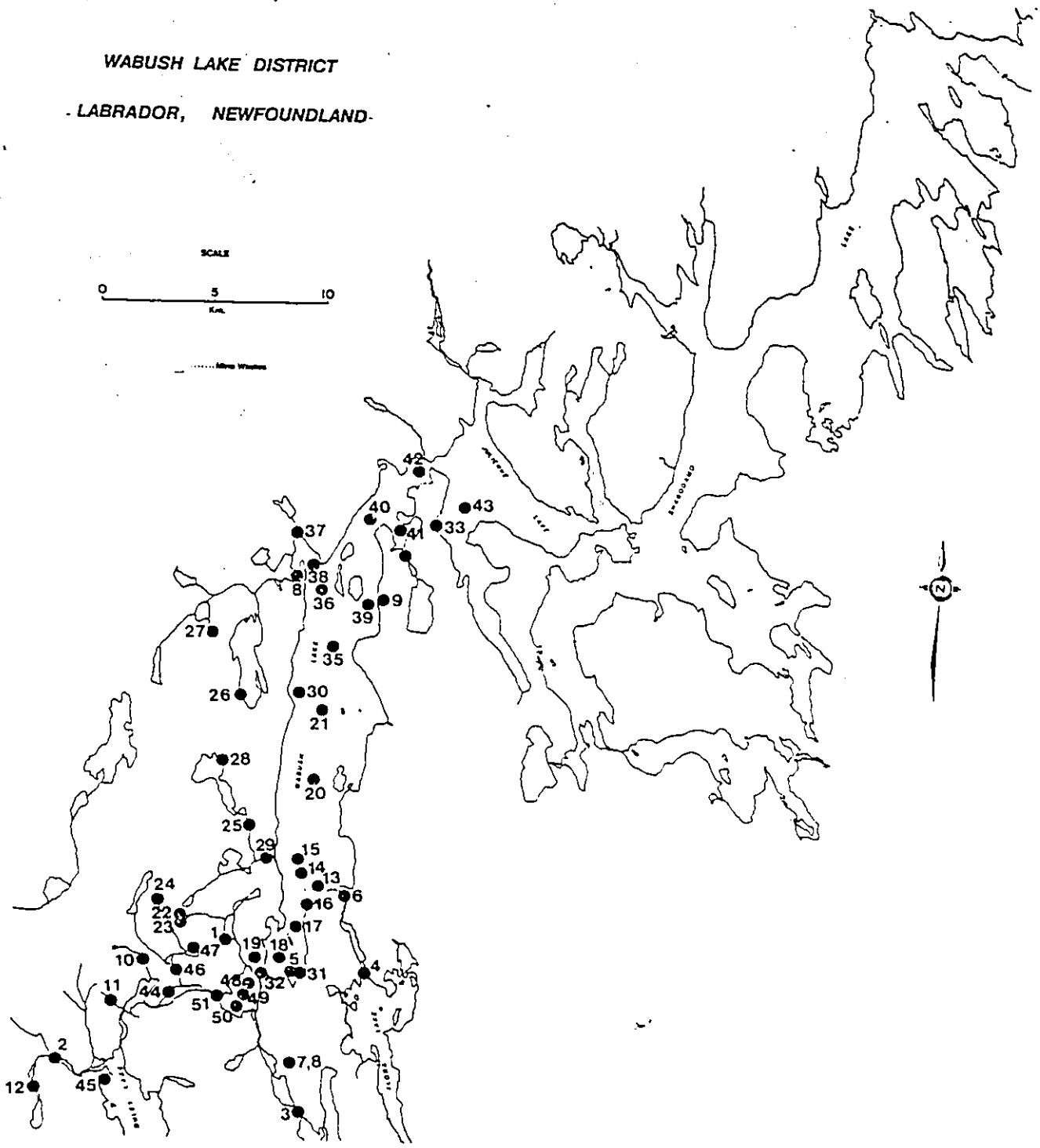

Figure 7: Water Sample Stations (1976)

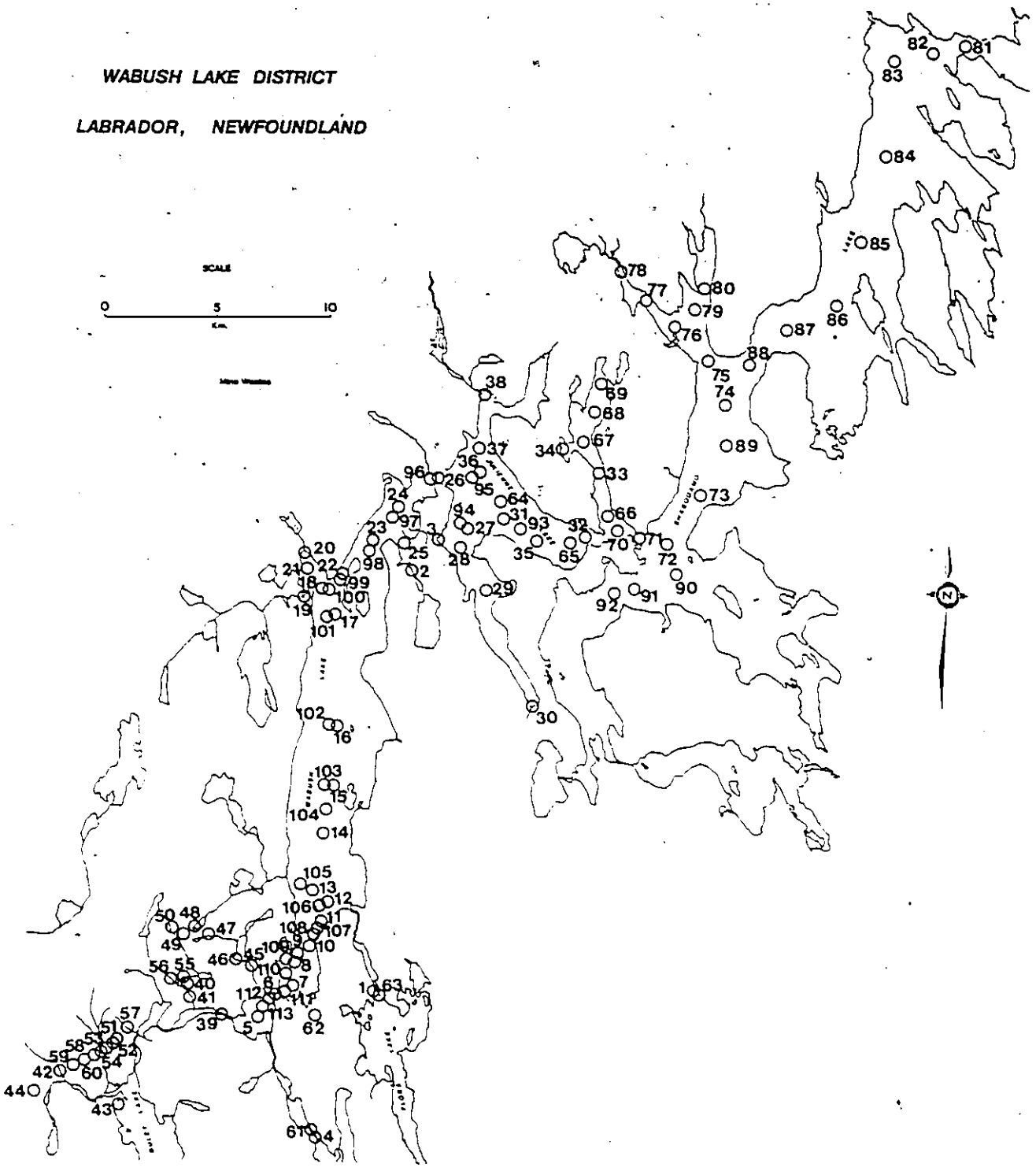

Figure 8: Water Sample Stations (1977)

TABLE 4: Lake Depths (Metres) - see Figures 8 and 9

1977 - Water Stations

No.	Depth
16	15
28	4
64	13
65	5
66	9
70	8
76	9
81	3
82	2
92	6

Sediment Stations

No.	Depth	No.	Depth	No.	Depth
1	5	16	7	30	3
2	5	17	16	31	14
3	38	18	18	32	13
4	16	19	15	33	22
5	11	20	15	34	40
6	4	21	50	35	39
7	8	22	3	36	33
8	6	23	9	37	11
9	16	24	10	38	5
10	13	25	8	39	3
11	10	26	8	40	2
12	10	27	7.5	42	49
14	10	28	9	43	42
15	10	29	9		

drinking water in Labrador City in June 1977. The sources of drinking water for Wabush (1976 number 3 (no data), 1977 numbers 4 & 61) and Labrador City (1976 number 1 and 1977 number 46) were also sampled.

2.2 LAKE AND STREAM SEDIMENTS, SOILS AND TAILINGS

Figure 9 shows the locations at which sediment or soil samples were taken during 1976 and 1977. The lake sediments were obtained by using a Shipek grab sampler lowered by rope from a boat. The depth of the lake at each station (Table 4 & Fig. 10) and a physical description of each sample was noted immediately upon sample recovery (Table 1 in Appendix). Bulk samples of the Iron Ore Company of Canada tailings were gathered from the mine waste dump at the edge of Wabush Lake. Separate containers for each layer were used to retain lake sediment samples which were stratified.

2.3 MINERAL AND ROCK SAMPLES

Since the principal aim of this study is to determine the distribution and fate of asbestiform amphiboles (or other asbestiform mineral particles) in the environment, as many different amphibole bearing rocks from as many locations as possible were collected, including specimens from the active mining area of Iron Ore Company of Canada and Wabush

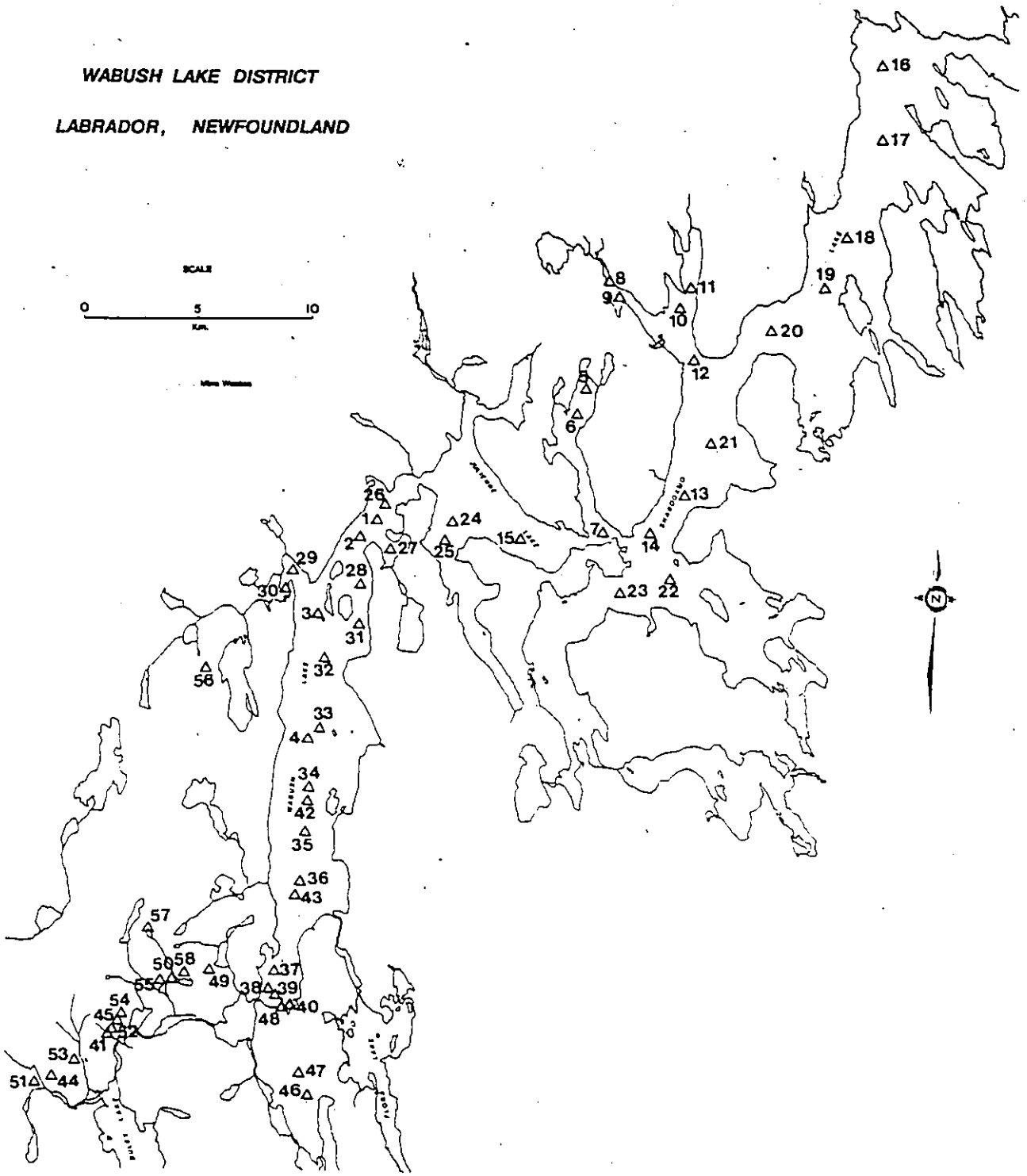

Figure 9: Sediment and Soil Sample Stations

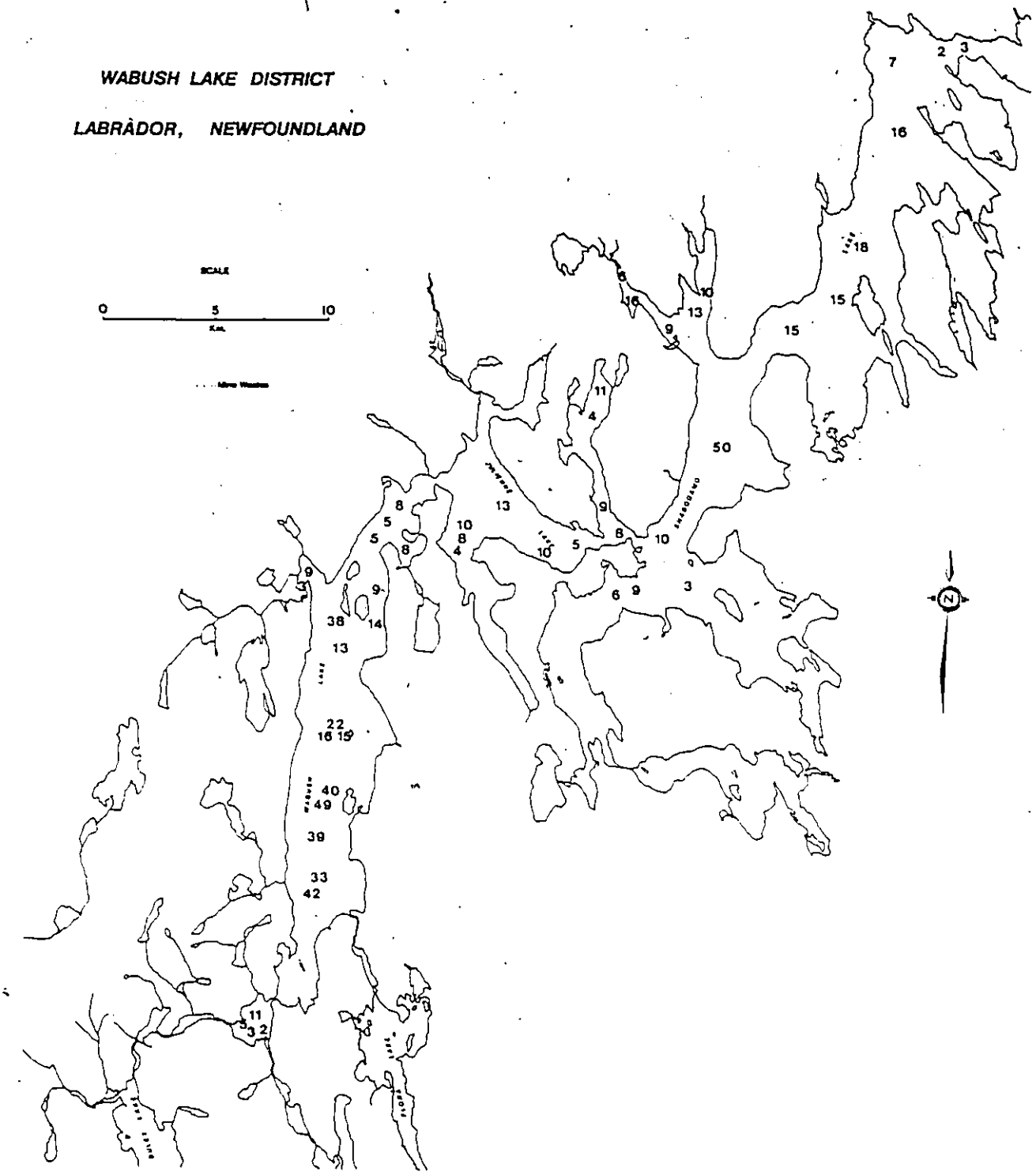

Figure 10: Lake Depths (Metres)

Mines. Most samples are from the Wabush Iron Formation (Table 2 in Appendix) but a representative suite of rocks found in the area (some of which contain no amphiboles) was also taken. The location of sampling points is shown in Figure 11.

Figure 11: Rock specimen locations. At point A, samples L-45, -29, -46 and -47 were collected over a distance of 150 metres from west to east respectively. At point B, samples L-22, -23, and -51 were collected 60 metres apart from west to east respectively. Samples L-32 to L-44 were taken from the Wabush Mines open pits at point C.

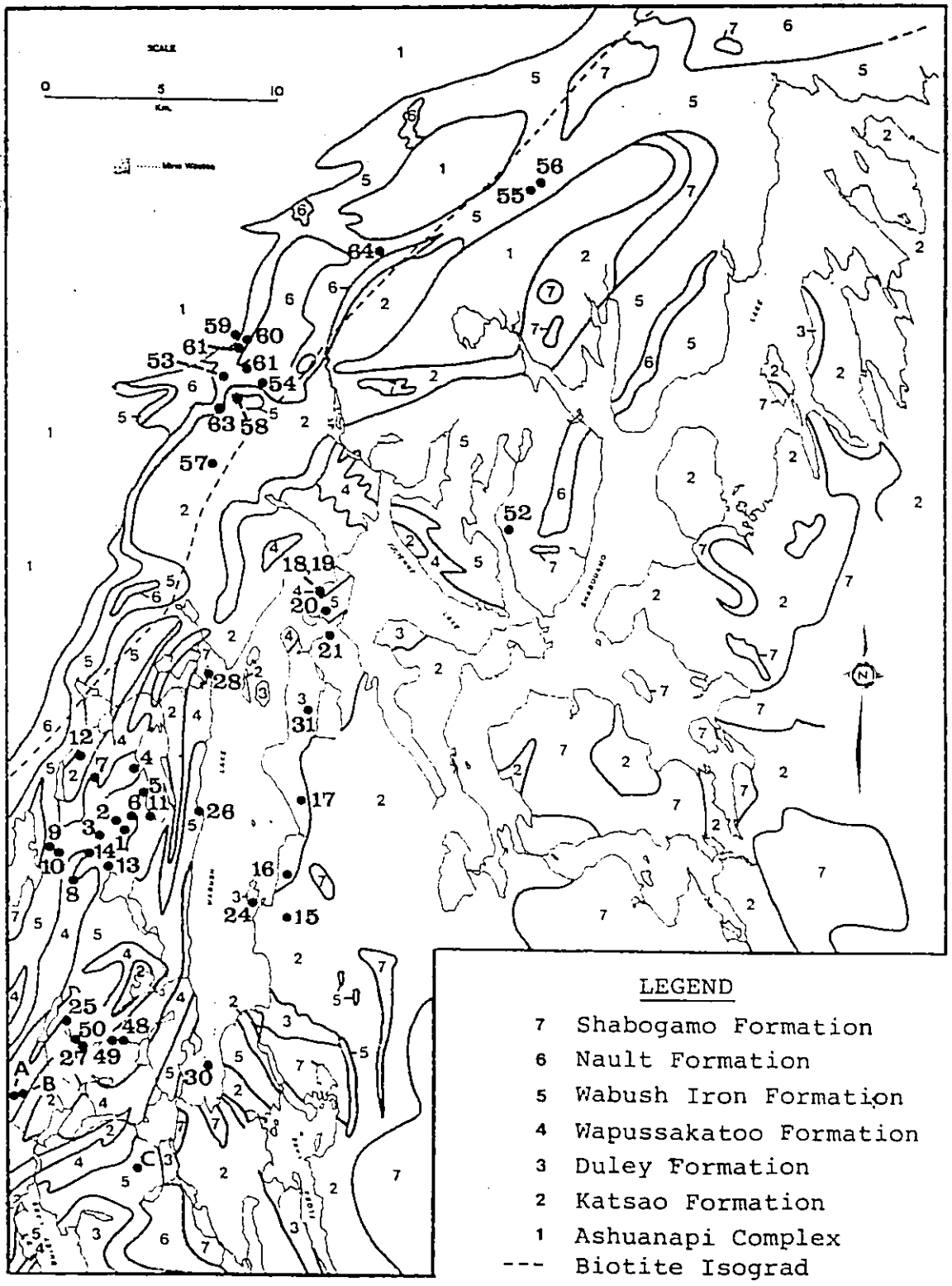
SCALE
0 5 10
Km
LEGEND
7 Shabogamo Formation
6 Nault Formation
5 Wabush Iron Formation
4 Wapussakatoo Formation
3 Duley Formation
2 Katsao Formation
1 Ashuanapi Complex
--- Biotite Isograd

CHAPTER THREE

ANALYTICAL METHODS

3.1 ENUMERATION, SIZE ANALYSIS AND IDENTIFICATION OF FIBRES IN WATER SAMPLES

Preparation of Electron Microscope Grids

All water samples were filtered through a 0.45 µm Nucleopore filter within two days of acquisition. The maximum volume of water filtered was 1 litre per sample. The actual volume filtered was dependent on the quantity of suspended material since some filters were clogged very rapidly. Each filter was folded inside out (using tweezers so as not to disturb the filtrate) and placed in a 10 ml. glass vial. Upon returning to the laboratory, a measured amount of deionized distilled fibre free water was added to the vials. The vials containing the filters were then sonified using an ultrasonic probe at 20,000 Hz for five minutes to remove the particulates from the filters. One to ten microlitre aliquots of solution were placed on carbonized Parlodion-coated 200 mesh copper or nickel electron microscope grids and allowed to dry in an upside down position with the aid of a high intensity lamp. Nickel grids were used for samples requiring analysis by energy dispersive X-ray fluorescence spectroscopy since the copper Lα line

is close to the sodium Kα line resulting in poor sodium analyses if copper grids are used.

The grids were initially examined at low power (~500 x magnification) on a Philips 300 transmission electron microscope to see if the grids were optimally loaded or if a substantial number of the grid openings were cracked or broken. New grids were prepared to replace those rejected.

Enumeration and Size Analysis of Fibres

Up to 100 fibres per grid square on 6 grid squares were enumerated on a Philips 300 transmission electron microscope. Any mineral particle having an aspect ratio of 3:1 or greater was included in the count. Fibres were designated as either amphibole cleavage fragments or other mineral fibres based on their morphology. The cleavage of amphiboles is relatively easy to recognize under the electron microscope. The presence of diatoms, other organics, and other mineral particles was noted for some samples.

All grids were enumerated to determine fibre concentrations; selected grids were chosen for size analysis. Sizing of the fibres (length and width) was carried out using the diameter of circles present on the microscope viewing screen as references. Mass concentrations of fibres in the samples were then calculated using the enumeration and size data. The standard deviation for individual grid square counts was determined and indicate the degree of homogeneity of the sample on the grid.

Energy Dispersive X-ray Fluorescence Spectroscopy Analysis of Fibres

Fibres and other mineral particles were analyzed on selected grids in a Philips 300 transmission electron microscope with an attached EDAX 707 analyser using a Si(Li) detector. The beam size ranged from 0.3 to 0.5 μm and the channel resolution was 4 to 40 e V. Data from the pulse-height generator was smoothed using a computer program. Elemental intensities were converted to weight per cent oxides, using reference standards, and the fibres were nominally identified using the standards and a computer program. Some of the longer fibres were analyzed at various points along their length to determine the variation in composition with length. The size of each fibre analyzed was recorded.

3.2 ANALYSIS OF TAILINGS, SEDIMENTS AND SOILS

X-ray Fluorescence

Portions of selected soil and sediment samples and a bulk sample of tailings were dried in a drying oven at 120°C for several hours then ignited in an electric furnace at 900°C. The ignited powder was used to prepare glass beads which consisted of 3 grams of flux (50% lithium metaborate and 50% lithium tetraborate) and 0.5 grams of sample. The beads were analyzed for major elements in a Philips 1540 X-ray fluorescence sequential analyzer using a chromium

radiation source at 50 kV and 50 m A. Results were re-calculated in weight per cent oxides and normalized to 100 per cent using a computer program.

X-ray Diffraction

The tailings were initially separated for X-ray diffraction analysis with a hand magnet to remove the highly magnetic material from a weighed 100 to 150 mesh fraction. A Franz isodynamic separator was used to further separate the sample. The fractions were weighed and a portion of each was ground to a fine powder using a clean agate mortar and pestle. The powders were mounted on clean petrographic glass slides with acetone. Analysis of the powders and a quartz standard was carried out on a Philips vertical goniometer using copper radiation (at 30 kV, 16 m A) with a nickel filter, a time constant of 2 seconds, a scan speed of 1 degree per minute, and a chart speed of 2 cm per degree.

The sediments were too fine to separate; they were composed mainly of clay-size particles. Bulk samples of some sediments were run to see if any minerals could be identified. None of the soil samples were analyzed by X-ray diffraction.

Analytical Transmission Electron Microscopy

Portions of selected sediment and soil samples were added to deionized distilled water and shaken to suspend the particles. Microlitre aliquots of the solution were placed on carbonized Parlodion-coated 200 mesh nickel electron microscope grids. Chemical analyses of fibres and other mineral particles present and size analyses of the fibres (for most sediments and the tailings) were done on a Philips 300 transmission electron microscope equipped with an EDAX 707 analyzer. Quantitative estimates of the fibre and mineral particle proportions were also made. Fibres only were studied in some of the sediment samples and all of the soils. Identification of minerals was made with the aid of reference standards and a computer program.

3.3 ANALYSIS OF AMPHIBOLES CONTAINED IN ROCK SAMPLES

Descriptions of the amphibole bearing rock samples which were collected from the Wabush Lake area appear in Table 2 of the Appendix. The morphology of the amphibole crystals and/or cleavage fragments, in hand specimen (and in some cases, thin section), is also presented.

Most of the amphiboles were large enough to pick directly out of the hand specimen. Some samples were

almost 100 per cent amphibole and required no further separation. Others which contained amphiboles that were too small to separate by hand were crushed and ground then separated using Carpo and Franz separators.

X-ray Fluorescence

Sample preparation techniques and operating conditions were identical to the analysis of tailings by X-ray fluorescence. Three amphibole samples and two reference standards were analyzed.

X-ray Diffraction

The samples were prepared for X-ray diffraction and run under the same operating conditions as outlined for the sediments and tailings. Quartz was used as a reference standard but was not mixed with the sample (some contained quartz impurities) because the quartz peaks interfered with some amphibole peaks. The peaks were difficult to index; consequently, a series of calculated patterns was produced with a computer program to assist in indexing. The cell refinement program PARAM of Stewart (1972) was used to obtain cell constants and volumes.

Energy Dispersive X-ray Fluorescence Spectroscopy

The amphibole samples were crushed and ground,

suspended in deionized distilled water, then pipetted directly onto carbonized Parlodion-coated 200 mesh nickel electron microscope grids. They were analyzed on a Philips 300 transmission electron microscope equipped with an EDAX 707 analyzer. Many analyses were done on several fibres to see if there was any compositional variation along individual fibres.

Electron Microprobe

The polished thin sections used in the microprobe were prepared for analysis by coating them first with cobalt and then with carbon to a thickness of several hundred Å. Analyses were carried out on an ETEC energy dispersive auto-probe located in the Mining Building at the University of Toronto using zinc from willemite as a standard for the energy spectrum, and a cobalt standard to which all elements analyzed were referred. The cobalt was initially checked against amphibole standards of similar composition to the amphiboles from the Wabush Lake area and correction factors were adjusted accordingly by J. Rucklidge. Data reduction was done on a computer program devised by J. Rucklidge.

Counts were made for either 50 of 100 seconds for each analysis using an accelerating voltage of 20 KV and a count rate around 2,000 counts per second. No significant change was noted in the standard deviation (which is

approximately 2%) of the analyses when the counting time was reduced from 100 to 50 seconds.

CHAPTER FOUR

ANALYTICAL RESULTS

4.1 WATER SAMPLES

Fibre Concentrations

Concentrations of fibrous minerals found in the water samples are given in Tables 3 (1976) and 4 (1977) of the Appendix. All mineral particles having an aspect ratio of 3:1 or greater are included in the results. For many of the 1977 samples, a distinction was made between amphibole fibres which exhibited good cleavage (Fig. 12) and other mineral fibres (mainly Fe-Mn, Mn-Fe-Si and Fe-rich) which had rounded ends and a rather corroded appearance (Fig. 13).

Figures 14 and 15 show the distribution of fibres in the surface waters for samples collected in 1976 and 1977 respectively. The highest concentrations were found in the river flowing from Flora Lake and just downstream from the Iron Ore Company of Canada tailings deposit in Wabush Lake. These high concentrations appear to be a direct result of mine waste dumping by the Iron Ore Company of Canada at the south end of Wabush Lake and by Wabush Mines at the west side of Flora Lake. The effect can be seen more clearly in Figure 16 where the fibre concentrations are low ($< 100 \times 10^6$

Figure 12: Electron photomicrograph of an amphibole exhibiting excellent cleavage (from water sample 77-112)

Figure 13: Electron photomicrograph of fibrous mineral particles in water sample 76-15

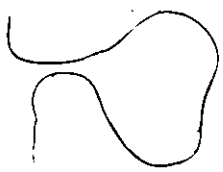

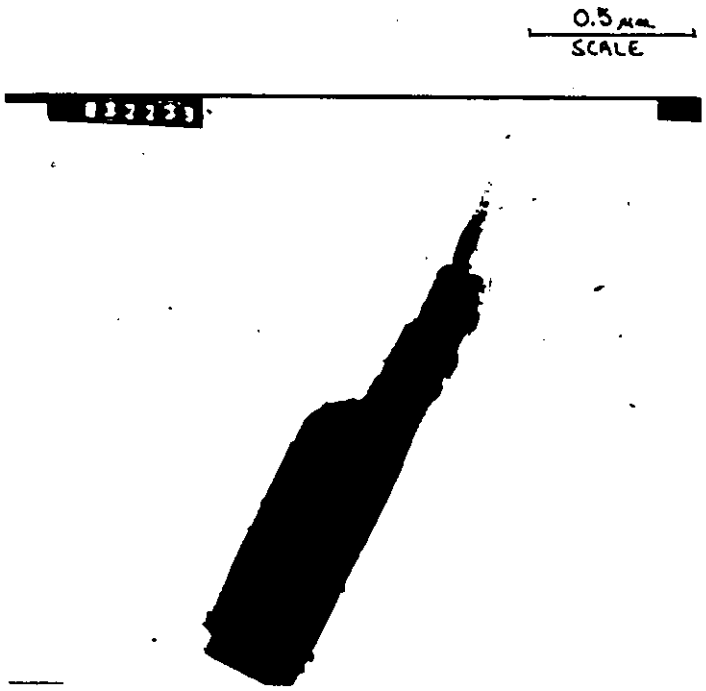
0.5 μm.
SCALE

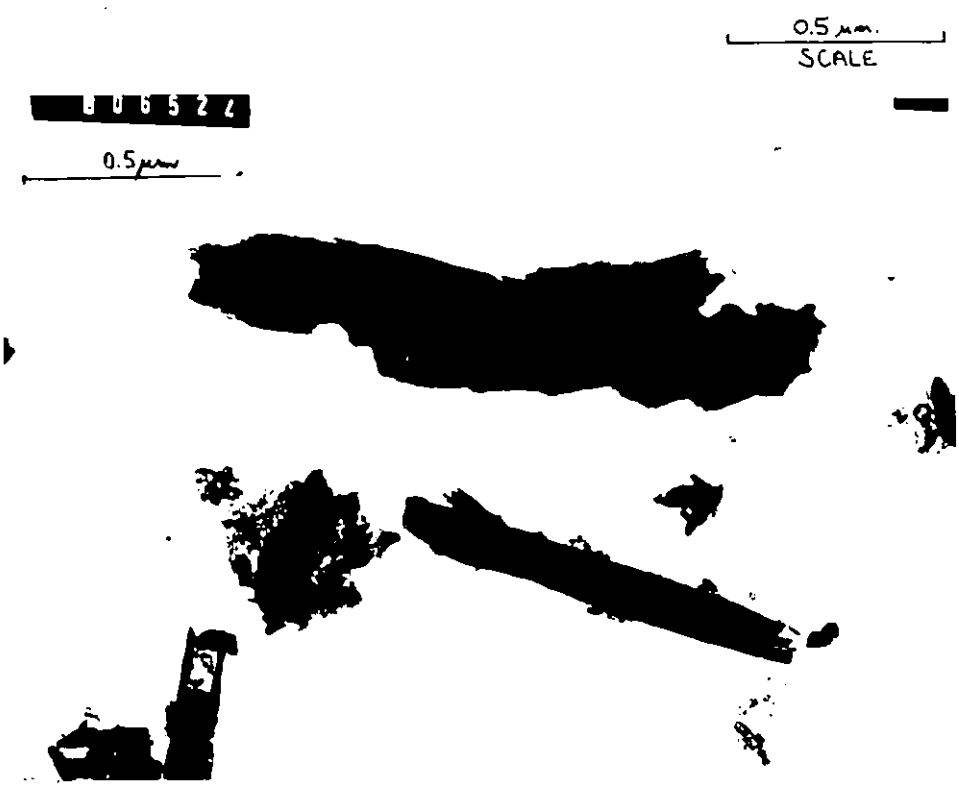
0.5 μm.
SCALE
0.5μm

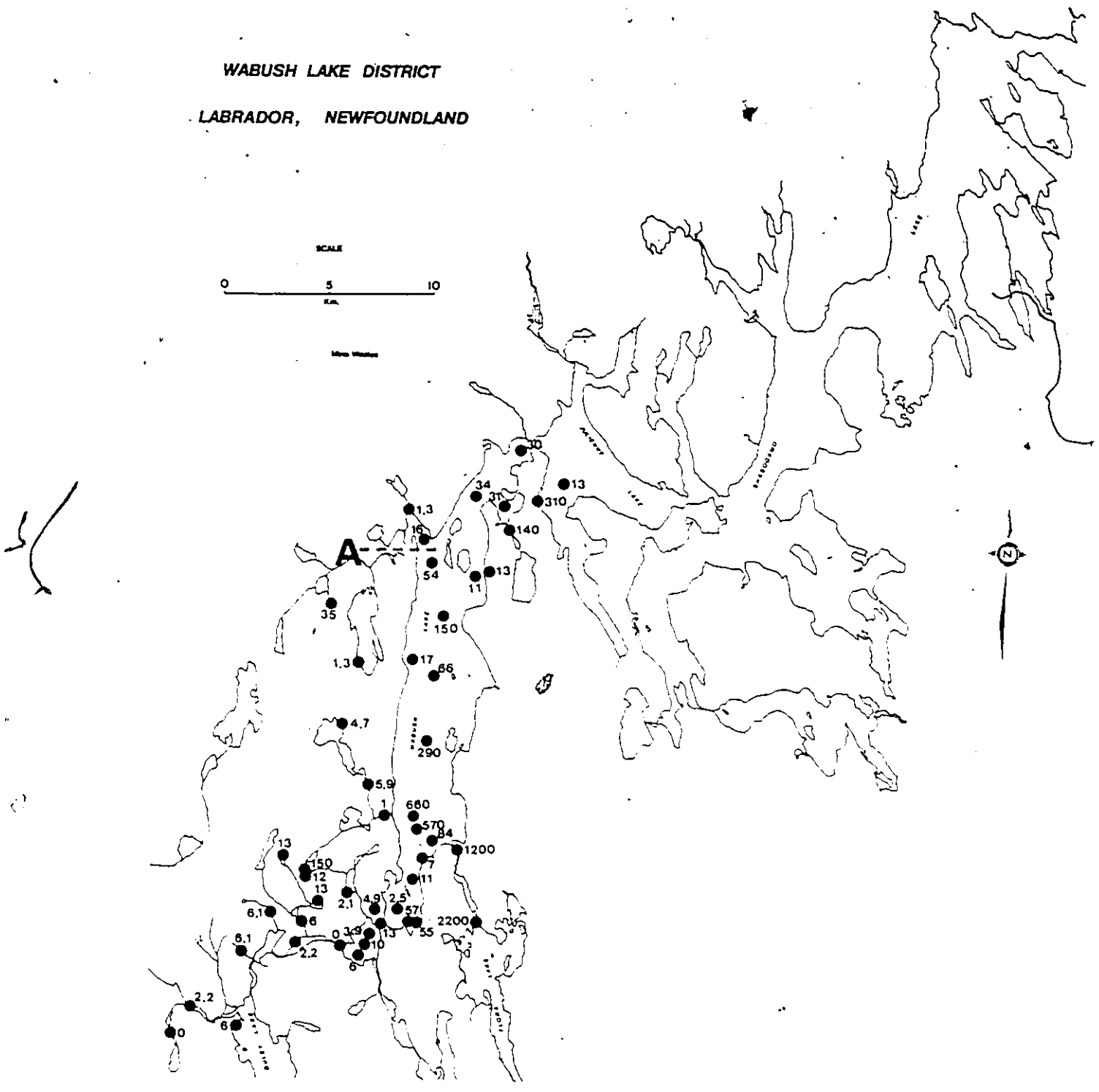

Figure 14: Fibre concentration in surface waters (fibres/ litre x 10^6), 1976 (see Fig. 16 for significance of A)

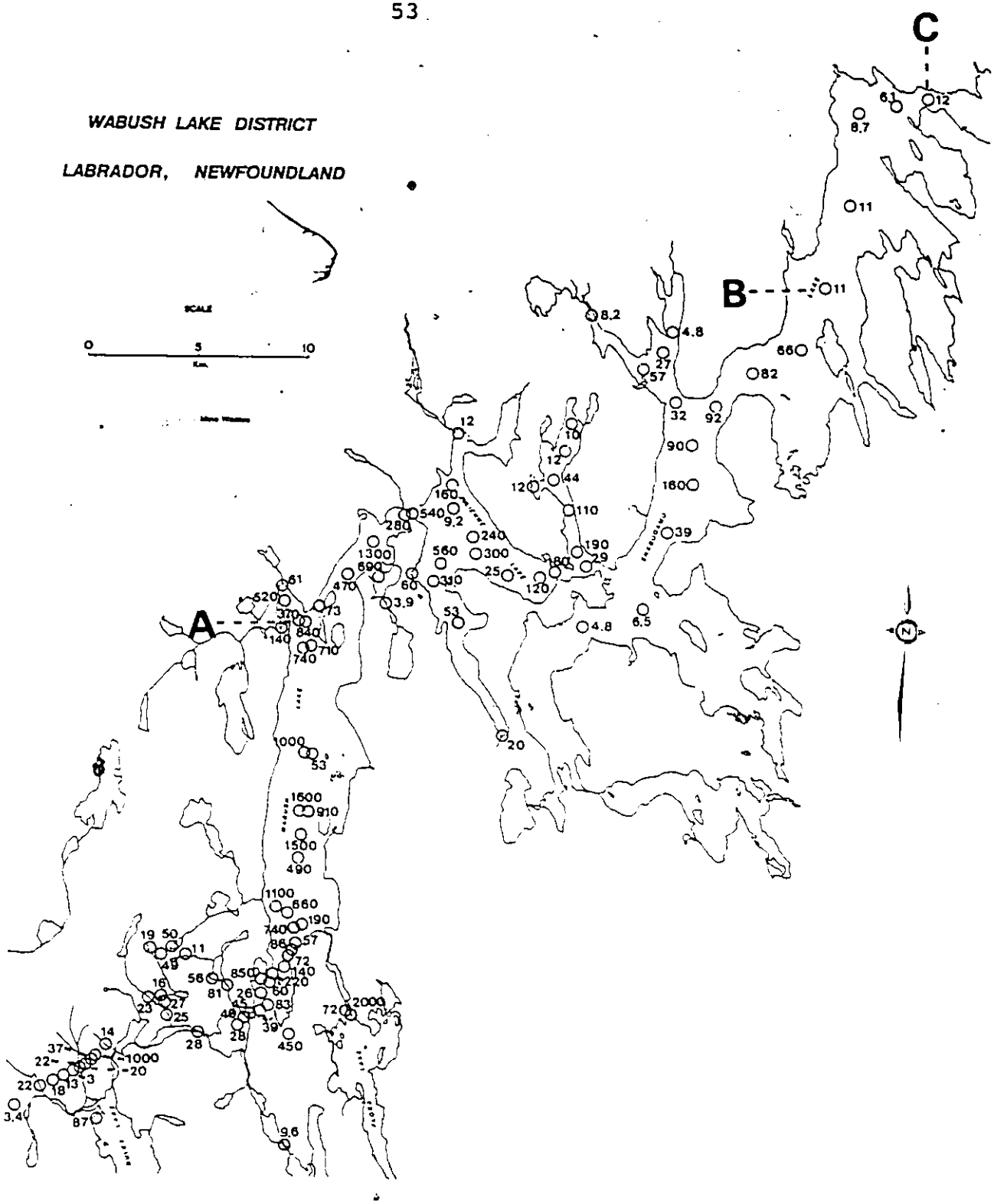

Figure 15: Fibre concentration in surface waters (fibres/ litre x ~~10⁶~~), 1977 (see Fig. 16 for significance of A, B, C)

Figure 16: Fibre concentration in water samples relative to distance from Iron Ore Company of Canada tailings deposit. Solid lines connect surface water concentrations for each sampling period. Numbers beside points on graph indicate sample depth in metres.

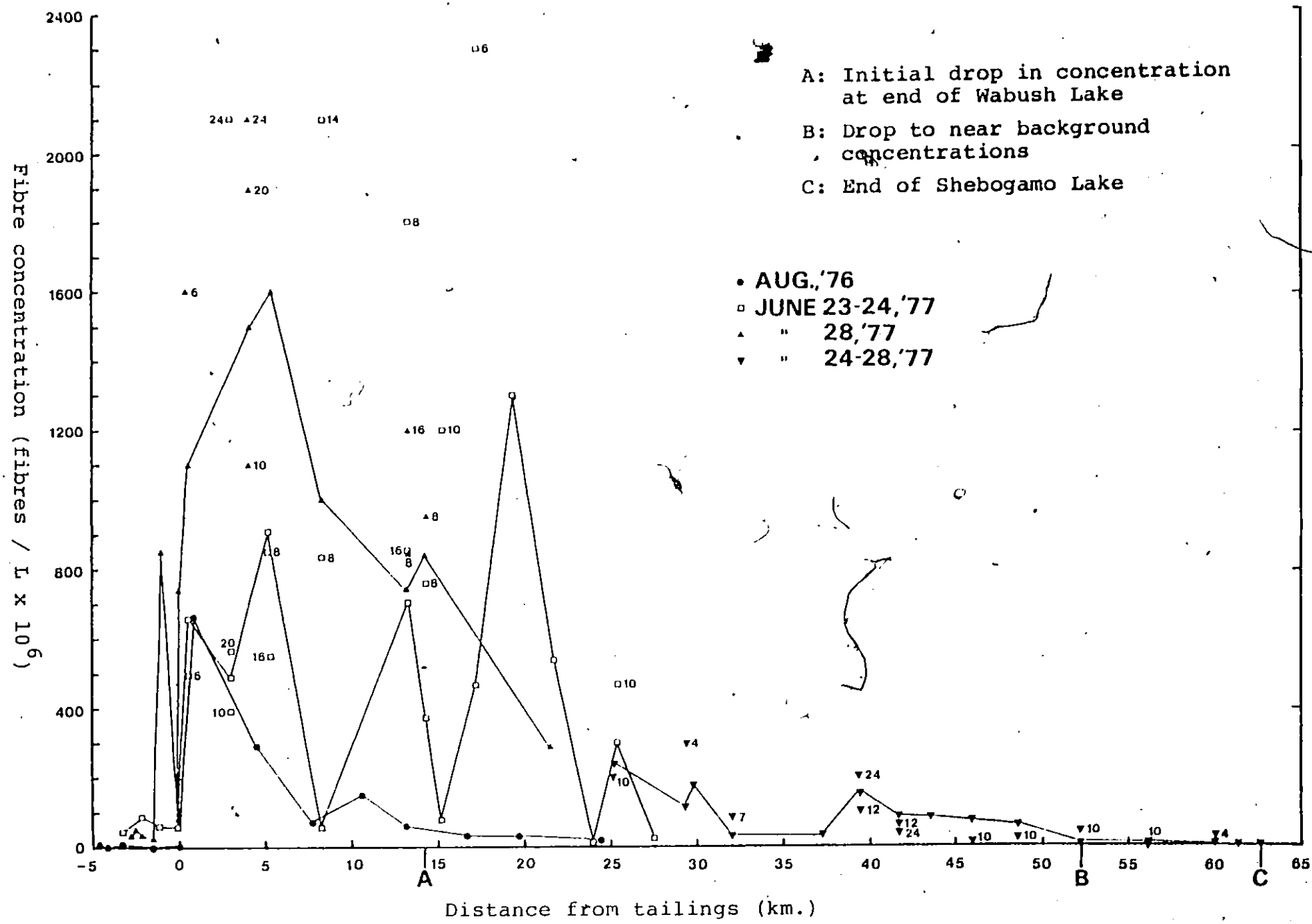
A: Initial drop in concentration at end of Wabush Lake
B: Drop to near background concentrations
C: End of Shebogamo Lake
• AUG.,'76
▫ JUNE 23-24,'77
▲ " 28,'77
▼ " 24-28,'77
Fibre concentration (fibres / L x 10^6)
Distance from tailings (km.)
A
B
C

fibres/litre) upsteam, and high (up to 2300 x 10^6 fibres/litre) just downsteam from the Iron Ore Company of Canada tailings. At point B (on Fig. 15 and 16), 52.1 km. downstream, fibre concentrations decrease to what appears to be a reasonable ambient level at around 10 x 10^6 fibres/litre.

Concentrations in samples taken at depth (shown on Fig. 16) seem to be higher in most instances than in surface waters, indicating that the fibres are settling out. Turbulence or currents in the lake waters may account for variations in this trend.

At station number 77-51, west of Labrador City, the stream water contained 1,000 x 10^6 fibres/litre, the highest concentration found outside Wabush and Flora Lakes. This sample was collected from a small stream at the north edge of the Fermont Highway near a road cut through a grunerite-actinolite rich section of the Lower Wabush Iron Formation (Fig. 32). Other stream samples from the same area had much lower concentrations (3 x 10^6 to 87 x 10^6 fibres/litre) and seem to be more representative of natural run-off from the iron formation. The channels north of Julienne and Shabogama Lakes which also drain from the iron formation had fibre concentrations between 4.8 x 10^6 and 110 x 10^6 fibres/litre. The mean fibre concentration of runoff waters from the Wabush Iron Formation is approximately 29.5 x 10^6 fibres/litre. In the active mining areas of the Iron Ore Company of Canada,

the concentrations are close to this mean runoff level, indicating that the mining of ore does not significantly change the fibre concentration in runoff waters.

Surface water samples 76-1 and 77-46 from the lake where the Labrador City drinking water intake pipe is located contained 2.1 ± 2.9 x 10^6 and 56 ± 5.7 x 10^6 fibres/litre respectively. Sample 77-61, located near the Wabush water supply contained 9.6 ± 4.4 x 10^6 fibres/litre. Samples of tap water (76-7 and 76-8) from the Sir Wilfrid Grenfell Hotel in Wabush had concentrations of 2.1 ± 2.9 x 10^6 and 5.8 ± 3.9 x 10^6 fibres/litre respectively. In June of 1977, drinking water from the Carol Lodge in Labrador City (samples CL-1 to CL-6) showed concentrations varying between 33 x 10^6 and 110 x 10^6 fibres/litre with a mean concentration of 56 x 10^6 fibres/litre.

Size Distribution of Fibres

The average aspect (length/width) ratios for fibres contained in water for those samples which were sized using the transmission electron microscope are given in Tables 3 and 4 of the Appendix. Size analysis results from surface water samples are plotted on Figure 17. There appears to be a decrease in aspect ratio of the fibres in a downstream direction from the Iron Ore Company of Canada tailings deposit due possibly to the settling out of larger, more

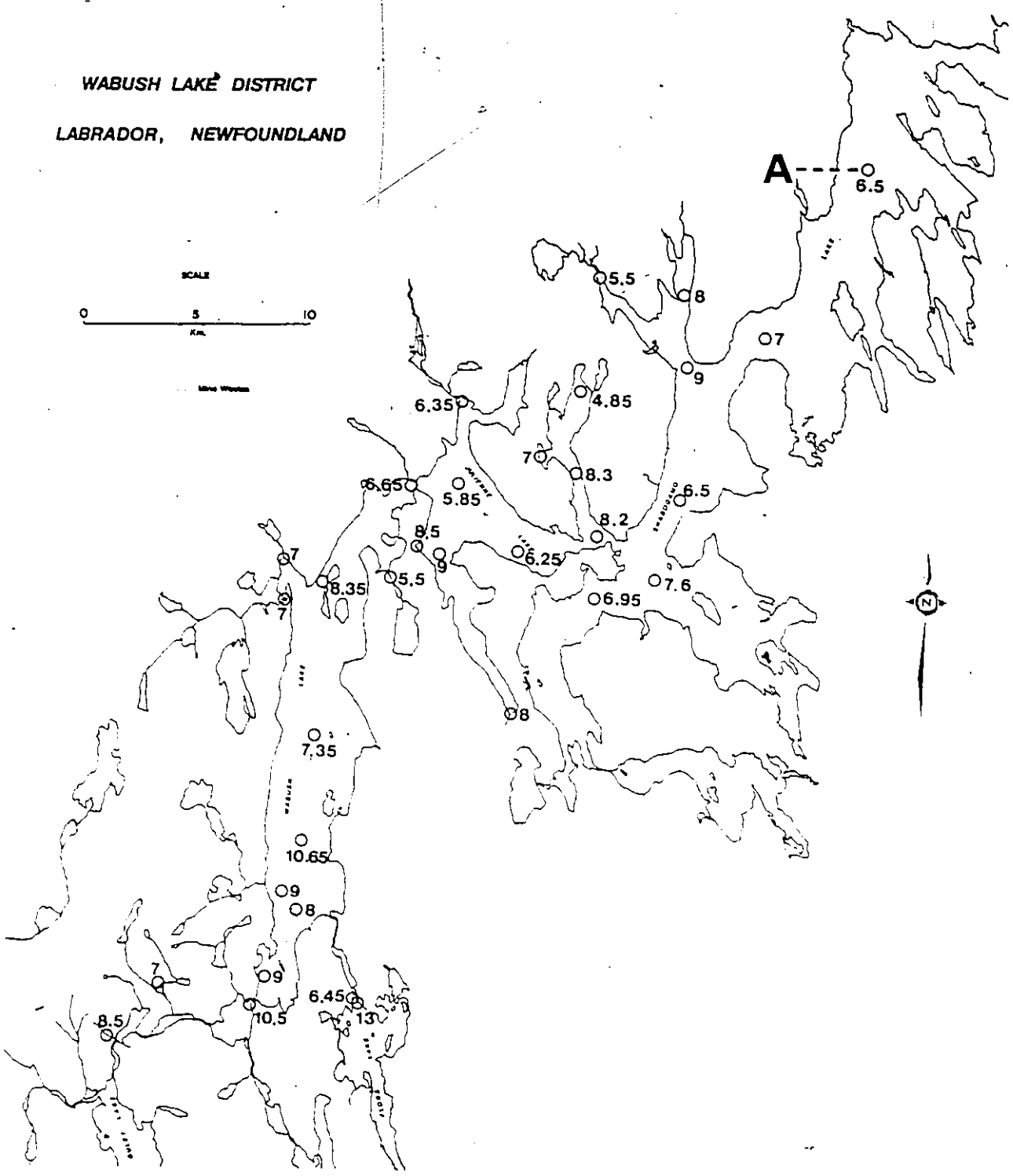

Figure 17: Average aspect ratio (length/width) of total fibres in surface waters, 1977

elongated fibres. This decrease can be better seen in Figure 18.

The average size of the fibres found in water samples was 3.5µm in length and 0.4µm in diameter with a range of 16µm to 2µm in length and 0.5µm to 0.05µm in diameter. In general, the "amphibole" fibres were more elongated than the iron and iron-manganese rich fibres.

Calculated Fibre Mass

The calculated fibre mass (calculated from size and estimated density) of fibres contained in some of the 1977 water samples are listed in the Appendix, Table 4 and plotted on the map (for surface waters only) in Figure 19. A graph of fibre mass versus distance from the Iron Ore Company of Canada tailings deposit (Fig. 20) shows a decrease in fibre mass in a downstream direction from the tailings indicative of fibres settling out of the water.

Energy Dispersive X-ray Fluorescence Spectroscopy of Fibres

Table 5 in the Appendix lists results of the energy dispersive X-ray fluorescence spectroscopy analyses of possible amphibole minerals found in selected lake and stream water samples. All analyses are of fibrous mineral fragments which had an aspect ratio of 3:1 or greater and exhibited good

Figure 18: Aspect ratio of fibres versus distance from Iron Ore Company of Canada tailings deposit. See Figure 17 for location of A.

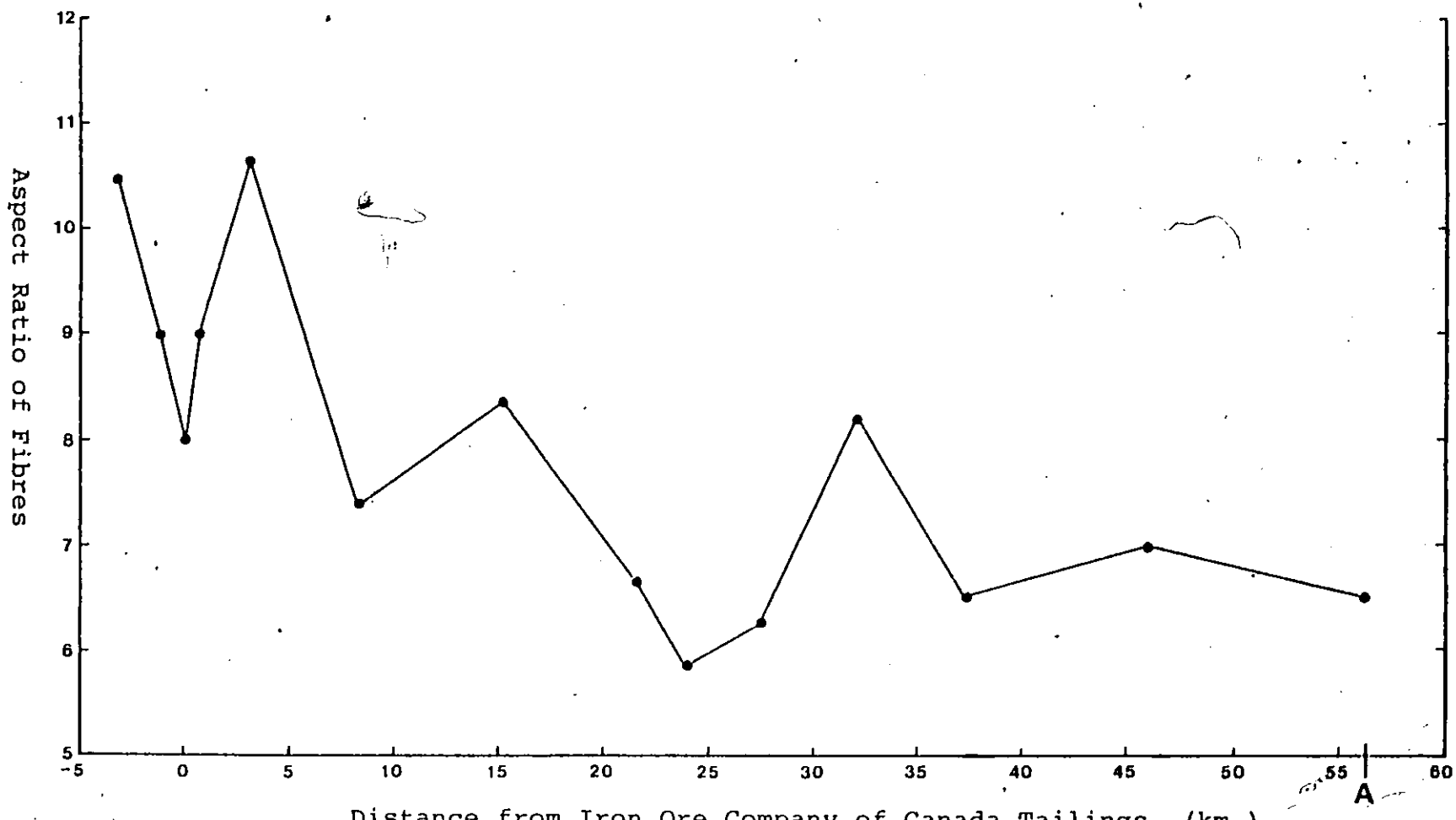
Aspect Ratio of Fibres
12
11
10
9
8
7
6
5
-5
0
5
10
15
20
25
30
35
40
45
50
55
60
A
Distance from Iron Ore Company of Canada Tailings (km.)

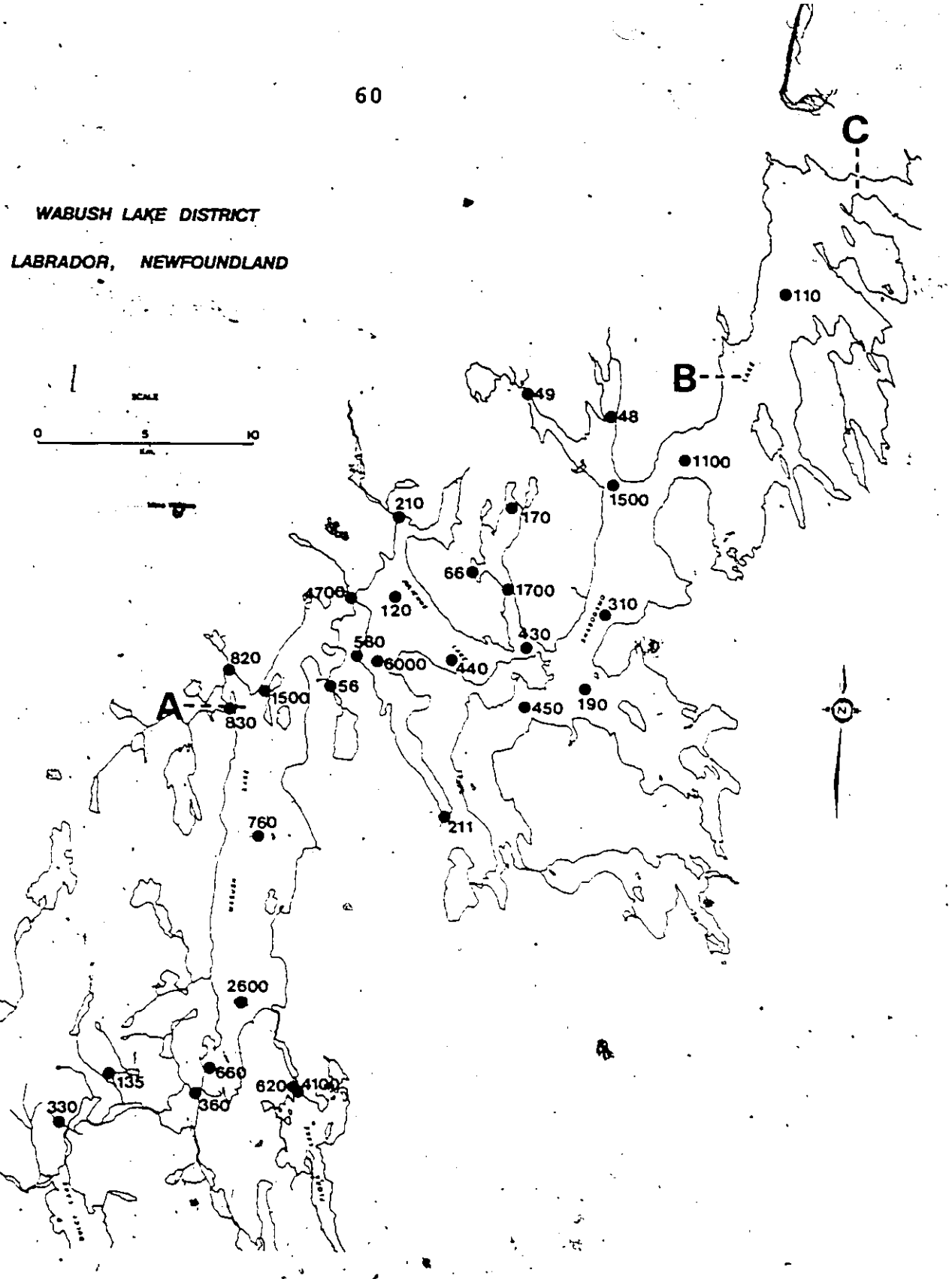

Figure 19: Fibre mass (NG/L x 10^6) in surface waters, 1977

Figure 20: Fibre mass versus distance from Iron Ore Company of Canada tailings deposit. Numbers in brackets refer to sample depth in metres. Solid line connects surface water samples. See Figure 19 for location of A, B and C.

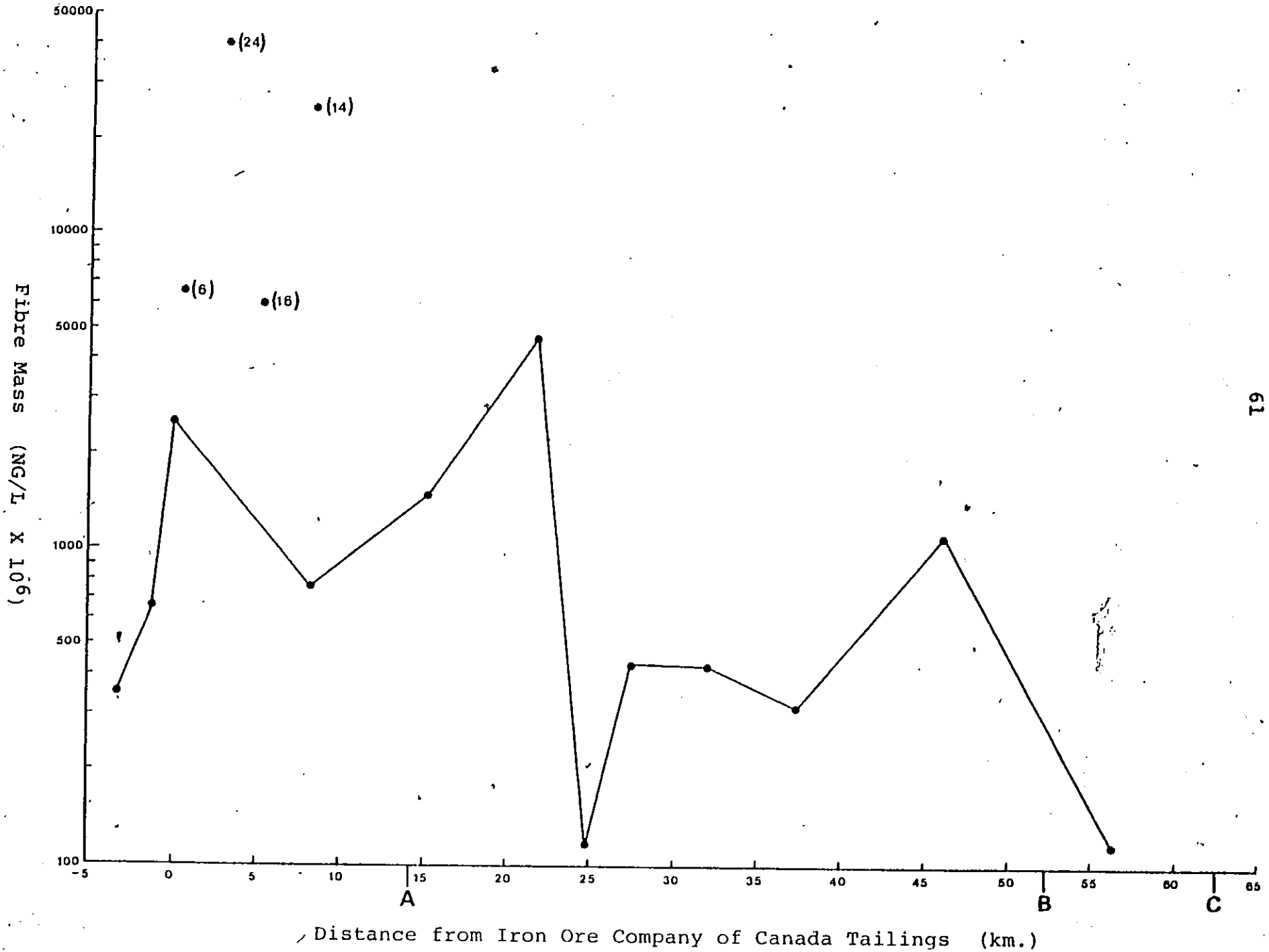
50000
10000
5000
1000
500
100
(24)
(14)
(6)
(16)
Fibre Mass (NG/L X 10⁶)
-5
0
5
10
15
20
25
30
35
40
45
50
55
60
65
A
B
C
Distance from Iron Ore Company of Canada Tailings (km.)

amphibole cleavage. A summary of these data, along with an indication of the mineralogy of other mineral particles present in the water samples, appears in Table 5. The fibres in samples CL-1 toCL-6 and other drinking waters were too small to analyze with any degree of certainty. Fibres in many other water samples collected were also too fine for analysis.

Many of the iron manganese-rich and iron-rich minerals analyzed in some water samples (Table 5) were fibrous in form. Some, which contained up to 86% MnO, had aspect ratios of 6:1 or greater and could be described morphologically as excellent fibres. No cleavages were apparent in these fibres. In general, those iron manganese-rich fibres which contained more iron, had lower aspect ratios and showed evidence of surficial weathering.

4.2 TAILINGS, SEDIMENT AND SOIL SAMPLES

X-ray Powder Diffraction

All of the sediment samples were too fine grained (silty clay to clay size particles) to separate pure mineral fractions for analysis. Several bulk samples that were run contained quartz, hematite, magnetite, and carbonates (possibly calcite, ankerite, dolomite and siderite). No amphibole peaks could be distinguished on the traces.

The magnetic separate which constituted approximately

TABLE 5: POSSIBLE MINERAL PARTICLES PRESENT IN WATER SAMPLES AS DETERMINED BY ENERGY DISPERSIVE X-RAY FLUORESCENCE SPECTROSCOPY (see Table 2A for amphibole compositions)

Sample	Cummingtonite	Mn-Cummingtonite	Grunerite	Anthophyllite	Actinolite	Riebeckite	Hornblende	Quartz	Iron Rich** Minerals	Iron Manganese rich Minerals
77-12	x	x	x	x				x	x	x
77133B		x		x				x	x	x
77-14B			x	x			x	x	x	
77-15C			x	x				x	x	
77-19			x					x		
77-20										x
77-30					x			x	x	x
77-31B						x			x	
77-32									x	x
77-33	x								x	
77-38			x	x				x	x	x
77-39									x	x
77-63									x	x
77-73A	x								x	
77-96									x	
77-98B			x						x	
77-104D				x					x	x
77-105D			x	x					x	x
77-108								x	x	x
77-112									x	x
77-113									x	x

x indicates mineral present

**(hematite, magnetite, goethite, siderite, etc)

4.5 weight per cent of the Iron Ore Company of Canada tailings was identified by X-ray powder diffraction as magnetite and hematite. Approximately 91.5 per cent of the remaining material was identified as quartz using a petrographic microscope to determine the refractive indices, and by X-ray powder diffraction. The carbonates could not be identified positively by X-ray methods.

X-ray Fluorescence Spectroscopy

Results of the X-ray fluorescence analysis of sediments, soils, and the Iron Ore Company of Canada tailings appear in the Appendix, Table 6. All analyses are normalized to 100 weight per cent. Oxide concentrations of top sediments from the lakes, stream sediments, and soil samples are plotted on Figures 21 to 30. Concentrations of three oxides (SiO_2, Al_2O_3 and FeO) in the top sediments of the lakes are plotted against distance downstream from the Iron Ore Company of Canada tailings deposit in Figure 31.

SiO_2 and FeO show opposing trends, with SiO_2 decreasing rapidly in a downstream direction from the tailings, then slowly increasing to the end of the Shabogamo Lake at point B, Figure 21. FeO increases rapidly away from the tailings, then decreases rapidly at the end of Wabush Lake (Fig. 23). It appears that most of the iron rich minerals (which have a higher specific gravity) settle out of the water before they

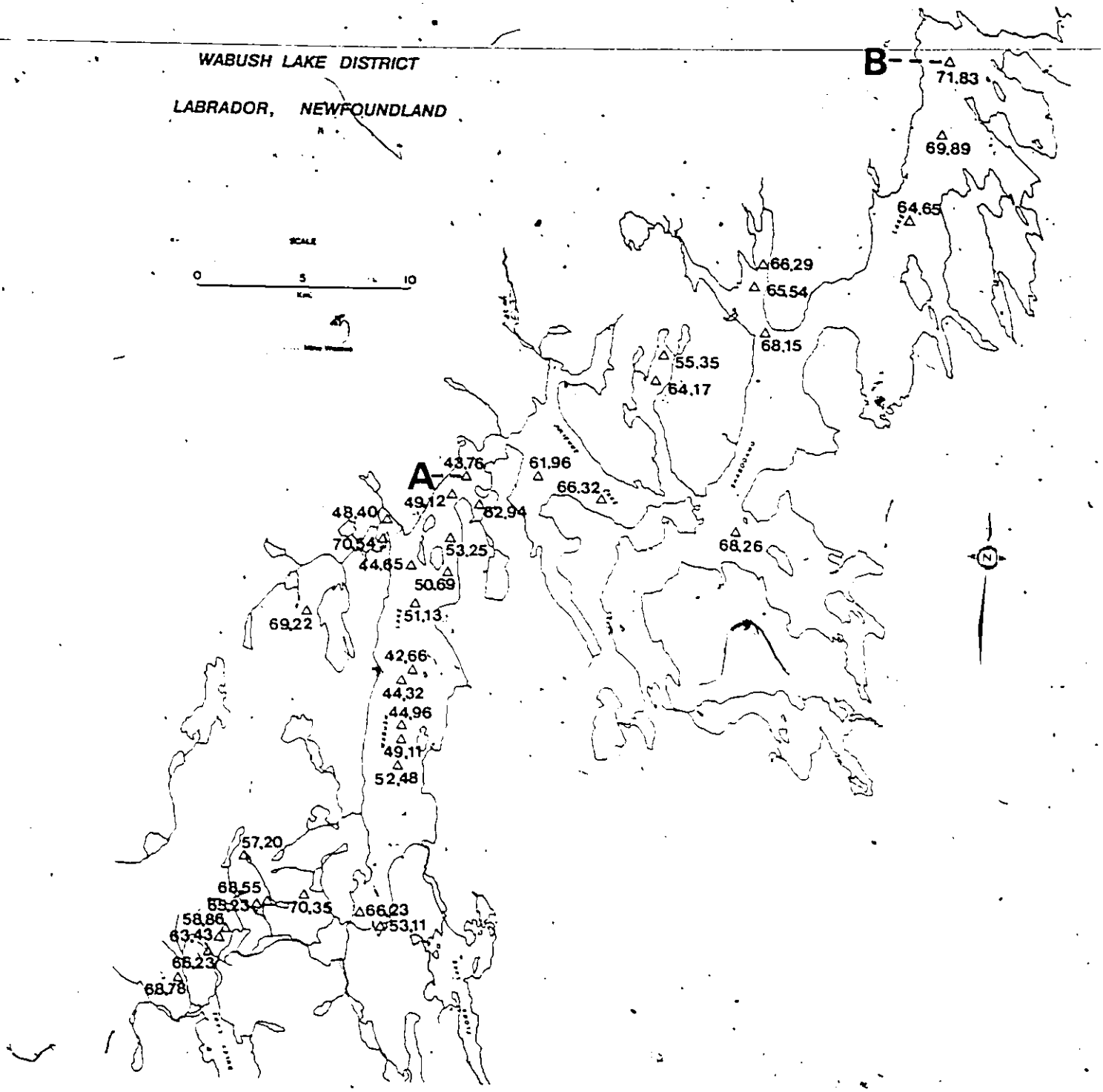

Figure 21: SiO_2 content (wt. %) of sediments and soils
I.O.C.C. tailings = 65.90

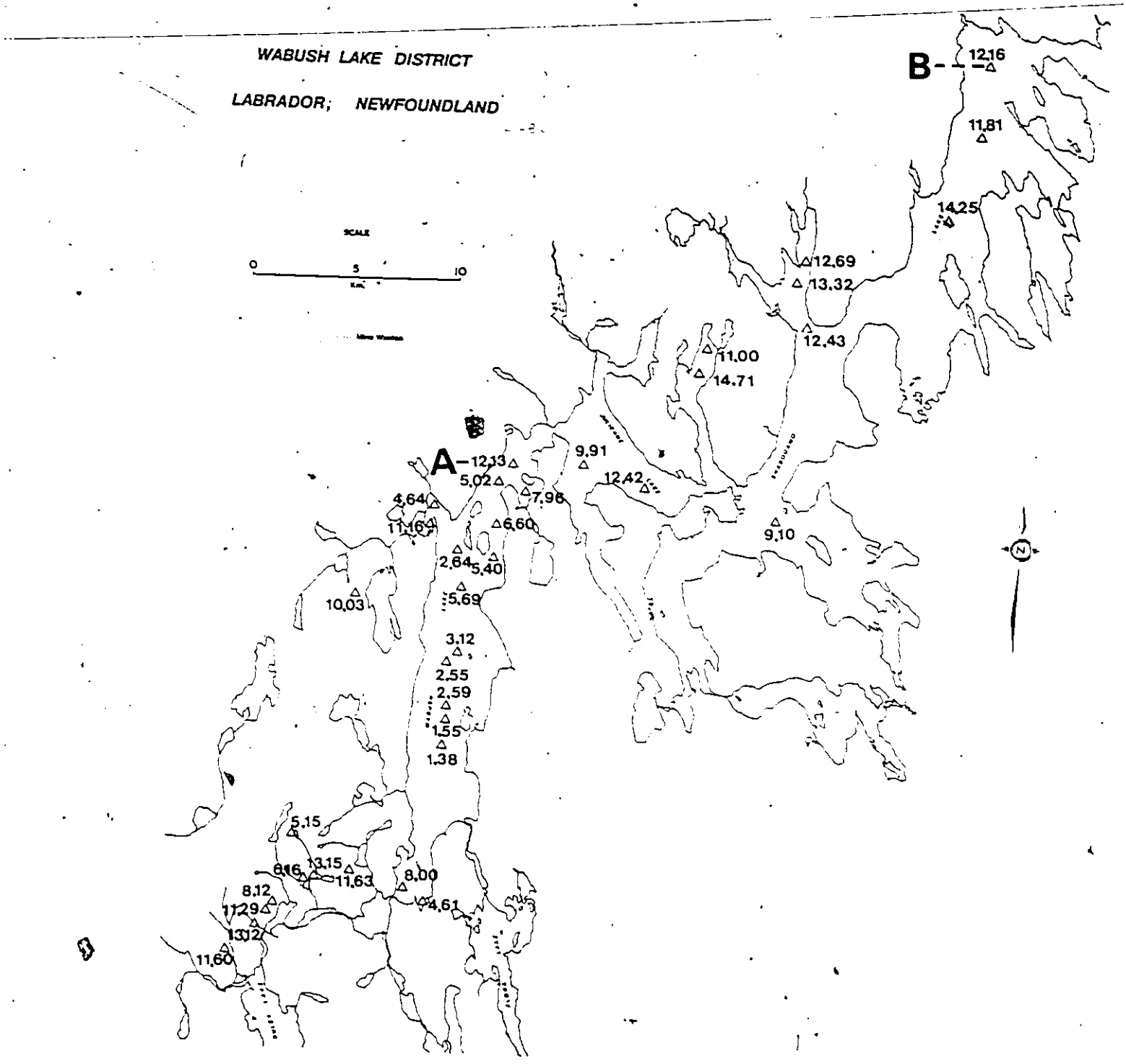

Figure 22: Al_2O_3 content (wt. %) of sediments and soils
I.O.C.C. tailings - 0.25

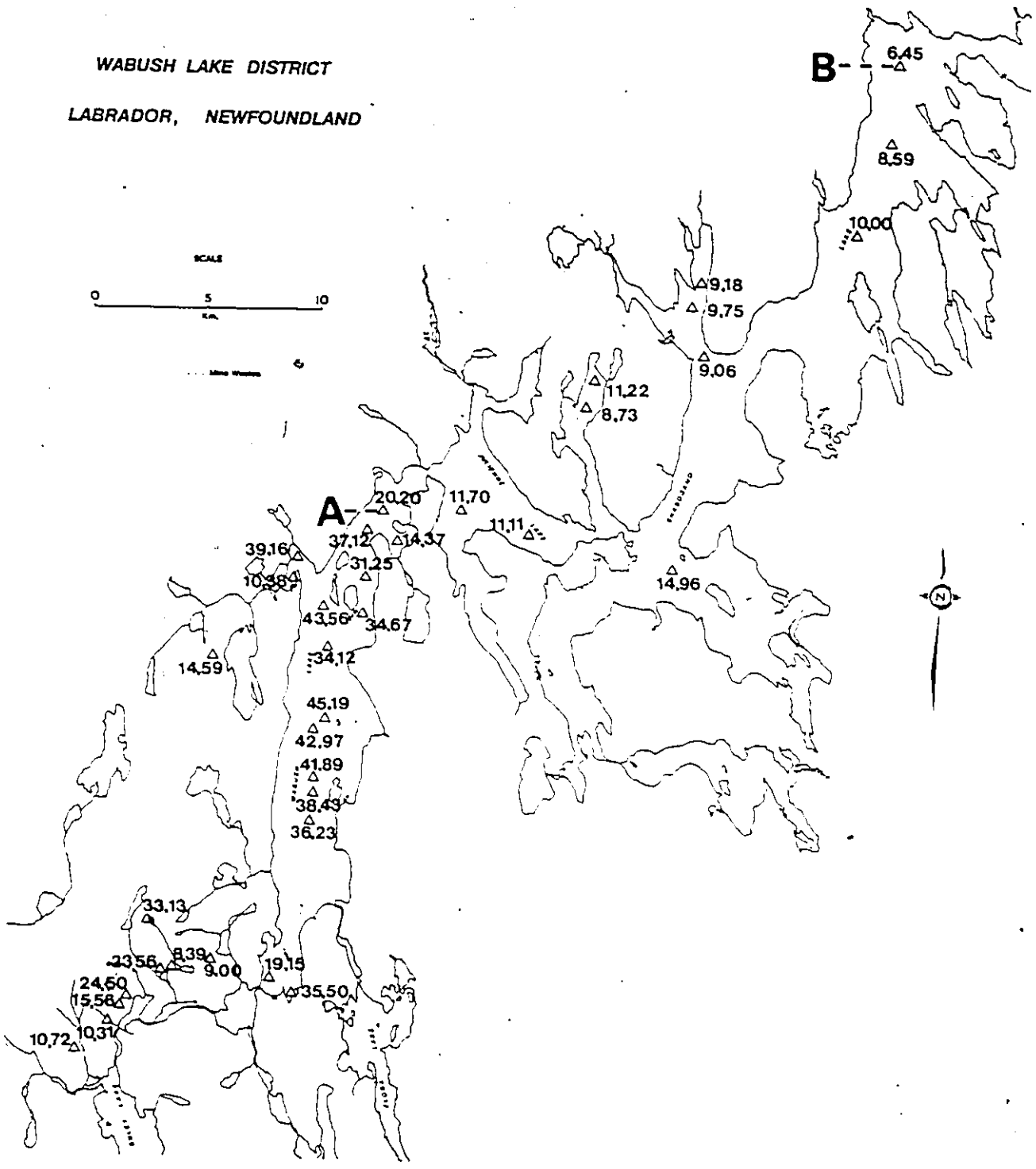

Figure 23: FeO content (wt. %) of sediments and soils
I.O.C.C. tailings = 29.94

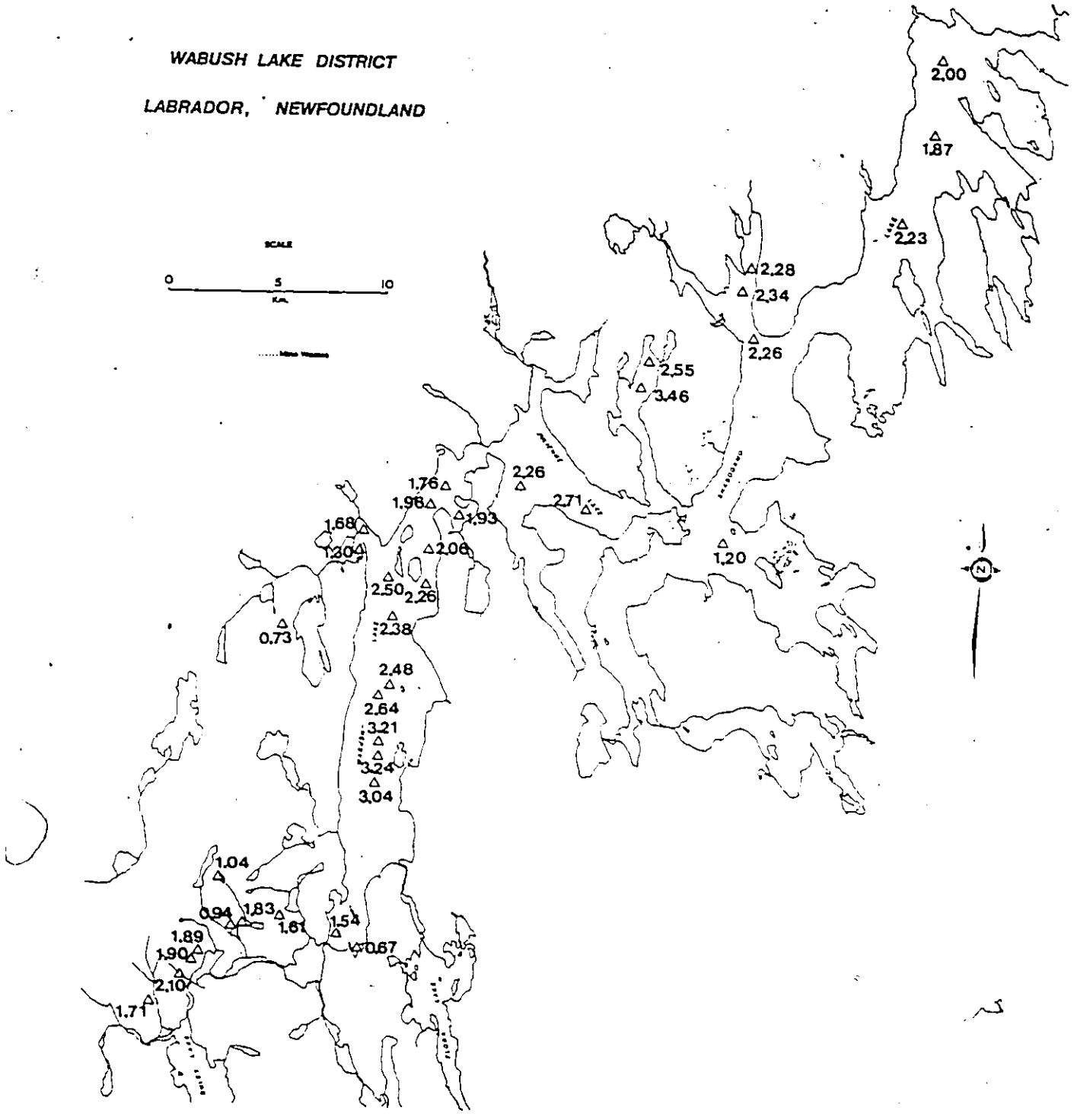

Figure 24: MgO content (wt. %) of sediments and soils
I.O.C.C. tailings = 1.17

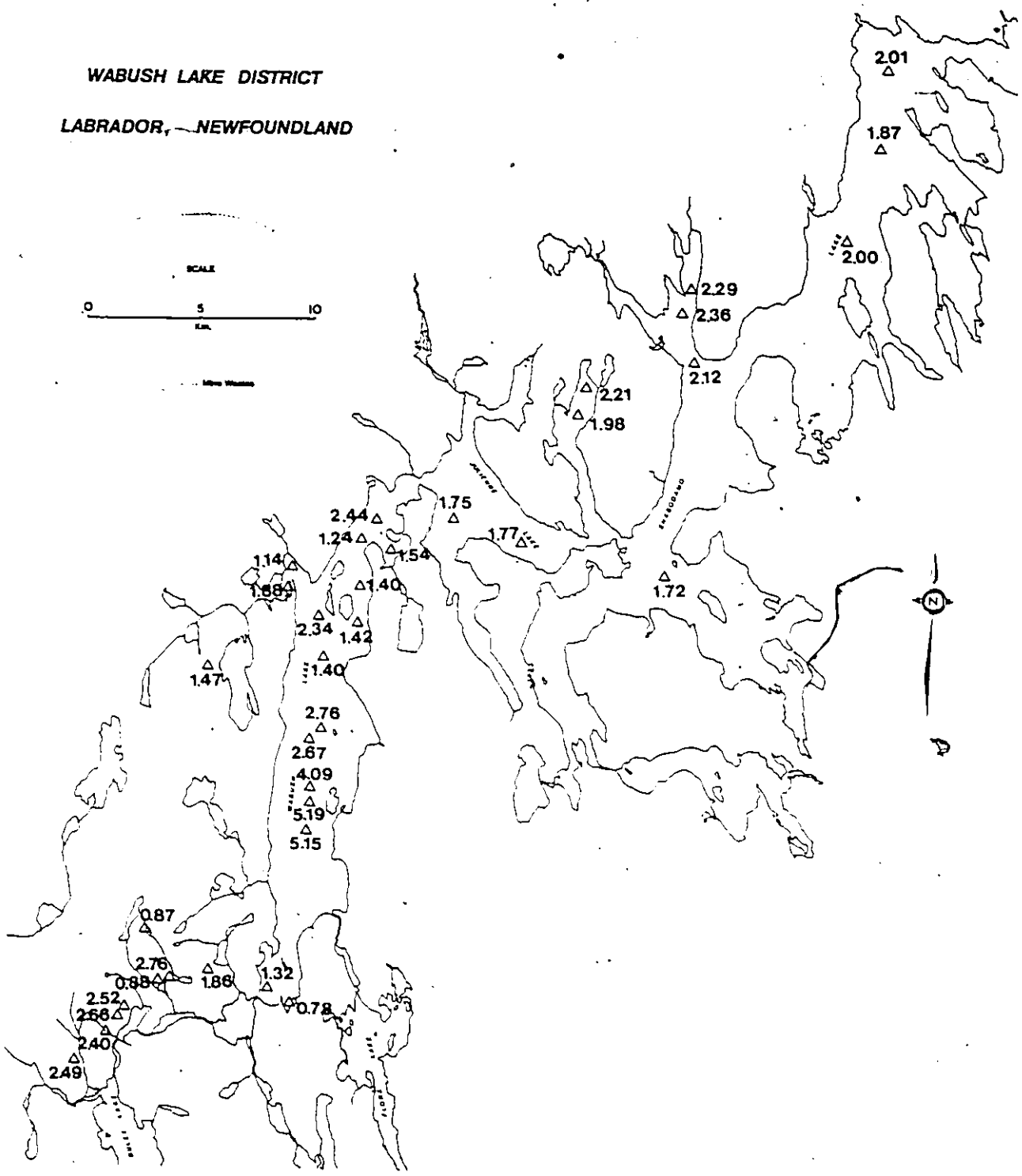

Figure 25: CaO content (wt. %) of sediments and soils
I.O.C.C. tailings = 1.93

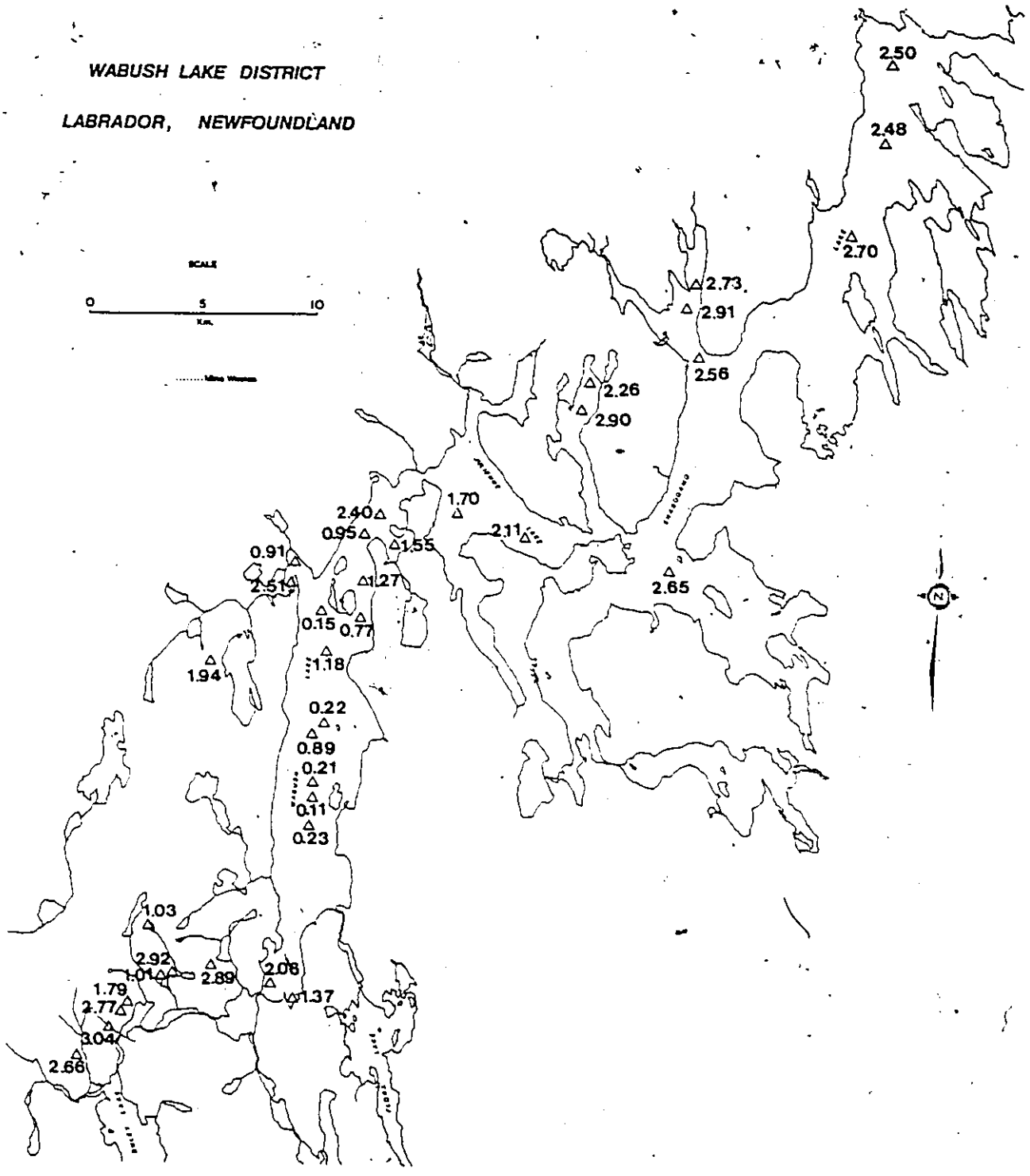

Figure 26: Na_2O content (wt. %) of sediments and soils
I.O.C.C. tailings = 0.27

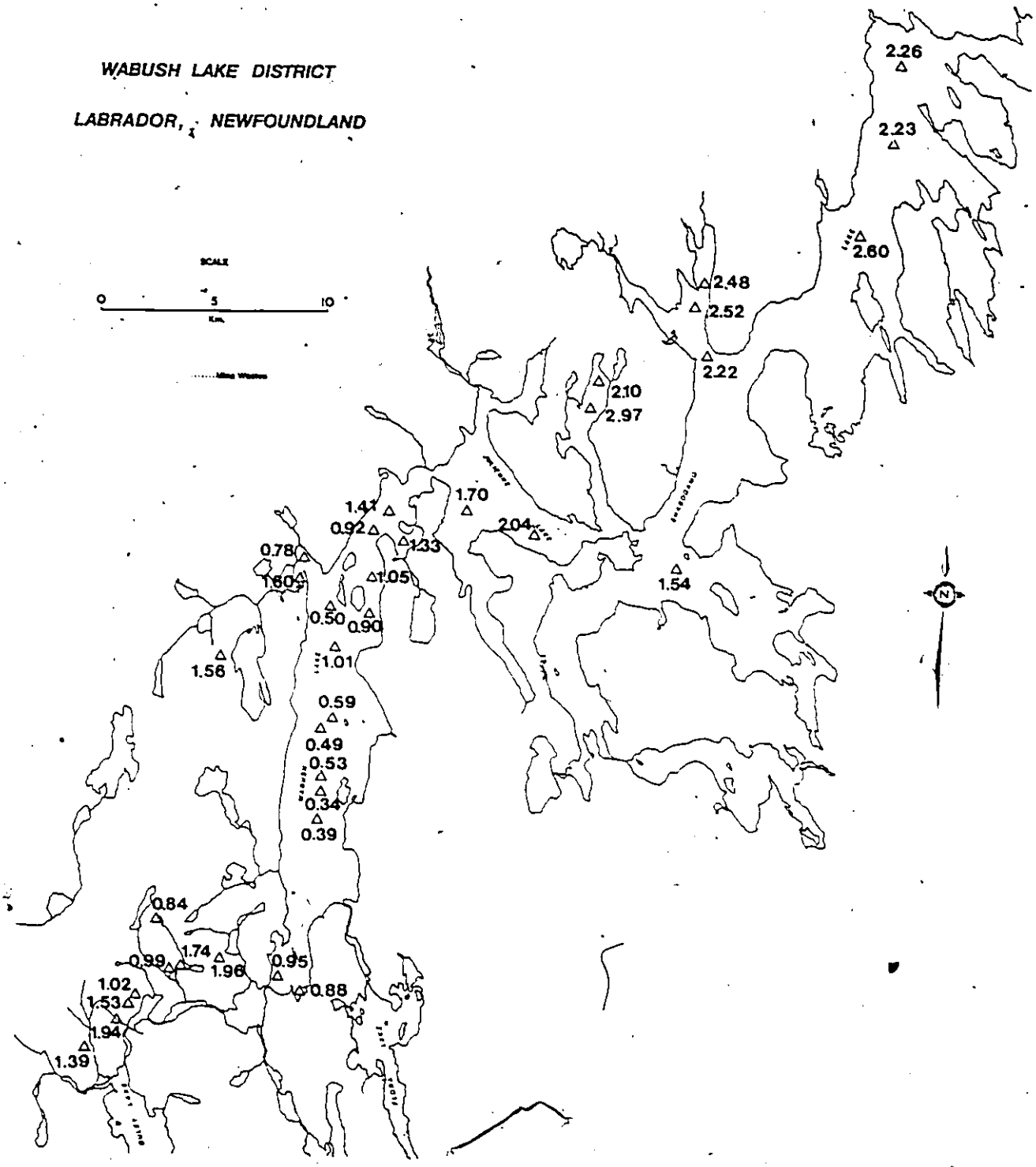

Figure 27: K_2O content (wt. %) of sediments and soils
I.O.C.C. tailings = 0.19

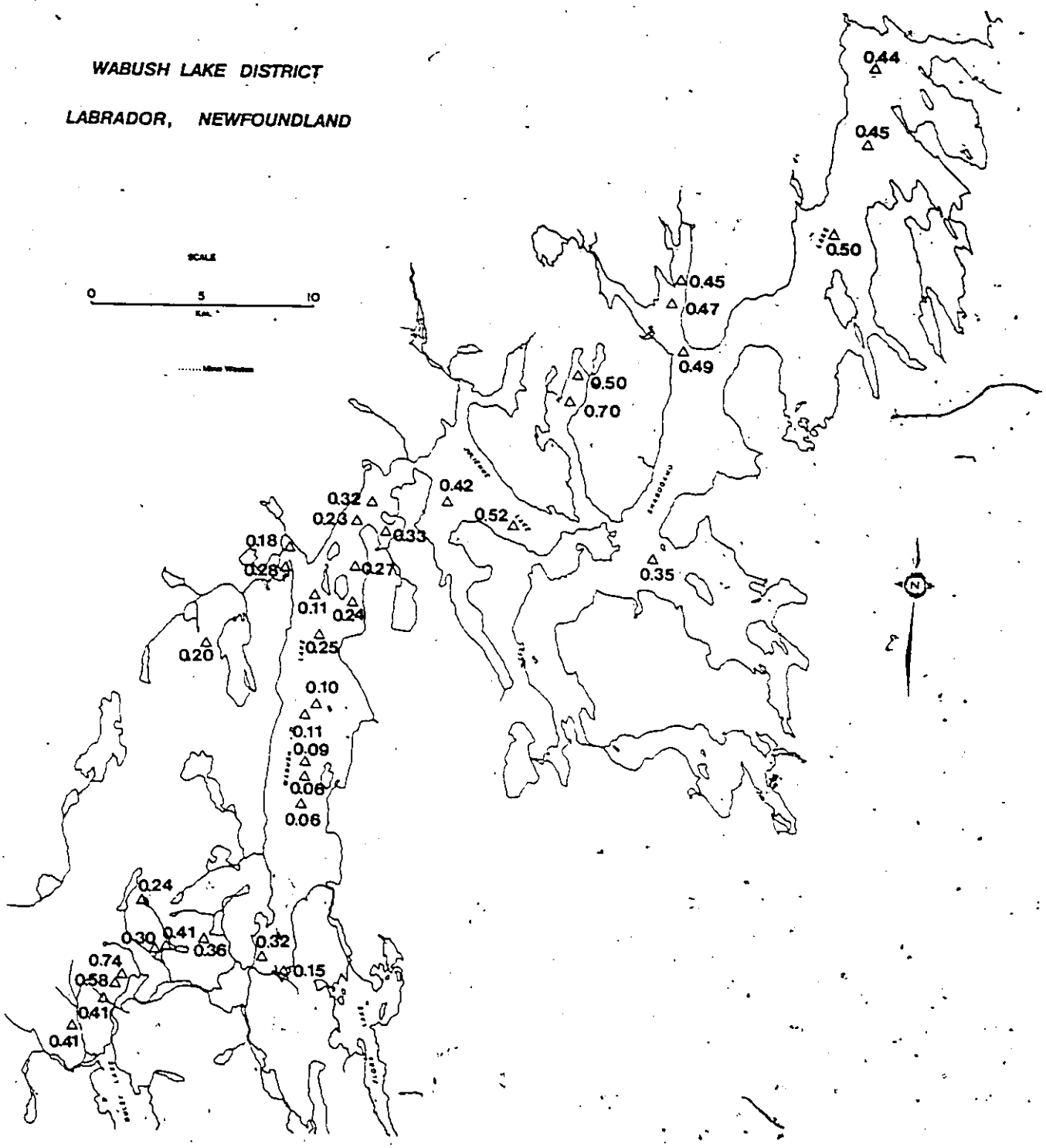

Figure 28: TiO_2 content (wt. %) of sediments and soils
I.O.C.C. tailings = 0.03

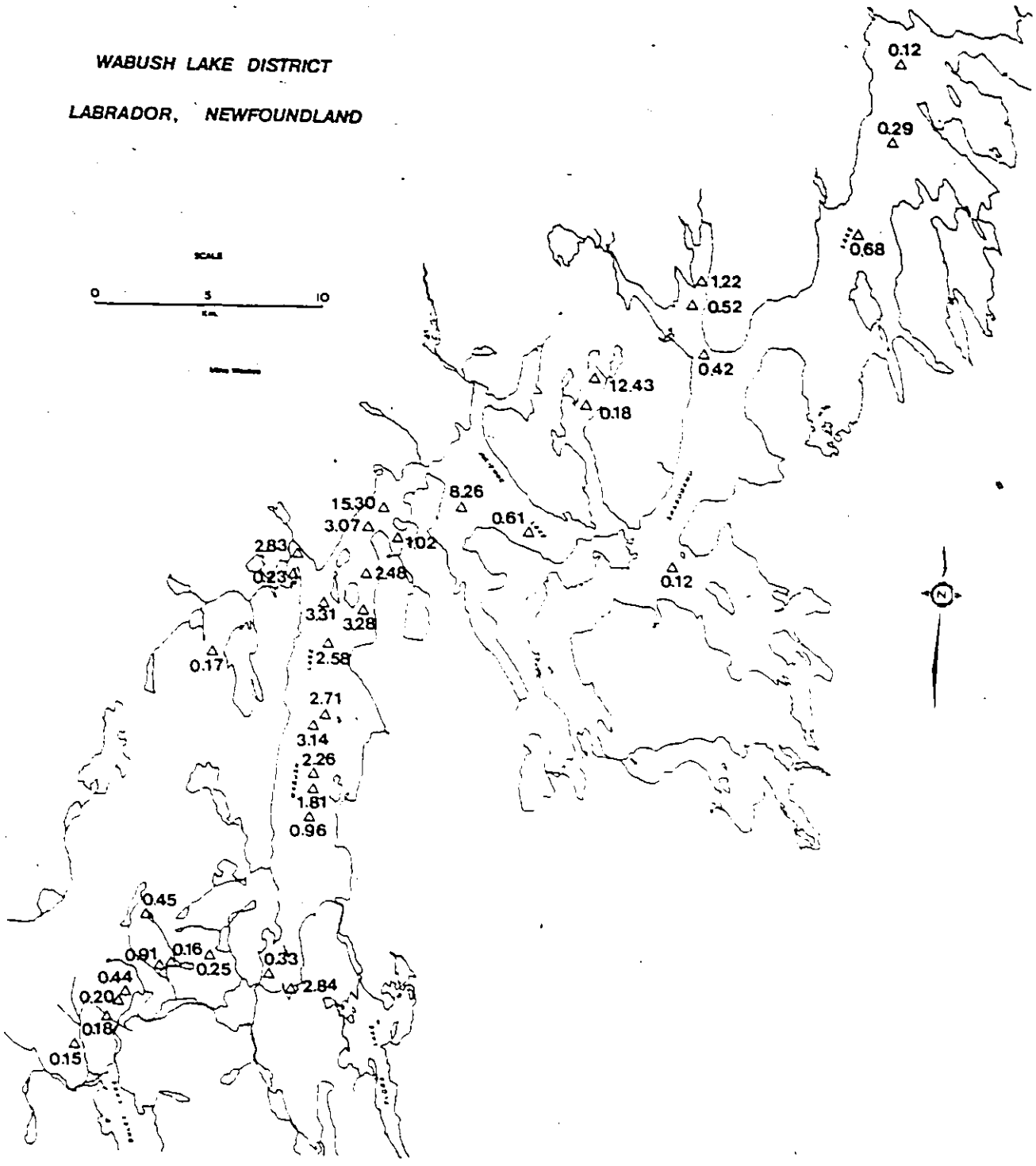

Figure 29: MnO content (wt. %) of sediments and soils
I.O.C.C. tailings = 0.29

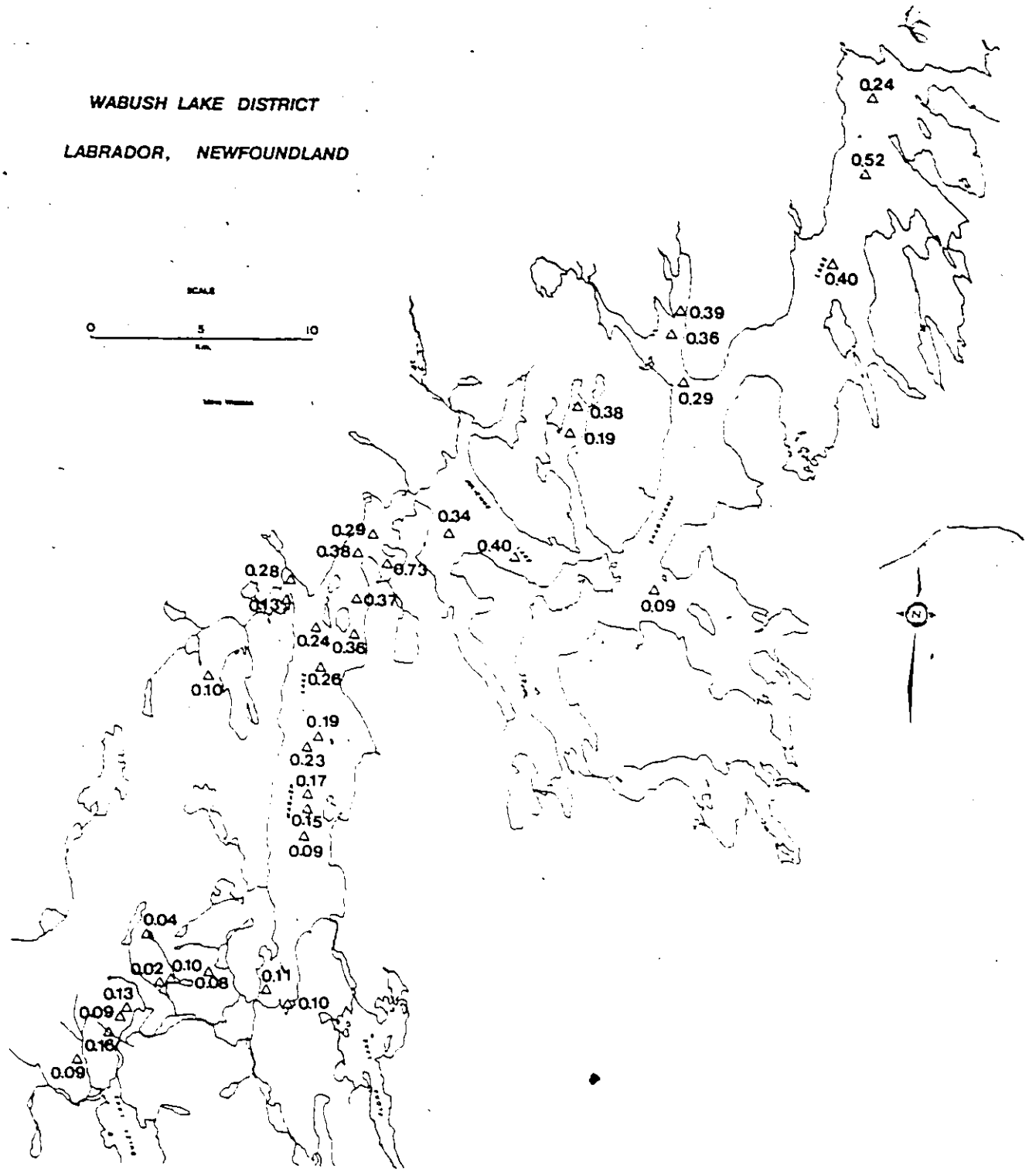

Figure 30: P_2O_5 content (wt. %) of sediments and soils
I.O.C.C. tailings = 0.05

Figure 31: Oxide concentration in top sediments versus distance down-stream from Iron Ore Company of Canada tailings deposit. See Figures 21 to 23 for location of A and B.

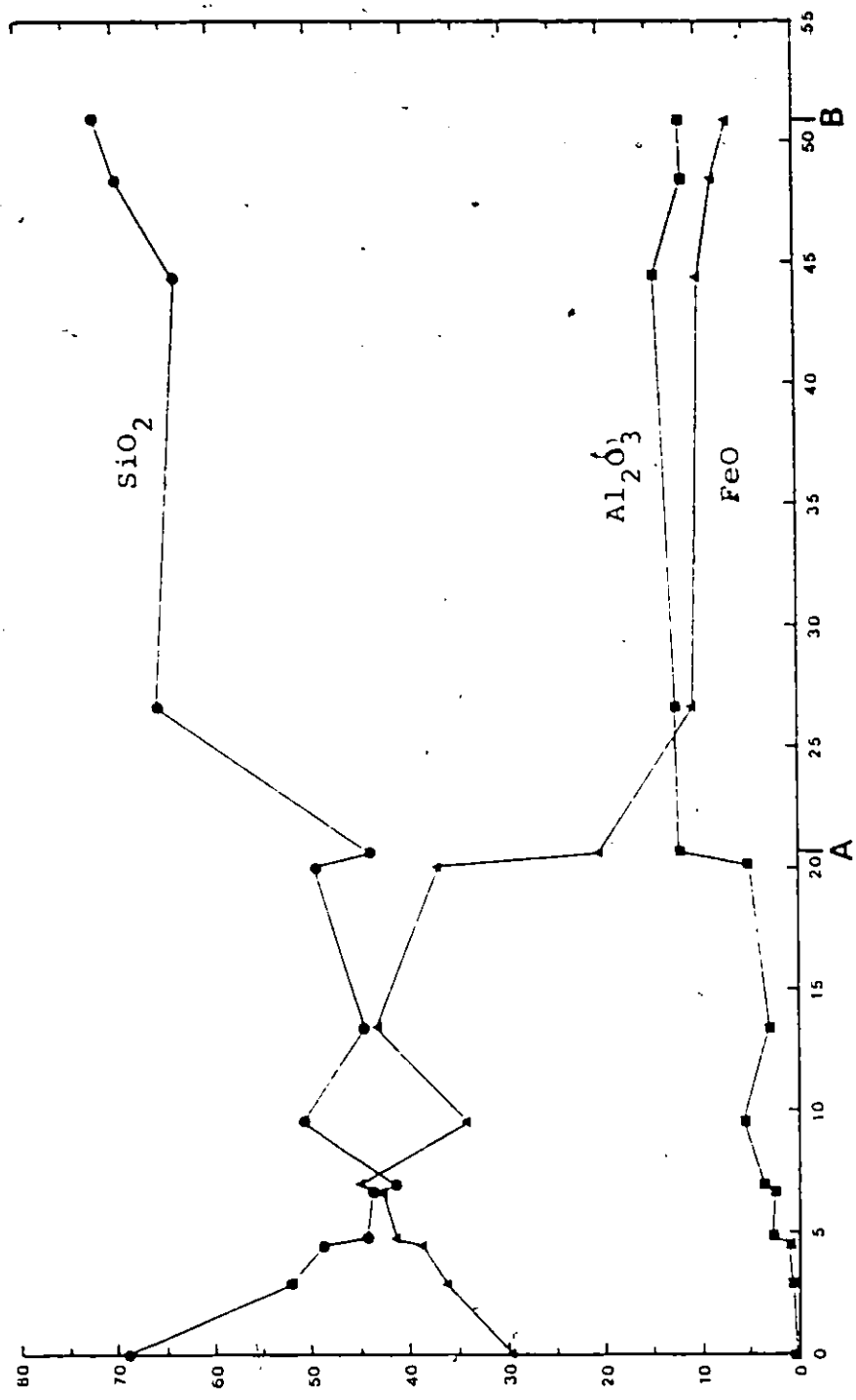
SiO_2
Al_2O_3
FeO
A
B
Weight % Oxide
Distance Downstream from Iron Ore Company of Canada Tailings (km.)

reach the end of Wabush Lake (Point A). Al_2O_3, which has a low concentration in the tailings, increases steadily downstream.

Concentrations of MgO, MnO and CaO in the top sediments parallel the variations in FeO content as one would expect since the Iron Ore Company of Canada tailings contain iron rich carbonates and iron-manganese-rich particles. The Na_2O, K_2O, TiO_2 and P_2O_5 content all increase steadily downstream from the tailings.

Table 6 compares the X-ray fluorescence analysis of the Iron Ore Company of Canada tailings to the average oxide concentrations found in lake and stream sediments and soils of areas surrounding Wabush and Shabogamo Lakes. These average concentrations represent the probable composition of sediments deposited as a result of natural weathering processes acting on rocks in the Wabush Iron Ore District. Some of the layered lake sediments that were analyzed approach this average composition in one or more layers. These layers were probably deposited prior to the opening of the iron ore processing plants in the Wabush Lake area.

Several lake sediment samples have anomalously high manganese contents (up to 24% MnO). Manganite (MnO.OH) was identified in these samples by X-ray powder diffraction using a Gandolfi camera. The manganite probably represents the alteration product of rhodochrosite ($MnCO_3$), rhodonite

TABLE 6: Comparison of oxide content of Iron Ore Company of Canada tailings to probable oxide content of sediments and soils produced by natural weathering processes. (All analyses by X-ray fluorescence spectroscopy, normalized to 100 weight per cent)

	Iron Ore Company of Canada tailings	Probable sediment and soil analysis as a result of natural weathering processes
SiO_2	65.90	64.74
Al_2O_3	0.25	10.40
FeO	29.94	15.43
MgO	1.17	1.74
CaO	1.93	1.92
Na_2O	0.27	2.33
K_2O	0.19	1.68
TiO_2	0.03	0.41
MnO	0.29	0.52
P_2O_5	0.05	0.16

($(Mn, Ca, Fe)SiO_3$), or other manganese rich minerals which are found in the Wabush Iron Formation.

Energy Dispersive X-ray Fluorescence Spectroscopy

Table 7 in the Appendix lists chemical analyses of mineral particles which appear to be amphiboles found in the sediments and soils, as determined by energy dispersive X-ray fluorescence spectroscopy. A summary of this information, along with other possible minerals present, is given in Table 7. Amphibole grains only were analyzed in the soil samples, numbers 47 to 58.

The top sediments in Wabush Lake contained up to 50% iron-rich and iron manganese-rich particles. Energy dispersive X-ray fluorescence spectroscopy analyses of some of these are given in Table 8. The majority of these mineral particles, some of which contained >85% MnO, are believed to be manganite, rhodochrosite, or rhodonite.

Table 9 lists the reasonably identifiable minerals found in the Iron Ore Company of Canada tailings. The major minerals present, reflect reasonably well, the minerals found in the top sediments of Wabush Lake. Anthophyllite, which is a common amphibole in the Middle Wabush Iron Formation (the ore body) is found in the tailings and in fairly high proportions in some of the Wabush Lake sediments.

TABLE 7: POSSIBLE MINERALS PRESENT IN SEDIMENTS AND SOILS AS DETERMINED BY ENERGY DISPERSIVE X-RAY FLUORESCENCE SPECTROSCOPY (see Table 2A for amphibole compositions)

Sample	Cummingtonite	Mn-Cummingtonite	Grunerite	Anthophyllite	Tremolite-Actinolite	Gedrite	Riebeckite	Hornblende	Quartz	Iron rich minerals**	Iron Manganese rich minerals	Almadine garnet	Ankerite
1-Top			x			x			x	x	x		
1-Bottom		x		x		x			x	x	x	x	
3	x		x	x		x			x	x	x		x
4	x		x	x		x			x	x	x		
5						x			x	x	x		
9-Bottom			x			x			x	x	x	x	
11	x		x			x			x	x	x	x	
14-Bottom			x			x			x	x	x		
16						x			x	x	x		
20-Bottom	x		x			x			x		x		
31-Top	x		x	x	x	x			x	x	x		
31-Bottom						x			x	x	x		
33-Top			x	x					x	x	x		x
33-Middle				x		x			x	x	x		
33-Bottom			x	x		x		x	x	x	x		
34			x	x					x	x	x		x
35			x	x			x		x	x	x	x	x
38-Top	x		x	x			x		x	x	x		
38-Bottom					x	x			x	x	x		
39-Bottom			x	x		x			x	x	x		
42			x	x				x	x	x	x		x
44	x		x	x									
47	x		x				x						
48			x										
49		x	x										
50			x		x								
51	x		x	x	x								
52			x		x			x					
53			x		x								
54			x										
55			x		x								
56	x												
57			x										
58			x										

x indicates mineral present **(hematite, magnetite, goethite, siderite, etc).

TABLE 8: Energy Dispersive X-ray fluorescence spectroscopy analyses of iron-manganese rich and iron-manganese-silica rich mineral grains in lake top sediments.

SiO_2	Al_2O_3	FeO	MgO	CaO	Na_2O	K_2O	TiO_2	MnO	P_2O_5	S	Cl	Cr_2O_3
4.83	3.29	83.44	0	0.26	0	0	0.22	7.03	0	0.35	0.10	0.49
8.61	4.19	73.50	0	1.56	0	0.34	0.03	10.47	0	0.17	0.61	0.52
1.24	0.07	67.30	0.19	0.14	0	0	0.18	30.61	0.17	0	0	0.11
5.44	8.61	59.19	0	0.24	0	0.65	0	25.53	0	0.05	0	0.29
25.08	11.31	19.54	2.25	1.07	0	3.97	0.27	36.21	0.02	0.19	0	0.10
24.02	10.82	24.81	3.39	0.94	0	3.47	0.89	31.04	0	0.16	0.21	0.25
7.70	0.99	68.28	0	1.16	0	0.34	0	21.06	0	0.20	0	0.25
10.24	1.68	67.85	0	1.06	0	0	0	19.17	0	0	0	0
8.92	1.06	68.83	0	0.76	0	0	0	19.45	0.32	0	0	0.64
18.69	1.52	21.99	1.05	2.33	0	0.24	0	54.18	0	0	0	0
13.18	2.03	69.55	0.23	2.24	0	0.17	0.11	11.67	0.28	0	0	0.53
13.66	1.76	69.38	0.24	0.11	0	0	0	14.85	0	0	0	0
7.84	3.76	34.02	0.41	0.24	0	0.45	0	53.00	0	0.03	0.23	0
3.28	0.16	45.34	16.97	0.48	0.06	0.05	0	33.12	0	0.03	0.16	0.34
6.23	0.52	80.58	0	0.04	0	0	0	12.17	0	0	0.33	0.13
6.81	0.35	36.92	0	0.90	0	0.57	0	54.30	0.09	0	0	0.07
5.23	0	60.41	11.65	0.84	0.28	0.09	0	20.36	0.25	0.01	0.07	0.81
10.03	0.93	51.14	2.26	0.93	0	0.49	0	33.22	0	0.08	0.17	0.76
4.81	4.46	59.02	0.04	0.55	0	0.03	0.09	30.04	0	0.51	0.19	0.27
3.27	0.22	13.99	0.54	0.31	0	0	0.01	81.18	0	0	0	0.48

TABLE 9: Probable mineralogy of Iron Ore Company of Canada tailings as determined by energy dispersive X-ray fluorescence spectroscopy.

MAJOR MINERALS	- quartz
	- ankerite
	- iron rich minerals such as hematite, goethite, siderite and magnetite
	- iron-manganese and iron-manganese-silica rich minerals
MINOR MINERALS	- grunerite
	- anthophyllite
	- actinolite
	- hornblende
	- biotite
	- muscovite
	- chlorite
	- almandine

(see Table 2A for amphibole compositions)

Sediments and soils from areas outside of Wabush Lake apparently contain no anthophyllite.

4.3 AMPHIBOLES AND RELATED MINERALS CONTAINED IN ROCK SPECIMENS

Description of the rock and mineral samples collected in the Wabush Lake Iron Ore District are given in Table 2 of the Appendix. For most samples, the description and modal analyses are a combination of hand specimen and thin section observations. Some specimens, for which no description appears, were not used in this study.

Figure 32 shows an outcrop of the Lower Wabush Iron Formation near the entrance to the Labrador City dump on the north side of the Fermont Highway. Samples L-22, L-23 and L-51 were collected here. The main rock type found was a quartz-grunerite-actinolite schist with bands of medium brown coarse grained elongated grunerite alternating with dark green coarse grained actinolite. Figure 33 is a photomicrograph of L-22B showing elongated grunerite crystals in a grunerite rich layer.

Figure 34 is a close-up photograph of an outcrop of quartz-carbonate-grunerite schist located in the Lower Wabush Iron Formation near Lorraine Lake. Most of the grunerite in this outcrop, from which sample L-4 was collected, is fibrous in form. Figure 35 is a photograph of an outcrop (sample

Figure 32: Outcrop of Lower Wabush Iron Formation near entrance to Labrador City dump (sample site of L-22, L-23 and L-51)

Figure 33: Photomicrograph of elongated, twinned grunerite crystals in sample L-22B

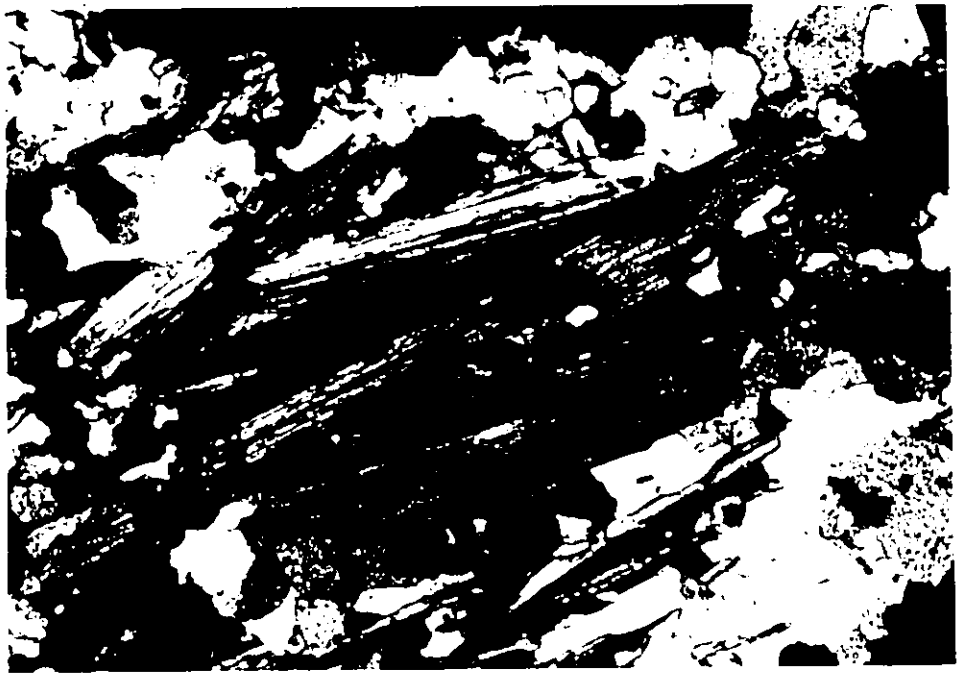
0.1 cm.
SCALE

Figure 34: Outcrop of fibrous grunerite (sample L-4) in the Lower Wabush Iron Formation, near Lorraine Lake

Figure 35: Outcrop of acicular grunerite crystals (sample L-6) in the Lower Wabush Iron Formation.

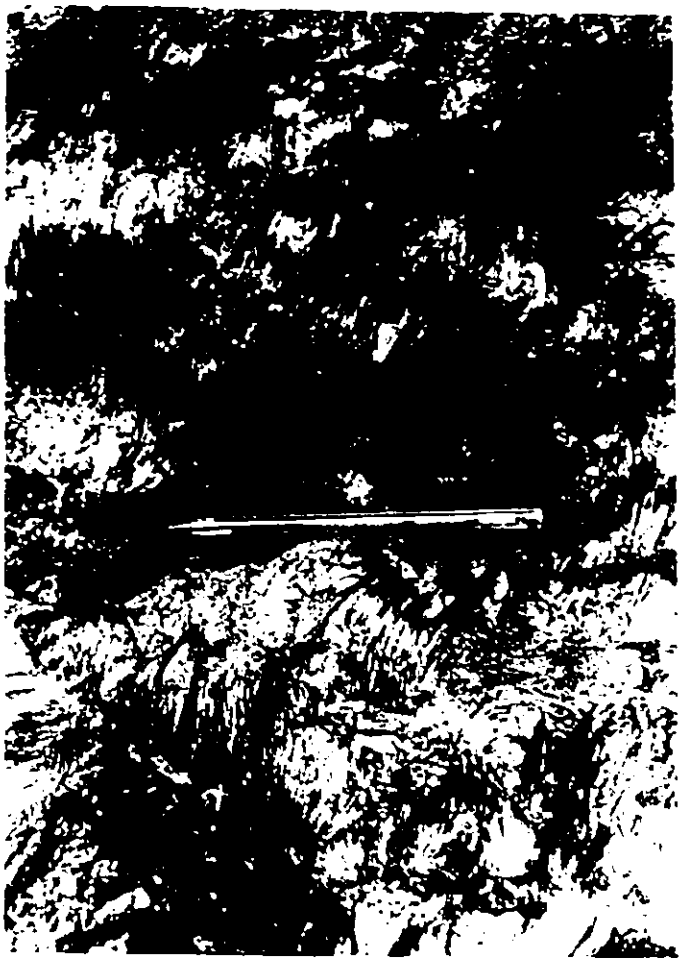

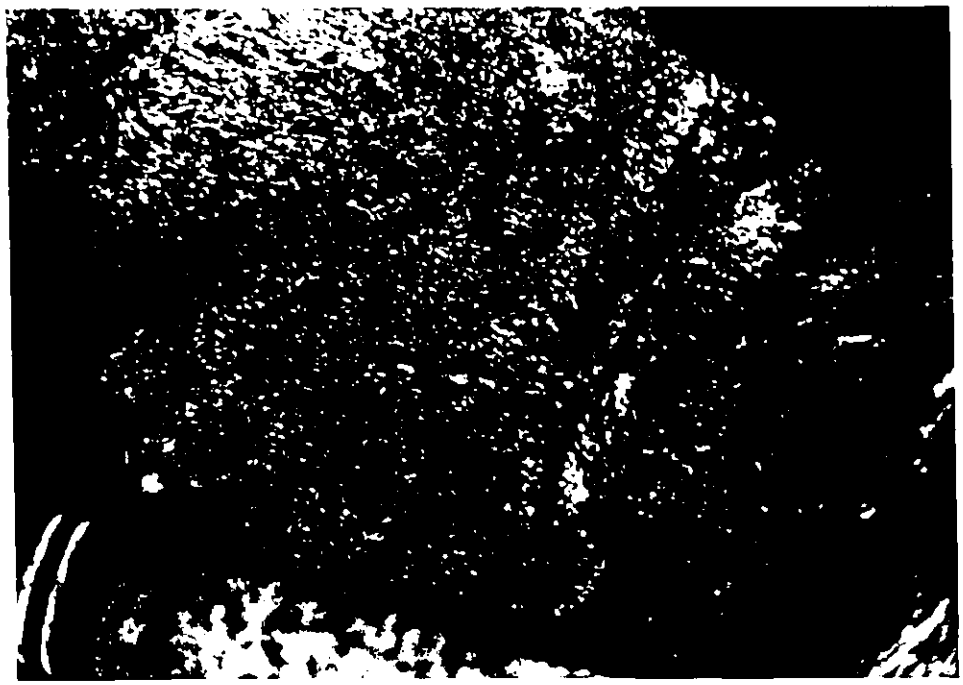

L-6 collected here) which is not as fibrous, but contains abundant acicular grunerite crystals. Figures 36 and 37 are of grunerite rich outcrops of the Lower Wabush Iron Formation along the north side of the Fermont Highway from which samples L-29, L-46 and L-47 were collected. Most of the grunerites in these outcrops were light brown colour and acicular to fibrous in form.

Figure 38 (Kramer, 1977) shows the variations in morphology of grunerite in six samples collected from the Lower Wabush Iron Formation. All of these samples have approximately the same bulk chemical composition and mineralogy,even though they differ greatly in form, from asbestiform to equidemensional. Figures 39 and 40 are electron photomicrographs of grunerite fibres which were separated and crushed from sample L-53.

Analytical Results

Analytical data for the minerals studied by x-ray powder diffraction, electron microprobe, energy dispersive x-ray fluorescence spectroscopy and x-ray fluorescence spectroscopy are listed in Table 8 of the Appendix.

Figure 36: Grunerite rich outcrop of the Lower Wabush Iron Formation on the north side of the Fermont Highway, west of Labrador City

Figure 37: Grunerite rich outcrop of the Lower Wabush Iron Formation on the north side of the Fermont Highway, west of Labrador City

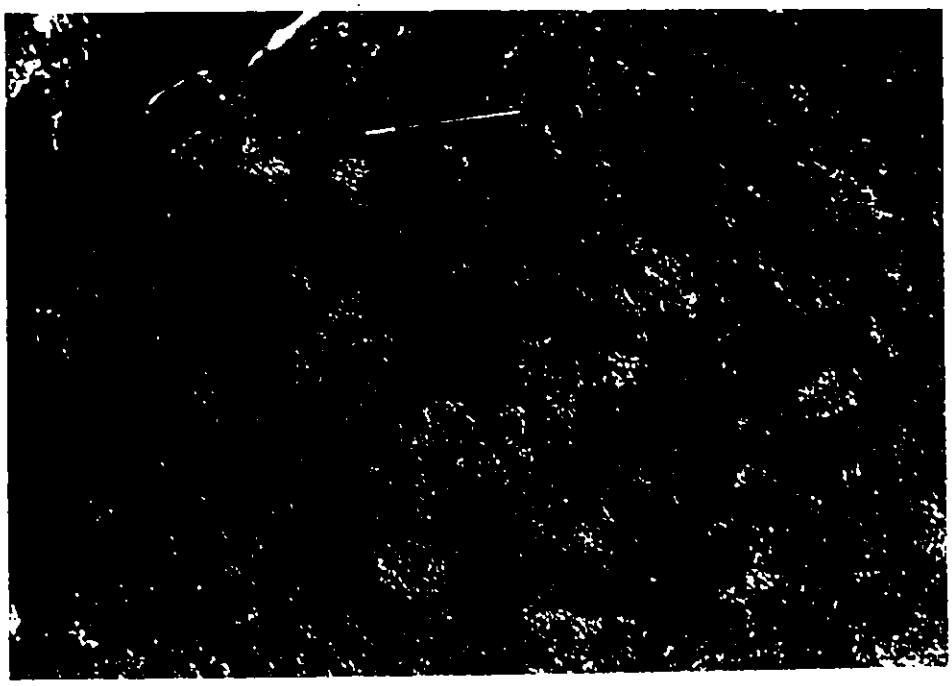

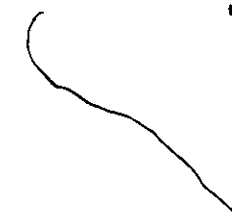

Figure 38: Asbestiform and equidimensional grunerite from Wabush Lake District, Labrador. A. asbestiform (fibrous) grunerite, scale units are in cm. B - F variations in fibres, cleavage fragments, and equidimensional grunerites sampled within 500 metres of each other; each numbered scale unit is 0.1 cm (from Kramer, 1977)

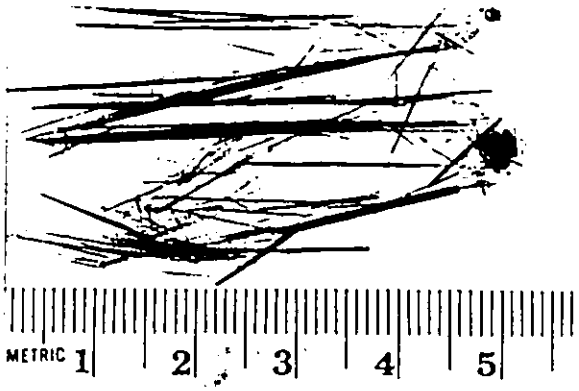

A

D

B

E

C

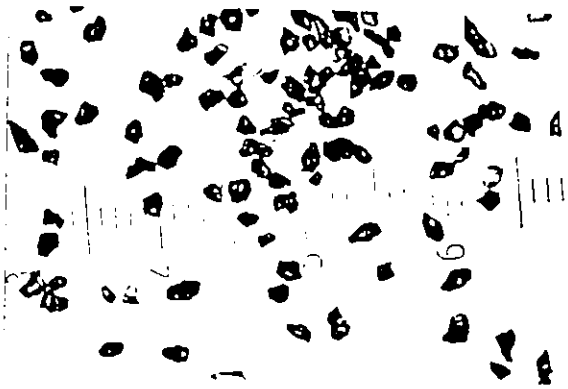

F

Figure 39: Electron photomicrograph of grunerite fibres from rock sample L-53

Figure 40: Electron photomicrograph of grunerite fibres from rock sample L-53


2 μm.
SCALE

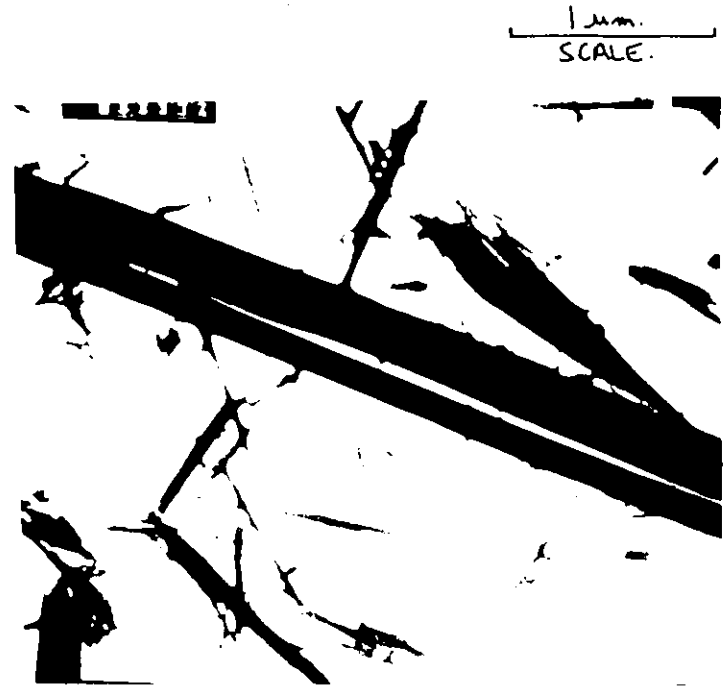
1 μm.
SCALE.

Table 2A in section 1.2 gives a chemical classification of amphiboles which will be referred to in this section. All chemical analyses are recalculated to 100 weight per cent. The structural formulae, based on 23 oxygens, from the probe analyses of the amphiboles which contain little or no aluminum, are almost all deficient in silica in the tetrahedral sites. Amphiboles from the Wabush Lake area studied by Klein (1960, 1964, 1966) and Chakraborty (1966) gave similar results. This deficiency could be due to either a consistent experimental error in the electron microprobe analyses or the Fe^{+3} occupancy of some of the tetrahedral sites.

In Figure 41, electron microprobe analyses of the anthophyllites and members of the cummingtonite-grunerite series are represented in terms of two end members, $Mg_7 Si_8O_{22}(OH)_2$ and $Fe_7Si_8O_{22}(OH)_2$. MgO and FeO are present in large and variable amounts compared to all other oxide components. All of the iron was considered as FeO since there is good evidence that the cummingtonite-grunerite series contains little or no Fe^{3+} (Klein, 1964)

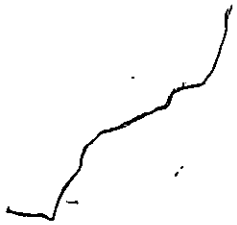

Figure 41: Diagram showing the mole per cent of MgO and FeO in anthophyllites and cummingtonite-grunerites from Wabush Lake District samples as determined by electron microprobe analysis. Analyses from Klein (1960, 1964, 1966) and Chakraborty (1966). (See text for explanation of regression lines)

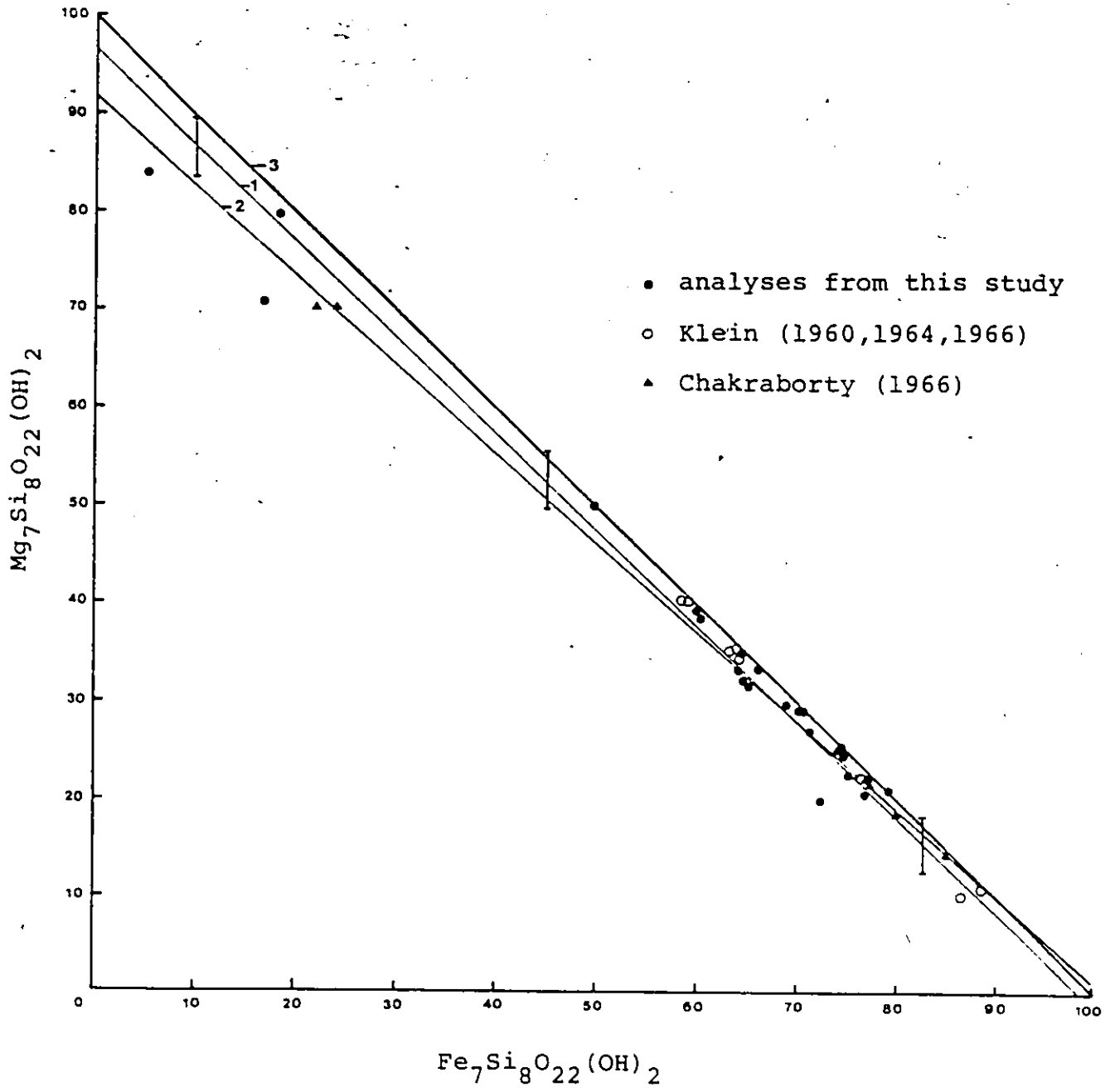
100
90
80
70
60
50
40
30
20
10
0
10
20
30
40
50
60
70
80
90
100
3
1
2
• analyses from this study
○ Klein (1960,1964,1966)
▲ Chakraborty (1966)
$Mg_7Si_8O_{22}(OH)_2$
$Fe_7Si_8O_{22}(OH)_2$

The molecular ratios, MgO:FeO were calculated as follows.

$$FeO = \frac{Fe^{+2} \text{ in octahedral positions}}{\text{total cations in octahedral positions}}$$

$$MgO = \frac{Mg^{+2} \text{ in octahedral positions}}{\text{total cations in octahedral positions}}$$

The electron microprobe date were averaged so that only one data point appears on Figure 41 for each sample (except for anthophyllite L-1 which had only 2 analyses). Linear regression analysis of all anthophyllite and cummingtonite-grunerite electron microprobe data (i.e. no sample averaging) gives the following: a straight line equation

$$y = -0.98\ x + 96.69 \text{ where } y = MgO \text{ and } x = FeO$$

in percent molecular fractions and a calculated correlation coefficient, γ_{xy}, of -0.98. The scatter, in the vertical (y) direction of the observed data points about the regression

line plotted on Figure 41 (No. 1) sometimes called the standard error of estimate ($S_{y/x}$) is 3.31. The bars drawn on the regression line represents vertical distances of $\pm S_{y/x}$ units ($\pm 3.31\%$ $Mg_7Si_8O_{22}(OH)_2$) from the regression line. Nineteen of the twenty-two points (86%) lie within $\pm S_{y/x}$ of the regression line. The scatter appears to be the greatest when MgO >Fe.

Analyses taken from Klein (1960, 1964, 1966) and Chakraborty (1966) are included on Figure 41 for comparison. These are all wet chemical analyses except for Klein's (1966) samples which were analyzed by an electron microprobe. Linear regression analysis of these 15 data points gives a straight line equation

$y = 0.91x + 91.96$ where y = MgO and x = FeO

and a correlation coefficient $\gamma_{xy} = -1.00$. This regression line is also shown on Figure 41 (No. 2).

In addition, the FeO + MgO = 100 line (y = x) is drawn on Figure 41 (No. 3). This line represents parallel substitution of Fe^{+2} for Mg^{+2} in the octahedral (xy) sites of anthophyllite and members of the cummingtonite-grunerite series. Neither calculated regression line on Figure 41 indicates that only Mg^{+2} and Fe^{+2} substitute in the octahedral sites. Other cations which may occupy these sites are Mn^{+2}, Ca^{+2}, Al^{+3} and K^{+}. Most samples analyzed contained some MnO (> 6% in L-1). One sample (L-57) contained

2.5% K_2O and 6% Al_2O_3. In most cases, the octahedral sites appear to be occupied by some Mn^{+2} cations. The data points which lie closest to the FeO + MgO = 100 line on Figure 41 are iron-rich amphiboles (grunerites) which contain more than 50% $Fe_7Si_8O_{22}(OH)_2$. The magnesium rich members (anthophyllites) plot further away. Calculated standard deviations of the molecular ratio FeO:MgO for all points plotted on Figure 41 show little variation between magnesium-rich and iron-rich members (all are close to 8%). The analyses are therefore equally as good for the iron-rich and magnesium-rich samples. Therefore, the magnesium-rich samples (anthophyllites) lying further from the FeO + MgO = 100 line have more substitutions of other ions in the octahedral sites. These sites are filled by manganese, aluminum, and minor calcium and sodium.

Almost no substitutions occur in the octahedral sites of the iron-rich members (grunerites).

The compositional trend of samples analyzed in this study closely follows the trend of samples studied by Klein (1960, 1964, 1966) and Chakraborty (1966) from the Wabush Lake area. Only 5 of the 35 data points (14%) lie outside the standard error of estimate, ± 3.31% $Mg_7Si_8O_{22}(OH)_2$. Four of these 5 data points are anthophyllites which contain appreciable amounts of MnO (up to 6.6%).

The cell constants calculated from the X-ray powder diffraction analysis of members of the cummingtonite-grunerite series were used to determine the FeO/Mgo ratios in Table 10. Column 1 in Table 10 lists these ratios calculated from a graph by Klein (1964) where V(cell volume) = 8.77.82 + 0.453 $Fe\overset{o}{A}^3$. Column 2 is calculated from the equation V = 873.41 + 0.53 $Fe\overset{o}{A}^3$ which appeared in Kramer (1976). Columns 3,4, and 5 are the FeO/MgO ratios as determined by electron microprobe, energy dispersive x-ray fluorescence spectroscopy and x-ray fluorescence spectroscopy respectively. For these calculations, only Mg^{+2} and Fe^{+2} were considered as occupying the octahedral sites. The equations used to calculate the FeO/MgO ratios from x-ray powder diffraction data do not allow for the calculation of other cation occupancy in the octahedral sites. A discussion and statistical study of these results appears in section 5.4.

A summary of the cell constants calculated from the x-ray powder diffraction data is shown in Table 11. Eighteen members of the cummingtonite-grunerite series, 4 actinolites, 1 tremolite, and 1 anthophyllite analyzed in this study are represented in Table 11. Values reported by Klein (1964) for 9 members of the cummingtonite-grunerite series, Klein (1966) for 2 actinolites, and Deer et al (1966) for anthophyllite and tremolite are included in the Table. The calculated values for the cell constants fall well

TABLE 10: FeO/MgO ratios of cummingtonite-grunerite samples from the Wabush Lake area (wt.% FeO ÷ wt.% MgO).

SAMPLE NO.	(1) XRD	(2) XRD	(3) PROBE	(4) EDS	(5) XRF
L-4	-	-	-	5.29	2.50
L-6	2.36	2.16	4.73	-	-
L-7	9.94	6.13	-	6.19	-
L-8	-	-	4.41	-	-
L-9	-	-	3.67	-	-
L-10	4.56	3.64	-	4.05	-
L-13	5.98	4.42	-	3.90	4.26
L-22A	2.99	2.62	6.55	6.58	4.99
L-22B	-	-	6.05	5.02	-
L-25	3.92	3.24	3,59	5.49	-
L-26	-	-	5.17	-	-
L-29A	3.30	2.83	4.35	7.62	-
L-29B	-	-	-	7.85	-
L-29C	-	-	5.41	-	-
L-45	3.14	2.72	-	-	-
L-46	-	-	3.29	-	-
L-47A	2.60	2.34	3.81	-	-
L-47B	2.68	2.40	3.46	-	-
L-48	3.63	3.05	-	-	-
L-51A	2.58	2.32	3.50	-	-
L-53	6.12	4.49	5.29	5.76	-
L-54	-	-	-	3.95	-
L-55	4.46	3.57	4.20	4.75	-
L-56	-	-	2.84	4.15	-
L-57	3.40	2.90	6.56	4.26	-
L-58	3.36	2.87	6.72	8.80	-
L-61	-	-	2.85	4.88	-
L-62	1.89	1.79	1.79	2.77	-
L-63	4.30	3.48	-	10.11	-

TABLE 11: AMPHIBOLE CELL CONSTANTS

	a(Å)	b(Å)	c(Å)	β(deg)	V(Å^3)
Cummingtonite-grunerite					
$\bar{x}$	9.55	18.30	5.34	101.90	913.05
Vx	0.07	0.14	0.22	0.12	0.30
Sx	0.01	0.03	0.01	0.12	2.75
Klein (1964)					
$\bar{x}$	9.56	18.22	5.32	102.10	905.94
Vx	0.40	0.56	0.26	0.27	0.78
Sx	0.04	0.10	0.01	0.27	7.11
Actinolite					
$\bar{x}$	9.88	18.14	5.30	104.59	919.64
Vx	0.42	0.31	0.47	0.59	0.43
Sx	0.04	0.06	0.03	0.62	3.97
Klein (1966)	9.803	18.083	5.292	104.35	909.95
	9.894	18.198	5.299	104.58	923.50
Tremolite					
L-17	9.827	18.062	5.279	104.65	906.47
Deer et al (1966)	9.84	18.05	5.275	104.7	-
Anthophyllite					
L-32	18.573	18.053	5.280	-	1770.49
Deer et al (1966)	~18.6	~18.0	~5.3	-	-

within the range of values obtained by Klein (1964, 1966) for samples analyzed from the Wabush Iron Ore District.

Chakraborty (1966) found that the FeO/MgO ratios of members of the cummingtonite-grunerite series increased from the carbonate facies to the silicate facies to the oxide facies of the Wabush Iron Formation. An attempt was made to verify this trend statistically, using the electron microprobe analyses, but no trend could be established. Some specimens collected in the silicate facies contained appreciable amounts of carbonate and no reference is made in the literature as to how much carbonate the iron formation must contain in order for it to be considered as a member of the carbonate facies rather than the silicate facies.

In addition, an attempt was made to correlate composition with crystal morphology for members of the cummingtonite-grunerite series. No systematic variation could be determined. Fibrous crystals had identical composition to some of the equidimensional and less elongated crystals.

Anthophyllite (L-1) contained more than 6 weight per cent MnO (Figure 42, electron microprobe analysis) which is more than twice the amount found in any anthophyllite by Chakraborty (1966). This anthophyllite occurred in a quartz specularite schist from the Middle Wabush Iron Formation and the fibres had no surficial manganese oxide

Figure 42: Photomicrograph of anthophyllite crystals in a quartz-specularite schist from the Middle Wabush Iron Formation (sample L-1)

0.1 cm.
SCALE

stains. Klein's (1966) anthophyllite (sample 14) contained 3.67 weight per cent MnO (electron microprobe analysis) and he noted that this was almost 1 per cent higher than any analyzed anthophyllites found in the literature.

Chakraborty (1966) noted that the analyses of manganoan cummingtonites from the Wabush Iron Formation were similar to analyses of anthophyllites, with Mn substituting for Mg. This suggests that these manganoan cummingtonites may be related to anthophyllites, rather than to cummingtonites. Comparison by Chakraborty of MnO and FeO content for anthophyllite, cummingtonite-grunerite, and manganoan cummingtonite shows an apparent linear relationship between anthophyllites and manganoan cummingtonites. As manganese enters into anthophyllite, its optical properties and chemical composition tend towards manganoan cummingtonite.

Four specimens of the actinolites analyzed, were found to be similar to Klein's (1966) sample 11B in both composition and unit cell constants (samples L-9, L-22B, L-25, and L64). Actinolite, L-59, from the Archean Ashuanipi Complex has a lower Fe:Mg ratio than the other actinolites and this is reflected in the unit cell dimensions. The actinolite in samples L-9, L-22B and L-25 was found interwoven with grunerite; samples L-59 and L-64 contained no other amphiboles. Tielines for the grunerite-

actinolite pairs are drawn on Figure 43. These grunerite-actinolite assemblages are useful in determining the maximum amount of CaO that can be contained in grunerites at the metamorphic conditions present during their formation. The tielines may be considered as part of a ternary system in which two points are known on the miscibility gap (Klein, 1966).

The maximum CaO content in manganese-poor cummingtonites and grunerites reported by Mueller (1960) in his study of their coexistence with actinolite is 2.5 per cent; Klein (1966) reported an analysis which contained 0.97 per cent. Most of the grunerites analyzed in this study contained less than one per cent CaO. The highest CaO content found was in one analysis of grunerite (L-6) which contained 2.41 weight per cent CaO, and an analysis of grunerite (L-47B) which contained 2.05 weight per cent CaO. All other analyses of these two grunerites gave less than half this amount of CaO. These data support the conclusion reached by Klein (1964, 1966) that the maximum CaO content possible in manganese-poor cummingtonites and grunerites is approximately 2 weight per cent and any higher values are somewhat suspect.

Magnesioriebeckite (L-60) occurs in a quartz limonite schist as scattered stellate groups of dark blue fibrous crystals (Fig. 44). The chemical composition of this

Figure 43: Diagram showing tielines for the grunerite actinolite pairs in assemblages L-9, L-22B and L-25. Klein's (1964) assemblage 11 is included for comparison

○ L - 9

▲ L - 22B

■ L - 25

● Klein,1964, assemblage 11

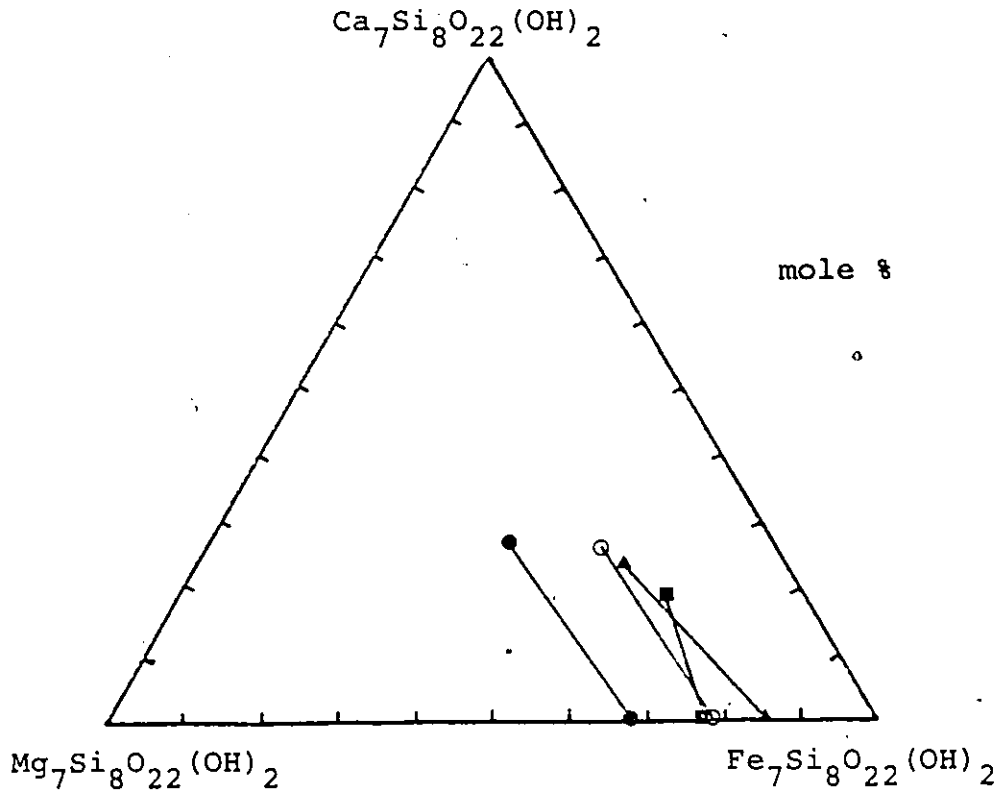

Figure 44: Photomicrograph of radiating fibrous magnesioriebeckite crystals (sample L-60)

0.2 cm.
SCALE

magnesioriebeckite can be considered as $Na_2(Mg_{2.4}Fe^{+2}_{0.6})Fe^{+3}_{2.2}Si_8O_{22}(OH)_2$. The magnesioriebeckite reported by Klein (1966) contained much more manganese (5.9 wt.%) and was part of an assemblage which contained specularite, cummingtonite, and magnesian rhodonite.

Only one sample of tremolite was analyzed, number L-17 from the Duley marble, east of Wabush Lake. Other minerals analyzed but not discussed are hedenbergite (L-22A), eulite (L-29A), ankerite (L-29C, L-46, L-55, L-56, L-57, L-62), and siderite (L-53). Results of these analyses appear in Table 8 of the Appendix.

CHAPTER FIVE

DISCUSSION AND CONCLUSIONS

5.1 CONCENTRATION OF FIBRES IN LAKE WATERS

Figure 16, a plot of fibre concentration versus distance from the Iron Ore Company of Canada tailings deposit shows fibre concentrations in Wabush Lake for three different sampling periods. The concentrations both upstream and downstream from the tailings are much higher for the samples taken in June 1977 as compared to August 1976. Some are more than one order of magnitude higher. This may be accounted for by the higher water levels and higher current velocity of the lake as a result of the spring run-off. Increased current velocity would carry suspended material (including fibres) much further down the lake before settling out. A significant increase in mine production could increase the number of fibres dumped into the lake but there was no substantial increase in production between 1976 and 1977.

5.2 CALCULATED SETTLING RATE OF FIBRES

In order to calculate settling rates of the fibrous minerals in Wabush Lake, the following assumptions are made:

a) complete mixing of the water in Wabush Lake, b) the sum of inflows to the lake is equal to the outflow at the north end of the lake (i.e. the lake is in equilibrium), c) the input to the lake is from two sources: the channels from Little Wabush Lake and Flora Lake (other sources are insignificant in comparison), d) the estimated maximum outflow velocity at the north end of Wabush Lake is 0.5 metres per second (estimated from the rapid but non-turbulent flow in the channel and flow rates for streams of similar configurations for which stream gauge data are available), e) the fibres follow Stokes' Law of Settling.

The outflow channel at the end of Wabush Lake (north end of the Julienne Peninsula) is 250 metres wide and 5 metres deep at the centre. Assuming a rectangular cross-section, an average depth of 2.5 metres, and a water velocity of 0.5 metres per second gives a calculated discharge rate of about 360 m^3 per second.

By dividing the lake into 7 sections and calculating the volume of each section (using data from Table 4 and Figure 10), the lake volume is estimated to be $11.225 \times 10^8 m^3$. This gives a residence time for the lake of about 36 days. The lake water velocity is then calculated by dividing the length of the lake (from the Iron Ore Company of Canada tailings dump to the outlet channel) by the residence time.

$$V = \frac{\text{length of lake}}{\text{residence time}} = \frac{20.33 \times 10^5 \text{cm}}{3.097 \times 10^6 \text{ sec.}} = 0.66 \text{ cm/sec.}$$

This velocity represents the horizontal velocity component acting on suspended particles in the lake.

The average size of fibres found in the water of Wabush Lake is 3.5 μm in length and 0.4 μm in diameter. A spherical particle of equal volume has a radius of 1.012×10^{-4} cm. By assuming a fibre density of 3.5 gm/cc (density of iron-rich amphiboles) and applying Stokes' Law, the settling velocity of the average fibre can be calculated as follows:

$$V = \frac{2}{9} \frac{d_1 - d_2}{N} gr^2$$

$$= 5.43 \times 10^{-4} \text{ cm/sec.}$$

where V = velocity of particle in cm/sec

r = radius of particle in cm

g = acceleration of gravity

N = viscosity of the fluid in poises

d_1 = density of particle

d_2 = density of fluid

Point A on Figures 14, 15 and 16 is 15 kilometres downstream from the Iron Ore Company of Canada tailings dump. By the time the average fibre has reached this position, it

will have settled about 12.3 metres. When it reaches the outlet channel at the north end of Wabush Lake it will have settled 16.8 metres which is greater than the maximum depth of the channel.

Using a fibre size of 3 μm x 0.3 μm instead of the average fibre size, the calculated settling velocity is 3.78×10^{-4} cm/sec. At point A, this fibre will have settled 2.70 metres and by the time it reaches the outlet channel the fibre will have settled 11.64 metres.

Many of the assumptions made in carrying out these calculations are very approximate. The water which carries the tailings from the Iron Ore Company of Canada pelleting plant into Wabush Lake is heavily loaded with sediment and does not mix evenly when it reaches the lake water. The lake appears to be stratified and does not completely mix since fibre concentrations do not show a steady increase with depth but at many locations downstream from the tailings the concentrations are rather erratic. In addition, the fibres may settle out more rapidly than spherical particles if they are oriented with their long axis in a vertical position and slower if their long axis is horizontal or inclined. The effects of wind generated currents and coagulation of fibres by biological processes were also not considered in the model. Coagulation would increase the particle size, thus increasing

the settling velocity and removing more fibres from the water than predicted in the model.

Since the majority of fibres found in the lake waters of Wabush Lake are iron and iron-manganese rich, their densities are much greater than 3.5 gm/cc which is used in these calculations. Therefore, they should settle out even more rapidly than amphibole fibres. This is borne out by the observation that sediments at the north end of Wabush Lake contain fewer iron and iron-manganese fibres than sediments closer to the tailings deposit. In Shabogamo Lake, "amphibole" fibres predominate in the sediments.

Figure 45 shows the depth that various sized fibres will settle as they move downstream from the tailings deposit. The fibres appear to follow the settling model to some extent in that the settling velocities calculated indicate that the majority of fibres should settle out before they reach the outlet channel at the north end of Wabush Lake. Probably only the very narrow fibres of volume less than about 0.1 μm^3 would go beyond the outlet channel (O in Fig. 45). Fibre concentrations in Shabogamo Lake surface waters are more than two orders of magnitude less than those in Wabush Lake surface waters and the fibres are much smaller in size, and tend to confirm this simple settling calculation.

Figure 45: Calculated depth of settling of various sized fibres versus distance downstream from the Iron Ore Company of Canada tailings. a represents an average fibre 3.5 µm x 0.4 µm, b is 3µm x 0.3 µm, and c is 6 µm x 0.1 µm. a, b and c have densities of 3.5 gm./cc. d represents an average sized fibre (3.5 µm x 0.4 µm) of iron and iron-manganese rich composition with a density of 4.5 gm/cc. (For positions of A,B &C see text and Figs. 14,15,16. O = outlet channel from Wabush Lake at north end of Julienne Peninsula)

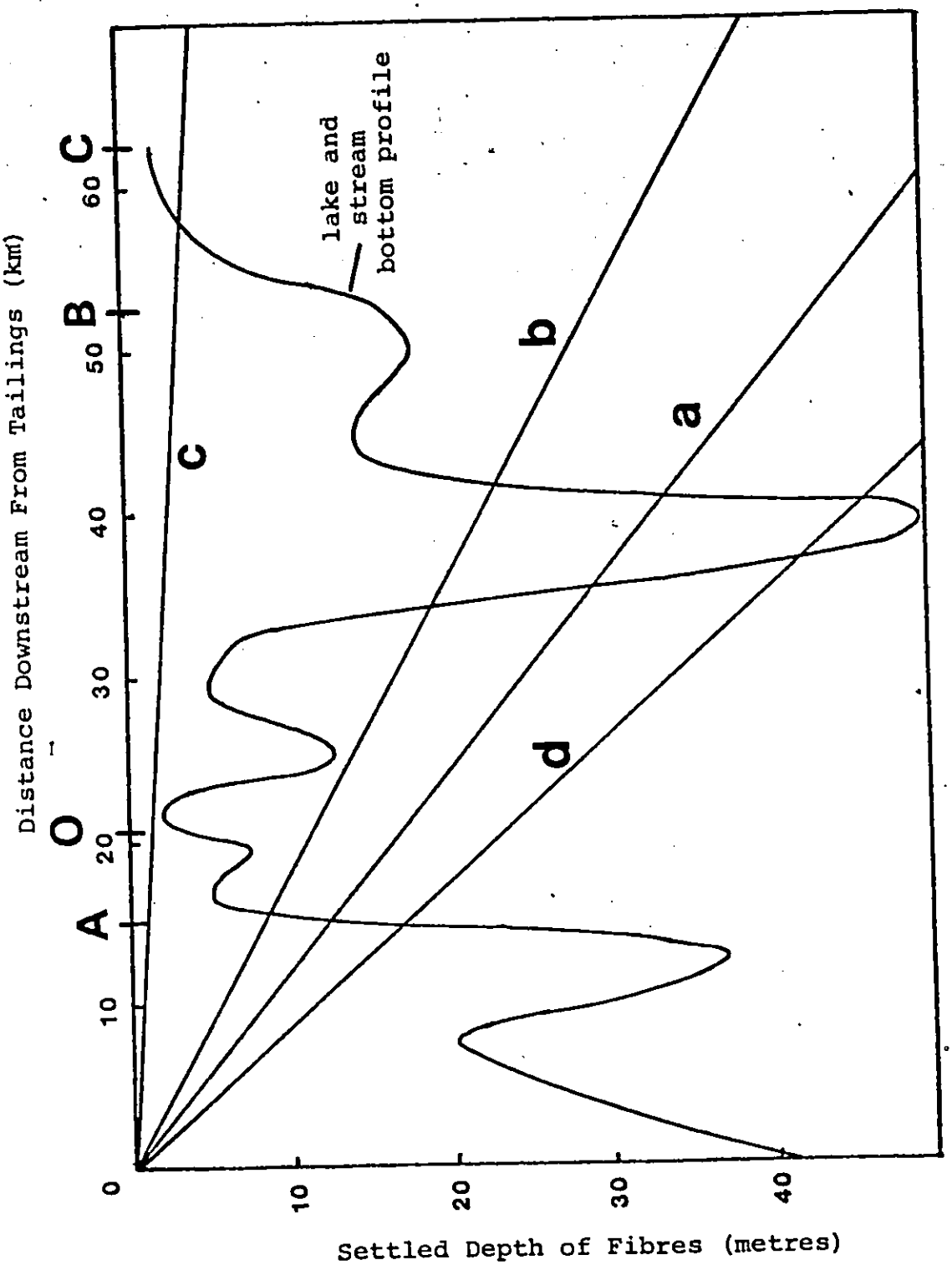
Distance Downstream From Tailings (km)
O
A
B
C
10
20
30
40
50
60
lake and
stream
bottom profile
a
b
c
d
0
10
20
30
40
Settled Depth of Fibres (metres)

5.3 COMPOSITION OF MINERAL FIBRES

The majority of the fibres found in the water samples of Wabush Lake were identified as iron and iron-manganese rich minerals by energy dispersive x-ray fluorescence spectroscopy. In Shabogamo Lake, and streams of the areas surrounding Wabush and Shabogamo Lakes, the mineral fibres were mainly of amphibole composition. The lake sediments follow a similar trend with iron and iron-manganese rich minerals predominant in the Wabush Lake bottom sediments and amphibole type fibres predominant in the Shabogamo Lake sediments. The Iron Ore Company of Canada tailings contained many iron and iron-manganese rich mineral fibres which were identified as magnetite, hematite, limonite, goethite, siderite, and/or manganite.

The fibrous minerals found in the rock samples collected were identified as amphiboles of the cummingtonite-grunerite series, anthophyllite, tremolite-actinolite (the least fibrous) and magnesioriebeckite. All of these amphiboles were identified as possibly present in the Iron Ore Company of Canada tailings, lake and stream waters, and sediments and soils of the Wabush Lake iron ore district.

No systematic variation was found in the cummingtonite-grunerite composition with respect to morphology. The excellent fibrous grunerites (L-4 and L-13) had compositions

similar to other grunerites which had much lower aspect ratios. The only compositional trend which could be related to morphology was noted in the iron and iron-manganese rich fibres found in lake water and lake sediment samples. The greater the iron content of these fibres, the lower their aspect ratio.

5.4 COMPARISON OF ANALYTICAL TECHNIQUES USED IN THE STUDY OF AMPHIBOLES IN ROCK SPECIMENS

FeO/MgO ratios of amphiboles from the cummingtonite-grunerite series are plotted on Figure 46. These ratios show the variation in analytical results between different analytical methods. Data used to construct this Figure can be seen in Table 10.

The electron microprobe is considered to be an excellent quantitative analytical tool when used in conjunction with good reference standards. The use of polished thin sections in this technique eliminates or greatly reduces the probability of weathering products remaining on the sample surface. The standard deviation of the MgO/FeO ratios (wt.% FeO ÷ wt % Mg) in cummingtonite-grunerites analyzed by the electron microprobe was calculated to be 0.34. This standard deviation was calculated by averaging the standard deviation of the FeO/MgO ratio of each sample

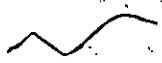

Figure 46: FeO/MgO ratios of amphiboles contained in rock samples

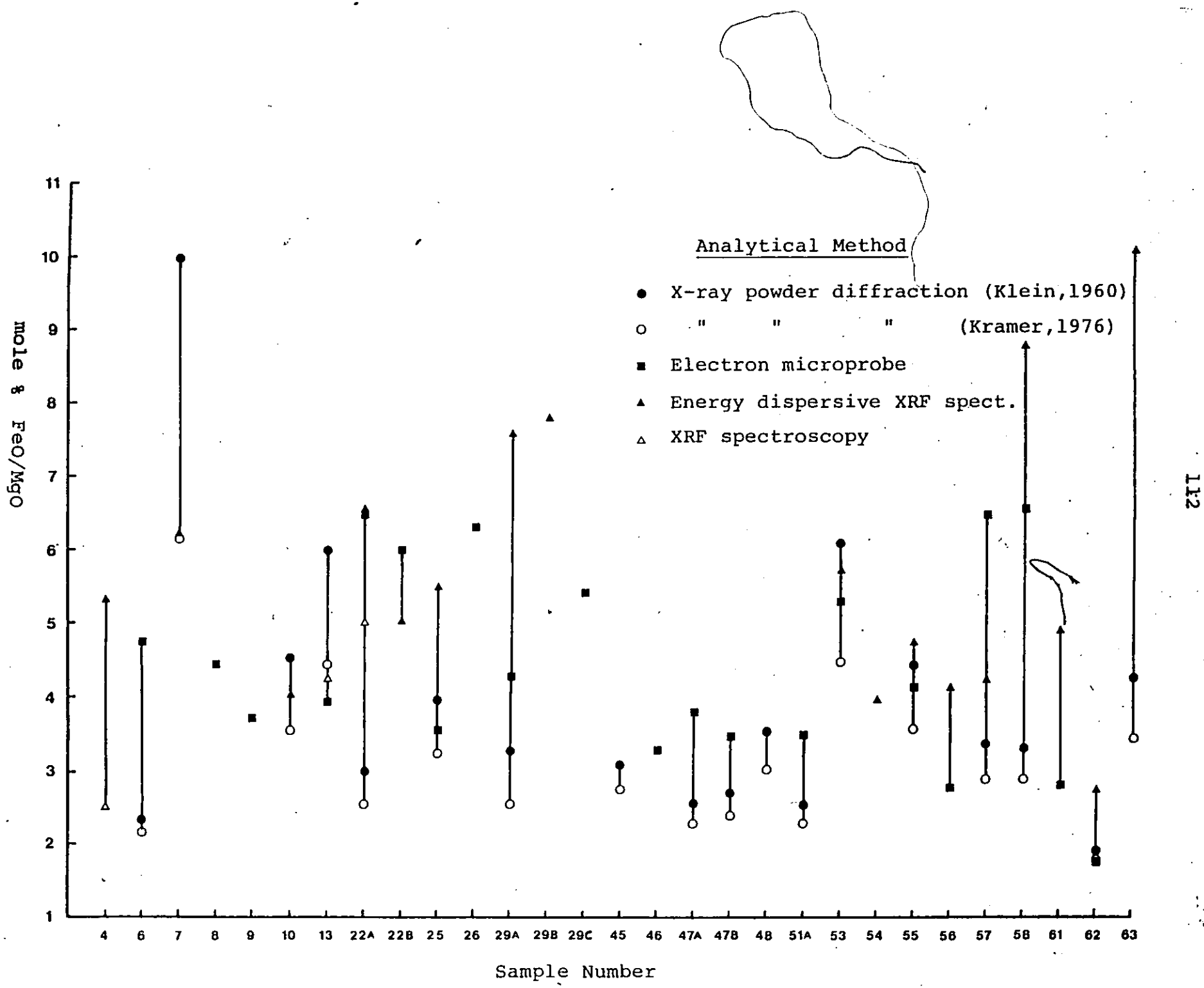
Analytical Method
X-ray powder diffraction (Klein,1960)
" " " (Kramer,1976)
Electron microprobe
Energy dispersive XRF spect.
XRF spectroscopy
mole % FeO/MgO
11
10
9
8
7
6
5
4
3
2
1
4 6 7 8 9 10 13 22A 22B 25 26 29A 29B 29C 45 46 47A 47B 48 51A 53 54 55 56 57 58 61 62 63
Sample Number

analyzed. The 95% confidence limits ($\pm 2S/\sqrt{n}$) are ± 0.18. The high standard deviation (up to ± 15% of the MgO/FeO ratio) within some samples indicates that the amphiboles contained in these samples have a wide compositional range. Several samples had a standard deviation of less than 1% (the precision of the instrument was calculated as 2%). The electron microprobe data represent the best analysis of the amphibole minerals in this study.

In order to compare the analyses obtained from different analytical techniques, the FeO/MgO ratios, for each sample analyzed by the electron microprobe and at least one other method (except for x-ray fluorescence spectroscopy) were tabulated (from Table 10). The means, standard deviations, and 95% confidence limits of the differences between the electron microprobe FeO/MgO ratios and each of the XRD (Klein, 1964), XRD (Kramer, 1976), and EDS FeO/MgO ratios were calculated and appear in Table 12.

The mean FeO/MgO ratio differences appearing in Table 12 were tested at the 5% significance level against the electron microprobe FeO/MgO ratio difference (which was taken as zero) to see if there was any real difference in the means. For $F(Z) = 1 - \alpha/2$, $Z_{0.25} = 1.960$. Since Z for the x-ray powder diffraction means is >1.960, the means are significantly different at the 5% significance level. However, $|Z|$ for the EDS mean falls within the limits of

TABLE 12: Comparison of FeO/MgO ratio differences for various analytical methods (see text for explanation)

	ANALYTICAL METHOD			
	XRD (Klein, 1964)	XRD (Kramer, 1976)	EDS	PROBE
$\bar{x}$	1.22	1.73	-0.87	-
S_x	1.52	1.38	1.55	0.34
95% confidence Limits	0.88	0.80	0.93	0.18
Z	2.71	4.22	-1.81	-

the 5% significance level. This indicates that the energy dispersive x-ray fluorescence spectroscopy analyses are better than the x-ray powder diffraction analyses when compared to electron microprobe results (note: this applies only to determination of FeO/MgO ratios and not to absolute values). The FeO/MgO ratios determined by energy dispersive x-ray fluorescence spectroscopy give the highest value in 11 out of 15 samples.

The differences between the ratios calculated from x-ray powder diffraction data (FeO/MgO calculated using equation for Kramer, 1976 - FeO/MgO calculated using equation from Klein, 1964) were plotted against the FeO/MgO electron microprobe ratios to see if any trends could be observed. Linear regression analysis showed no trends in the data; however, the ratios calculated using the equation from Kramer (1976) were higher in the majority of samples analyzed.

Absolute values obtained for the oxides (wt.%) by electron microprobe and energy dispersive x-ray fluorescence methods were compared for several grunerite samples. Results of this statistical evaluation appear in Table 13. At the 5% level of significance, $Z_{.025} = 1.960$. The only $|Z|$ values that fall within this range consistently are for manganese (except of sample L-57). Energy dispersive x-ray fluorescence spectroscopy appears in general to give variable SiO_2 and MgO and higher FeO (in all samples) results; the Al_2O_3

TABLE 13: COMPARISON OF EDS AND PROBE DATA (wt.% oxide)

	$\bar{X}$		Sd		Z
	PROBE	EDS	PROBE	EDS	
SAMPLE L-22A					
SiO_2	50.23	46.81	0.99	2.81	5.03
FeO	41.95	44.85	0.86	4.13	-3.19
MgO	6.41	6.75	0.26	2.27	-6.17
CaO	0.68	0.60	0.05	0.49	0.16
MnO	0.38	0.33	0.20	0.32	0.42
SAMPLE L-29A					
SiO_2	51.03	44.01	1.27	3.15	9.75
FeO	39.56	47.18	1.54	3.81	-8.66
MgO	9.10	6.16	0.38	1.74	9.48
CaO	0.21	0.13	0.16	0.15	8.00
MnO	0.11	0.10	0.17	0.17	0.14
SAMPLE L-53					
SiO_2	48.26	49.49	1.71	2.38	-1.30
Al_2O_3	7.77	0.06	1.91	0.11	9.07
FeO	36.96	42.65	0.83	2.80	-7.79
MgO	7.01	7.36	0.60	1.24	-0.92
SAMPLE L-55					
SiO_2	52.58	48.44	0.67	2.08	5.45
Al_2O_3	0	0.37	0	0.27	4.11
FeO	37.58	41.39	0.76	2.61	-4.05
MgO	9.07	8.67	1.19	1.52	0.55
CaO	0.67	0.31	0.09	0.57	2.00
MnO	0.07	0.14	0.17	0.12	-0.64

Table 13 continued

SAMPLE L-57

SiO_2	51.03	48.53	0.96	4.58	1.48
Al_2O_3	5.38	0.56	0.68	0.21	13.77
FeO	35.62	40.20	0.47	5.87	-2.19
MgO	5.46	9.37	0.43	2.17	-4.89
CaO	0.13	0.04	0.15	0.06	0.90
MnO	0.06	0.39	0.13	0.30	-2.75
K_2O	2.32	0.03	0.25	0.06	16.36

and K_2O determinations are unsatisfactory and extremely difficult to evaluate using this method.

The high FeO concentrations in the energy dispersive x-ray fluorescence spectroscopy analyses may be due to the fluorescence effects of iron or to the lack of sample penetration by the beam which may result in the analysis of an iron rich surface weathering product.

The use of energy dispersive x-ray fluorescence spectroscopy analyses to characterize amphibole fibres appears to be reasonably accurate for certain oxides and gives results which could be used to study compositional trends in microscopic size particles. Any trends observed in the analysis of fibres in water and sediment in this study could be considered as real trends. Absolute values however should be treated with caution.

5.5 CONCLUSIONS

Amphiboles of the cummingtonite-grunerite series are abundant in the Wabush Lake area. They are restricted in their occurrence to the Lower Wabush Iron Formation and the lower portion of the Middle Wabush Iron Formation. No trend in the FeO/MgO ratios, with respect to the facies in which the cummingtonite-grunerite occurs, is observed. These amphiboles generally have a fibrous morphology (i.e.

an aspect ratio of 3:1 or greater) and several occurrences of excellent elongated fibres are present. Their compositions are similar to those cummingtonite-grunerite series' members studied by Klein (1960, 1964, 1966) and Chakraborty (1966).

Anthophyllites are less abundant and occur only in the Middle Wabush Iron Formation (the oxide facies). They are usually found in stellate groups of radiating fibres but may also be found scattered throughout the oxide facies. One outcrop of the Lower Wabush Iron Formation contained radiating fibrous aggregates of dark blue magnesioriebeckite.

Amphiboles of the tremolite-actinolite series are also present. Tremolite is commonly found in the Duley Formation (marble) and actinolite is found closely associated with amphiboles of the cummingtonite-grunerite series in the Lower Wabush Iron Formation. These amphiboles do not often occur in a fibrous form.

Tailings or mine wastes are entering Wabush Lake from two sources. The Iron Ore Company of Canada deposits tailings from a pelleting plant directly into the south end of Wabush Lake. Tailings from Wabush Mines are dumped at the edge of Flora Lake and suspended material is carried into Wabush Lake via the stream channel directly east of the Iron Ore Company of Canada tailings deposit. Many fibrous minerals

are present in the Iron Ore Company of Canada tailings, most of which are iron and iron-manganese rich fibres. Amphibole fibres are less abundant but most amphiboles found in the rocks around Wabush Lake are present in the tailings.

A major proportion of the iron (fibres with high iron content are magnetite, hematite, limonite, goethite, and siderite) and iron-manganese (fibres with a high manganese content are manganite which is produced by the alteration of rhodochrosite, rhodonite, or other manganese rich minerals) fibres and a significant number of amphibole fibres settle out of the water in Wabush Lake before it reaches Shabogamo Lake. This is borne out by studies of the lake sediments and suspended particulates in the lake water samples. The application of Stokes' Law of settling to the mineral fibres also suggests that most fibres will be sedimented in Wabush Lake. Many fibres, believed to be amphiboles, which occur in the waters of Shabogamo Lake, Duley Lake, streams in the Wabush Lake area, and the drinking water samples are too small to analyze by energy dispersive x-ray fluorescence spectroscopy, the only analytical method available. The effect of weathering of the Wabush Iron Formation seems to be insignificant, with respect to addition of fibrous minerals to the water system, as compared to the dumping of tailings by the Iron Ore Company of Canada and Wabush Mines.

A comparison of analytical techniques used in the study of amphiboles of the cummingtonite-grunerite series suggests that energy dispersive x-ray fluorescence spectroscopy used in conjunction with a transmission electron microscope is a good semi-quantitative method for analyzing amphibole fibres in the micron to sub-micron range.

REFERENCES

ANDERSON, C. H. 1977. Environmental Protection Agency Interim Method for Determining Asbestos in Water. in Proc. of the Workshop on Asbestos, NBS Special Publ. 506.

ANDREWS, K. W., DYSON, D. J., KEOWN, S. R. 1971. Interpretation of Electron Diffraction Patterns. Plenum Press, N.Y. 239 p.

ASHBROOK, P. 1978. Ambient Concentrations of Mineral Fibres in Air and Water in Northeast Minnesota. Preliminary Report to Environmental Quality Council, Minnesota, August, 1978.

BEAMAN, D. R., and FILE, D. M. 1976. Quantitative determination of asbestos fibre concentrations. Anal. Chem. 48, 101-110.

BEAMAN, D. R., and WALKER, H. J. 1977. Mineral fibre identification using the analytical transmission electron microscope. in Proc. of the Workshop on Asbestos, NBS Special Publ. 506, 249-269.

BEESTON, B. E. P., HORNE, R. W., MARKHAM, R. 1973. Electron Diffraction and Optical Diffraction Techniques. North-Holland Publ. Co., Amsterdam. 444 p.

BILES, B., and EMERSON, T. R. 1968. Examination of Fibres in Beer. Nature, 219, 93-94.

BONNICHSEN, B. 1969. Metamorphic pyroxenes and amphiboles from the Biwabik Iron Formation, Dunba River area, Minnesota. Mineral. Soc. Am. Special Paper 2, 217-239.

BROWN, A. L., TAYLOR, W. F., CARTER, R. E. 1976. The reliability of measures of amphibole fibre concentrations in water. Environ. Res. 12, 150-160.

CHAKRABORTY, K. L. 1966. Ferromagnesian silicate minerals in the metamorphosed iron formation of Wabush Lake and adjacent areas, Newfoundland and Quebec. G.S.C. Bull. 143, 34 pages.

CHOPRA, K. S. 1977. Inter-Laboratory Measurements of Amphibole and Chrysotile Fibre Concentration in Water. in Proc. of the Workshop on Asbestos, NBS Spec. Publ. 506, 377-381.

COMMITTEE ON ASBESTOS ANALYSIS. 1977. An Interim Method for the determination of asbestos fibre concentrations in water by transmission electron microscopy. M.O.E., Ontario, November, 36 pages.

CUNNINGHAM, H. M., and PONTEFRACT, R. 1971. Asbestos fibres in beverages and drinking water. Nature, 232, 332-333.

DEER, W. A., HOWIE, R. A. ZUSSMAN, J. 1966. An Introduction to the Rock Forming Minerals. Longmans, Green and Co. Ltd., London, 160 p.

FAHRIG, W. F. 1960. Shabogamo Lake map sheet, Newfoundland and Quebec. Geol. Survey Canada, Map 1226A.

FINGER, L. W. 1967. The crystal structures and crystal chemistry of ferromagnesian amphiboles. Unpublished Ph.D. thesis, University of Minnesota.

FINGER, L. W. 1969. The crystal structure and cation distribution of a grunerite. Mineral. Soc. Amer., Special Paper 2, 92-100.

GASTIL, G., and KNOWLES, D. M. 1960. Geology of the Wabush Lake area, southwestern Labrador and eastern Quebec, Canada. Bull. Geol. Soc. Amer. 71, 1243-1254.

GILL, J. E., BANNERMAN, H. M., TOLMAN, C. 1937. Wapussakatoo Mountains, Labrador. Bull. Geol. Soc. Amer. 48, 567-586.

GILL, J. E., and JAMES, W. G. 1929. Report on the New Quebec Company Ungava expedition (unpublished report).

GLOSSARY OF GEOLOGY. 1973. American Geological Institute, Washington, D. C. second printing.

GROSS, G. A. 1968. Geology of Iron Deposits in Canada, Vol. 3, Iron Ranges of the Labrador Geosyncline. Geol. Survey of Canada, Economic Geology Rept. No. 22, 179 p.

HIRSCH, P. B., HOWIE, A., NICHOLSON, R. B., PASHLEY, D. W., WHELAN, M. J. 1965. Electron Microscopy of Thin Crystals. Butterworths, London.

JACKSON, G. D. 1962. The Geology of the Neal (Virot) Lake area, west of Wabush Lake, Labrador, with special reference to iron deposits. Unpublished Ph.D. thesis McGill University, Montreal.

KLEIN, C. 1960. Detailed Study of the amphiboles and associated minerals of the Wabush Iron Formation, Labrador. McGill University, unpublished M.A. thesis.

KLEIN, C. 1964. Cummingtonite-grunerite series; a chemical optical and X-ray study. Amer. Min. 49, 963-982.

KLEIN, C. 1965. Mineralogy and Petrology of the Wabush Iron Formation, Labrador City Area, Newfoundland. Unpublished Ph.D. thesis, Harvard University.

KLEIN, C. 1966. Mineralogy and Petrology of the metamorphosed Wabush Iron Formation, Southwestern Labrador. Jour. Petrology, 7, pt. 2, 246-305.

KNOWLES, D. M., and GASTIL, R. G. 1959. Metamorphosed iron formation, S. W. Labrador. Bull. Can. Inst. Mineral. and Met., 52, 503-510.

KNOWLES, D. M. 1967. The structural development of Labrador Trough formation in the Grenville Province, Wabush Lake area, Labrador. Ph.D. thesis, Columbia University, 190 p.

KRAMER, J. R. 1976. Fibrous Cummingtonite in Lake Superior. Can. Mineral., 14, 91-98.

KRAMER, J. R. 1977. Fibrous and asbestiform minerals. in Proc. of Workshop on Asbestos, NBS, Special Publ. 506, 19-32.

KRANCK, S. H. 1961. A study of phase equilibria in a metamorphic iron formation. J. Petrol. 2, 137-184.

LEINEWEBER, J. P. 1977. Statistics and the significance of Asbestos fibre analysis. in Proc. of the Workshop on Asbestos, NBS, Special Publ. 506, 281-294.

LOW, A. P. 1895. Report on explorations in the Labrador Peninsula along East Main, Koksoak, Hamilton, Manicougan and portions of other rivers in 1892-1895. Geol. Survey of Canada Annual Report.

McCRONE, W. C. 1977. Identification of asbestos by polarized light microscopy. in Proc. of the Workshop on Asbestos, NBS, Special Publ. 506, 235-248.

McCRONE, W. C., and STEWART, I. M. 1974. Asbestos. Amer. Lab., 6,(4), 10-18.

MASSEY, N. W. 1979. Personal Communication

MUDROCH, O. 1979. Personal Communication

MUELLER, R. F. 1960. Compositional characteristics and equilibrium relationships in mineral assemblages of a metamorphosed iron formation. Amer. J. Sci. 258, 449-497.

MUMTAZZUDIN, M. 1958. The Geology of the area between Carol Lake and Wabush Lake, Labrador. Unpublished M.Sc. thesis, McGill University, Montreal.

NORD, G. J. Jr. 1977. State-of-the-Art of the Analytical Transmission Electron Microscope. Symposium on Electron Microscopy and X-Ray Diffraction in Environmental and Occupational Health.

O'LEARY, J., CANNELL, R., HONSBERGER, D. 1972. Geology of ore deposits, Geology at the Scully Mine. Canadian Mineral. & Met. Bull. January, 1-5.

PATTNIAK, A., and MEAKIN, J. D. 1973. Development of an instrumental monitoring method for measurement of asbestos concentrations in or near sources. U.S. Environmental Protection Agency, Washington, D. C., EPA 650/2-73-016.

RIVERS, T. 1978a. Wabush Lake-Sawbill Lake Map Sheets, Preliminary Project Report 78-10, Newfoundland Dept. of Mines & Energy, 87-92.

RIVERS, T. 1978b. Flora Lake-Wabush Lake Map Sheet, Newfoundland, Newfoundland Department of Mines and Energy, Map 7872. Scale 1:50,000.

RUDD, C. A., BARRETT, C. S., RISSELL, P. A., CLARK, R. L. 1976. Selected area Electron Diffraction and Energy Dispersive X-ray Analyses for the Identification of Asbestos Fibres, A Comparison. Micron, 7, 115-132.

STEWART, J. M. 1972. The X-ray system-version of 1972. Computer Sci. Centre, Univ. Maryland, Tech. Rept. TR-192.

WENK, H. R. 1976. Electron Microscopy in Mineralogy. Springer-Verlag, Berlin, 564 p.

ZOLTAI, T., and STOUT, J. H. 1976. Comments on asbestiform and Fibrous Mineral Fragments Relative to Reserve Company Mining Deposits. Minnesota Pollution Control Agency, Minneapolis, 37 pages. + Appendices.

ZUSSMAN, J. 1967. Physical Methods in Determinative Mineralogy. Academic Press, London and New York.

APPENDIX

TABLE 1: SEDIMENT AND SOIL DESCRIPTIONS

# 1	Top	- 1 cm red brown clayey silt
	Bottom	- layered, 1 to 3 cm layers, green brown and dark brown clayey silt
	Depth	- 5 m
# 2	Top	- 1 cm brown red clayey silt
	Bottom	- green brown clayey silt with a 1 cm dark brown layer 5 cm from the surface
	Depth	- 5 m
# 3		- brown red clayey silt
	Depth	- 38 m
# 4		- brown red silty clay
	Depth	- 16 m
# 5		- dark brown and brown green layers of silt (0.5 to 1 cm layers), odd sand grain
	Depth	- 11 m
# 6		- medium green colour silt, some sand grains
	Depth	- 4 m
# 7	Top	- <0.5 cm red brown clayey silt
	Bottom	- medium brown silt with dark brown grains approximately 0.25 cm diameter, some sand grains
	Depth	- 8 m
# 8	Top	- 0.25 cm red brown very fine clayey silt
	Middle	- 0.25 cm dark brown silt, some sand grains
	Bottom	- medium green clayey very fine sand
	Depth	- 6 m
# 9	Top	- <0.25 cm red brown clayey silt
	Bottom	- medium brown green silty clay, some sand, several hard dark brown layers (0.5 cm thick) near top
	Depth	- 16 m

# 10		- medium brown clay
	Depth	- 13 m
# 11		- medium brown clay, odd sand grain
	Depth	- 10 m
# 12		- medium brown clay
	Depth	- 10 m
# 13	no data	
# 14	Top	- 0.25 cm green silty sand
	Bottom	- red brown clayey very fine sand, odd course sand grain
	Depth	- 10 m
# 15		- red brown silt
	Depth	- 10 m
# 16		- medium brown find sand, odd coarse grain
	Depth	≥ 7 m
# 17	Top	- 0.5 cm hard crusty layer of silt, banded red brown and dark brown
	Bottom	- green silt
	Depth	- 16 m
# 18		- red brown silt with odd light green layer (0.5 cm thick) of silt
	Depth	- 18 m
# 19	Top	- 0.25 cm red brown clayey silt
	Bottom	- gray brown clayey very fine silt
	Depth	- 15 m
# 20	Top	- 0.5 cm red brown clayey very fine silt
	Bottom	- green silt with odd dark brown layer
	Depth	- 15 m
# 21	Top	- 0.5 cm dark brown and red brown (hard) clayey very fine silt
	Bottom	- green clayey very fine silt, odd thin dark brown layer
	Depth	- 50 m

# 22		- medium to coarse sand
	Depth	- 3 m
# 23	Top	- 0.25 cm red brown clayey very fine silt
	Bottom	- green gray sandy silt with 0.5 cm dark brown layers
	Depth	- 9 m
# 24	Top	- 1 cm red brown clayey very fine silt
	Middle	- 1 to 1.5 cm dark brown clayey silt with odd sand grain
	Bottom	- green gray clayey silt with several 0.5 cm dark brown layers
	Depth	- 10 m
# 25	Top	- 2 cm red brown clayey silt with a 0.5 cm black brown layer
	Bottom	- green brown clayey very fine silt
	Depth	- 8 m
# 26	Top	- 1 cm red brown clayey silt
	Middle	- 4 cm brown green clayey silt with odd sand grain
	Bottom	- black and green layers of clayey silt
	Depth	- 8 m
# 27	Top	- 0.5 cm red brown clayey silt
	Bottom	- green gray clayey silt
	Depth	- 7.5 m
# 28	Top	- 0.5 to 1 cm brown red clayey silt
	Bottom	- medium brown silty clay
	Depth	- 9 m
# 29	Top	- 0.5 cm brown clayey silt to silty clay
	Middle	- 0.5 cm black silt
	Bottom	- green gray clayey silt
	Depth	- 9 m
# 30		- red brown silty very fine sand with some coarse grains
	Depth	- in river channel

# 31	Top	- 0.5 cm brown red clayey silt
	Middle	- 0.5 cm black clayey silt
	Bottom	- green brown clayey silt with 0.5 cm black clayey silt layers
	Depth	- 14 m
# 32		- brown red clayey silt to silty clay with some coarse grains
	Depth	- 13 m
# 33	Top	- 2.5 cm brown red silty clay
	Middle	- 4 cm dark brown red clay
	Bottom	- green brown silty clay with some coarse grains
	Depth	- 22 m
#34		- brown red clay, hardened near bottom of sample
	Depth	- 40 m
# 35		- brown red clay with specularite from tailings mixed in
	Depth	- 39 m
# 36	Top	- 1 to 2.5 cm brown red clay
	Bottom	- fine sandy silt (tailings)
	Depth	- 33 m
# 37	Top	- 2.5 cm brown red (dark) clay
	Bottom	- deep dark red clay
	Depth	- 11 m
# 38	Top	- 5 cm brown red silty clay, odd coarse grain
	Bottom	- green gray silty sand
	Depth	- 5 m
# 39	Top	- 3 to 5 cm brown red clayey silt, many coarse grains
	Bottom	- green gray silty sand
	Depth	- 3 m

40 Top - 3 to 5 cm brown red clayey silt, many coarse grains
Bottom - green brown silty sand
Depth - 2 m

41 - poorly sorted coarse sand with some silty layers
Depth - from stream along north side of Fermont Highway

42 - red brown clay
Depth - 49 m

43 Top - 2 cm red brown clay
Bottom - same as tailings
Depth - 42 m

44 - poorly sorted coarse sand with odd large pebble
- collected from north side of Fermont Highway

45 - poorly sorted medium to coarse sand from small stream on north side of Fermont Highway near the city dump

46 - poorly sorted medium sand from sand pit

47 - well sorted fine sandy soil

48 - well sorted coarse sand from spit into Wabush Lake

49 - poorly sorted fine sand from sand pit

50 - mixture of sand, peat, and silt at edge of stream

51 - medium sorted fine sand from south side of Fermont Highway

52 - poorly sorted silty sand along highway near city dump

53 - poorly sorted fine sand from sand pit

54 - poorly sorted silty sand from north side of Fremont Highway

55 - poorly sorted silty sand

56 - very poorly sorted brown red fine sand from west of Lorraine Lake

57 - poorly sorted red brown silty sand

58 - cross bedded sand and gravel deposits in road cut
- sands are very fine (A) and medium (B) and are both well sorted

TABLE 2: ROCK SPECIMEN DESCRIPTIONS

For the samples described below, fine = < 1 mm., medium = 1 to 2 mm., coarse = > 2 mm.

L-1

Quartz Specularite schist
Middle Wabush Iron Formation, Smallwood Mine, I.O.C.C.

- 25% fine to medium grained elongated specularite (gives the rock its schistosity.
- 70% quartz, medium grained, granular
- 5% stellate groups of white radiating anthophyllite fibres parallel to schistosity and individual acicular crystals scattered throughout sample

L-2

Quartz carbonate schist or gneiss
Lower Wabush Iron Formation, Smallwood Mine, I.O.C.C.

- 20% fine grained quartz, some bands contain much more quartz
- carbonate (calcite and ankerite) constitutes remainder of rock

L-3

Limonite
Lower Wabush Iron Formation, Smallwood Mine, I.O.C.C.

- yellow brown limonite, earthy, crumbles easily, found in vein 0.5 m thick

L-4

Grunerite fibres
Lower Wabush Iron Formation

- outcrop several metres diameter consisting of quartz veins and fibrous grunerite which was picked out of the rock
- grunerite fibres up to 10 cm. long, pale yellow brown colour.

L-5

Quartzite
Wapussakatoo (Carol) Formation

- almost 100% coarse grained euhedral quartz

L-6

Quartz grunerite carbonate gneiss
Lower Wabush Iron Formation

- 10% quartz, fine to medium grained, granular
- 40% grunerite, fibrous to acicular, crystals up to 1.5 cm
- 10% magnetite, medium grained, euhedral, concentrated in certain bands
- 40% ankerite, medium to coarse grained

L-7

Quartz grunerite schist
Lower Wabush Iron Formation

- rock contains quartz rich and carbonate rich bands, with more grunerite in quartz rich ones
- some bands contain up to 80% grunerite
- grunerite-coarse grained, acicular, brown colour, up to 1.5 cm crystals, oriented parallel to schistosity
- finer grained grunerites, 0.5 cm, cut across foliation
- odd stellate group (<0.5 cm. dia.) of actinolite

L-8

Quartz grunerite gneiss
Lower Wabush Iron Formation

- quartz rich and grunerite rich bands
- grunerite, light to dark brown colour, acicular, coarse grained, appear like dis-oriented clusters of stellate groups in the grunerite rich bands
- some crystals 1.0 cm long
- hematite (10% of rock) scattered through the quartz rich bands
- quartz is white, medium grained, granular

L-9

Quartz grunerite actinolite gneiss
Upper Wabush Iron Formation

- coarse grained, acicular, medium green colour bands of interwoven actinolite and grunerite alternating with medium to coarse grained quartz bands
- amphibole crystals oriented parallel to gneissic banding

L-10

Quartz grunerite schist
Lower Wabush Iron Formation

- bands of grunerite alternating with quartz rich bands
- grunerite is light to medium brown colour, coarse grained, acicular (crystals up to 2 cm) oriented parallel to banding
- minor medium grained ankerite and siderite

L-11

Biotite schist
Katsao Formation

- contains biotite, quartz, alkali feldspar, some plagioclase, and minor hornblende

L-12

Hornblende garnet schist

- contains red garnet porphyroblasts up to 2 mm diameter

L-13

Grunerite fibres
Lower Wabush Iron Formation

- fibres picked from an outcrop of quartz grunerite schist
- grunerite is fibrous, light yellow brown colour,
- some fibres up to 10 cm long

L-14

Gabbro
Shabogamo Formation

- more than 90% calcium plagioclase, coarse grained, randomly oriented laths
- minor pyroxene, magnetite and biotite

L-15

Biotite schist
Katsao Formation

- similar to sample L-11

L-16

Marble
Duley Formation

- coarse grained, euhedral, white and clear calcite crystals
- weathered surface is light yellowy green

L-17

Tremolite
Duley Formation

- marble similar to L-16 but contains scattered masses of radiating tremolite crystals
- tremolite is white to pale green, acicular
- some crystals up to 5 cm long

L-20

Quartz specularite schist
Upper Wabush Iron Formation

- rock contains quartz rich and specularite rich bands
- quartz is medium grained, euhedral, contains blebs of specularite
- specularite grains are micaceous, fine grained, and oriented parallel to banding

L-21

Marble
Duley Formation

- similar to L-16

L-22A

Quartz grunerite schist
Lower Wabush Iron Formation

- bands of almost 100% grunerite alternating with quartz-rich bands
- quartz is fine grained, euhedral, granular
- odd thick band of green fine to medium grained hedenbergite
- minor anhedral to euhedral magnetite
- grunerite is coarse grained, medium brown colour, acicular (crystals up to 1.5 cm) has glassy appearance, and is oriented parallel to gneissic banding

L-22B

Quartz grunerite actinolite schist
Lower Wabush Iron Formation

- quartz is euhedral, fine grained
- grunerite is medium brown colour, coarse grained acicular, constitutes more than 50% of rock, oriented
- several bands containing dark green medium grained elongated actinolite, oriented parallel to foliation
- some ellipsoidal magnetite grains (1 cm long) oriented parallel to foliation

L-23

Quartz specularite anthophyllite schist
Upper Wabush Iron Formation

- anthophyllite occurs in thin layers (<0.2 cm thick) crystals are coarse grained, fibrous and light gray colour
- quartz specularite layers up to 0.75 cm thick
- odd quartz vein containing thin layers of light green muscovite

L-24

Marble
Duley Formation

- medium grained white calcite
- rock is very friable due to weathering
- odd large quartz inclusion

L-25

Quartz grunerite actinolite schist
Lower Wabush Iron Formation

- 25% actinolite, greenish brown colour, medium grained acicular
- 25% grunerite, medium to dark brown, coarse grained acicular (up to 1 cm)
- quartz represents majority of remaining constituents
- amphibole and quartz bands alternate
- the grunerite rich amphibole bands are coarser grained

L-26

Quartz grunerite schist
Lower Wabush Iron Formation

- 75% fine grained, euhedral, granular quartz
- 20% fine grained, grayish acicular grunerite
- 5% fine grained magnetite
- orientation of amphibole gives rock its schistosity

L-27

Quartz specularite schist
Upper Wabush Iron Formation

- 85% fine to medium grained granular quartz
- 15% fine to medium grained specularite

L-28

Quartzite
Wapussakatoo Formation

- medium to coarse grained, white to light gray quartz

L-29A

Quartz grunerite schist
Lower Wabush Iron Formation

- 5% brown fine grained eulite
- 30% fine grained, acicular (needles up to 0.5 cm) pale brown grunerite
- 65% fine to medium grained euhedral quartz
- grunerite oriented parallel to foliation
- some thick bands (> 2 cm) are almost 100% grunerite
- rock has been intensely weathered, making it very friable and the grunerite almost fibrous
- the eulite is closely associated with grunerite

L-29B

Quartz grunerite schist
Lower Wabush Iron Formation

- similar toL-29A but contains 10% anhedral magnetite scattered throughout and no pyroxene

L-29C

Quartz grunerite schist
Lower Wabush Iron Formation

- 80% dark green very coarse grained grunerite
- 10 % fine to medium grained, granular quartz
- 10 % medium grained ankersite

L-30

Muscovite schist
Katsao Formation

- muscovite plates up to 1 cm across
- quartz crystals as large as 2 cm present

L-31

Marble
Duley Formation

- similar to L-24

L-32

Quartz specularite anthophyllite rock
Upper Wabush Iron Formation, south pit, Wabush Mines

- 20% anthophyllite occurring in radiating groups of fibres up to 1.5 cm long, white in colour
- 50% fine to medium grained, euhedral, granular quartz
- 30% specularite, medium grained, minor siderite

L-33 to L-44

- collected from Wabush Mines. None of these samples contained significant amounts of amphiboles and were collected only to get a representative suite of rocks from the mine

L-45

Quartz grunerite schist or gneiss
Lower Wabush Iron Formation

- outcrop 10 m x 2 m
- bands of quartz rich and grunerite rich in 5- 10 cm bands
- grunerite is dark brown green in colour, coarse grained, acicular (almost platey) oriented to give grunerite layers a schistose appearance
- quartz rich layers are almost entirely composed of coarse white quartz crystals

L-46

Quartz grunerite schist
Lower Wabush Iron Formation

- 15% fine grained, beige colour, acicular grunerite which is oriented to give rock its schistosity
- 20% fine grained euhedral quartz
- rest of rock is carbonate
- limonite stains throughout rock

L-47A

Quartz grunerite schist
Lower Wabush Iron Formation

- 50% fine grained, light brown, acicular grunerite
- some large grunerite crystals up to 1 cm long
- 50% euhedral fine grained quartz
- odd euhedral magnetite octahedron
- rock is intensely folded and the schistosity is due to alignment of the grunerite

L-47B

Quartz grunerite schist
Lower Wabush Iron Formation

- quartz rich and grunerite rich bands varying in thickness from 0.3 cm to 3.5 cm
- grunerite (> 80% in grunerite rich bands) is medium to coarse grained, medium to dark brown, acicular, and oriented to give rock a schistose appearance
- quartz (> 95% in quartz rich bands) is fine grained, white, and granular
- odd magnetite grain present

L-48

Quartz grunerite schist
Lower Wabush Iron Formation

- fine to medium grained, light brown, acicular grunerite
- minor dark brown grunerite up to 0.75 cm long crystals
- grunerite crystals oriented
- rock has limonite staining throughout

L-49

Quartz grunerite schist
Lower Wabush Iron Formation

- 20% fine to medium grained, medium brown, acicular grunerite
- 20% fine grained granular quartz
- 60% fine to medium grained carbonates
- carbonates and quartz concentrated in separate bands
- grunerite irregularly dispersed throughout rock but oriented to give rock a foliated appearance

L-50

Quartz specularite schist
Upper Wabush Iron Formation

- fine grained granular quartz and fine grained specularite

L-51A

Quartz grunerite schist
Lower Wabush Iron Formation

- banded with alternating quartz rich and grunerite rich bands
- quartz is fine grained, euhedral, granular
- grunerite is coarse grained, medium brown colour, acicular (crystals up to 1.5 cm long) glassy in appearance, and oriented parallel to banding
- the grunerite rich bands are almost 100% grunerite

L-51B

Quartz grunerite schist
Lower Wabush Iron Formation

- medium to coarse grained, light brown, acicular grunerite
- some bands almost pure grunerite
- fine to medium grained white quartz
- grunerites oriented to give rock foliated appearance
- 10% elongated magnetite particles up to 0.75 cm long

L-52

Quartz grunerite specularite schist
Upper Wabush Iron Formation

- grunerite is light brown, medium grained, acicular and concentrated in thin bands
- some limonite staining

L-53

Quartz grunerite schist
Lower Wabush Iron Formation

- 30% light beige, acicular to fibrous (some fibres up to 5 cm long) grunerite
- quartz is fine to medium grained and elongated parallel to schistosity
- some bands are almost pure grunerite
- minor limonite staining, minor medium grained siderite

L-54

Quartz grunerite schist
Lower Wabush Iron Formation

- similar to L-53 but has several carbonate rich bands containing ankerite

L-55

Quartz grunerite schist

- fine grained, light beige colour, acicular grunerite oriented parallel to schistosity
- fine grained, granular quartz
- some ankerite rich bands
- limonite staining on weathered surface

L-56

Quartz grunerite schist
Lower Wabush Iron Formation

- fine grained, beige colour, acicular grunerite oriented parallel to schistosity
- fine grained granular quartz
- several thick ankerite rich bands
- intense limonite staining on weathered surfaces

L-57

Quartz grunerite schist
Lower Wabush Iron Formation

- light beige, fibrous grunerite concentrated in thin bands, gives schistosity to rock
- quartz is fine to medium grained (approx. 30%)
- ankerite is medium to coarse grained (approx 50%) and concentrated in bands

L-58

Quartz grunerite schist
Lower Wabush Iron Formation

- fine grained, light brown, acicular grunerite concentrated in highly contorted bands
- fine grained, granular carbonate (calcite and siderite) and quartz bands
- rock is intensely deformed

L-59

Actinolite schist
Ashuanapi Complex

- fine grained, medium green colour (actinolite) constitutes major rock component

L-60

Quartz limonite riebeckite schist
Lower Wabush Iron Formation

- 50% fine grained euhedral quartz
- 30% limonite
- 20% fibrous magnesioriebeckite arranged in scattered stellate groups, oriented parallel to schistosity, dark blue in colour
- some limonite staining on weathered surfaces

L-61

Quartz grunerite schist
Lower Wabush Iron Formation

- 30% fine grained, acicular to fibrous grunerite oriented to give schistosity to rock
- 70% fine grained, euhedral, granular quartz
- some limonite staining

L-62

Quartz cummingtonite schist
Lower Wabush Iron Formation

- 20% fine grained, intensely deformed, light brown colour, fibrous to acicular cummingtonite
- thin ankerite and quartz bands parallel the schistosity
- intense limonite staining in the ankerite bands

L-63

Quartz grunerite schist
Lower Wabush Iron Formation

- > 50% fine grained, light brown, acicular grunerite concentrated in intensely deformed thin bands
- fine grained quartz, highly concentrated in some bands

L-64

Actinolite schist
Lower Wabush Iron Formation

- fine to medium grained, green coloured actinolite
- fine to medium grained granular carbonates in thin bands alternating with fine grained, granular quartz rich bands

TABLE 3: MINERAL FIBRES IN 1976 WATER SAMPLES

Sample No.	Concentration (fibres/Lx10^6)	Standard Deviation (x10^6)	Average Length/ Width Ratio	Sample Depth (Metres)
76-1	2.1	2.9	-	0
76-2	2.2	3.0	-	0
76-3	no data			
76-4	2,200	590	-	0
76-5	57	32	-	0
76-6	1,200	200	-	0
76-7	2.1	2.9	-	-
76-8	5.8	3.9	-	-
76-9	13	3.9	-	0
76-10	6.1	5.2	-	0
76-11	6.1	2.4	-	0
76-12	0	-	-	0
76-13A	84	25	-	0
76-13B	140	66	-	3
76-14	570	130	13.1:1	0
76-15A	660	130	-	0
76-15B	3,700	200	-	9
76-16	7.0	2.7	-	0
76-17A	11	4.4	-	0
76-17B	15	11	-	6
76-17C	16	4.3	-	15
76-18A	2.5	2.9	-	0
76-18B	59	25	30:1	10.5
76-19	4.9	0	-	0
76-20A	290	140	10:1	0
76-20B	9.4	3.8	-	9
76-20C	360	90	21:1	21
76-21A	66	20	-	0
76-21B	100	35	40:1	9

TABLE 3: Continued

76-22	150	18	-	0
76-23	12	8.2	-	0
76-24	13	5.4	-	0
76-25	5.9	3.9	-	0
76-26	1.3	2.6	-	0
76-27	35	14	-	0
76-28	4.7	5.6	-	0
76-29	1.0	2.0	-	0
76-30	17	8.4	-	0
76-31	55	20	-	0
76-32	13	7.3	50:1	0
76-33	310	31	-	0
76-34	140	20	-	0
76-35A	150	25	-	0
76-35B	190	41	-	9
76-35C	51	3.8	-	21
76-36A	54	18	-	0
76-36B	220	25	-	9
76-36C	54	23	-	21
76-37	1.3	2.6	-	0
76-38A	16	12	-	0
76-38B	2.3	2.7	-	9
76-39A	11	11	-	0
76-39B	57	8.3	-	9
76-40A	34	10	-	0
76-40B	8.6	8.4	-	9
76-41A	31	8.4	5:1	0
76-41B	15	9.1	-	3
76-42A	30	12	10:1	0
76-42B	8.9	4.9	-	7.5
76-43	13	8.0	-	0
76-44	2.2	2.5	-	0
76-45	6.0	2.4	-	0
76-46	6.0	4.6	-	0
76-47	13	7.3	-	0

TABLE 3: Continued

76-48	3.9	7.9	-	0
76-49	10	4.1	-	0
76-50	6	6.1	-	0
76-51	0	-	-	0

TABLE 4: MINERAL FIBRES IN 1977 WATER SAMPLES

Sample No.	Concentration (fibres/Lx10^6)	Standard Deviation (X10^6)	Fibre Mass Amphibole NG/L	Other NG/L	Total NG/L	Average Length/Width Ratio	Sample Depth (Metres)
CL-1	39	10	-	480	480	8.5:1	
CL-2	33	9.0	-	-	-		
CL-3	44	10	-	-	-		
CL-4	65	17	200	1100	1300	7.5:1 amph. 5.25:1 other 6.65:1 total	
CL-5	47	12	-	-	-		
CL-6	110	13	1300	360	1660	7.25:1 amph. 9.35:1 other 7.85:1 total	
77-1	72	18	-	620	620	6.45:1 total	0
77-2	3.9	4.6	-	56	56	5.5:1 total	0
77-3	60	15	-	580	580	8.5:1 total	0
77-4	no data						
77-5	no data						
77-6	45	11	270	90	360	11.5:1 amph. 8.75:1 other 10.5:1 total	0
77-7	83	18	-	-	-		0
77-8	60	16	-	660	660	9.0:1 total	0
77-9	220	28	-	-	-		0
77-10	140	33	-	-	-		0
77-11	57	6.5	-	-	-		0

TABLE 4: continued

77-12	190	27	-	2600	2600	8.0:1	total	0
77-13A	660	46	-	-	-			0
77-13B	500	150	-	6600	6600	9.0:1	total	6
77-14A	490	40	-	-	-			0
77-14B	390	53	-	-	-			10
77-14C	570	120	-	-	-			20
77-14D	2100	270	40,000	0	40,000	10.65:1	total	24
77-15A	910	130	-	-	-			0
77-15B	850	27	-	-	-			8
77-15C	550	75	3000	3000	6000	7.0:1 9.0:1 7.9:1	amph. other total	16
77-16A	53	10	-	760	760	7.35:1	total	0
77-16B	830	100	-	-	-			8
77-16C	2100	270	25,000	0	25,000	8.5:1	total	14
77-17A	710	73	-	-	-			0
77-17B	1800	260	-	-	-			8
77-17C	850	39	-	-	-			16
77-18A	370	59	-	-	-			0
77-18B	760	85	-	-	-			8
77-19B	140	49	230	600	830	6.5:1 7:1 7:1	amph. other total	0
77-20	61	8.0	-	820	820	7.0:1	total	0
77-21	520	71	-	-	-			0
77-22A	73	7.9	-	1500	1500	8.35:1	total	0
77-22B	1200	580	-	-	-			10

TABLE 4: continued

77-23A	470	120	-	-	-		0
77-23B	2300	170	-	-	-		6
77-24	1300	160	-	-	-		0
77-25	690	78	-	-	-		0
77-26	540	26	-	-	-		0
77-27A	560	30	-	-	-		0
77-27B	530	120	-	-	-		8
77-28A	310	37	4900	111	6000	7:1 amph. 10:1 other 9:1 total	0
77-28B	110	38	-	-	-		3
77-29A	53	9.5	-	-	-		0
77-29B	19	5.4	35	87	122	9:1 amph. 7.35:1 other 8:1 total	10
77-30	20	6.6	130	81	211	9:1 amph. 7:1 other 8:1 total	0
77-31A	300	72	-	-	-		0
77-31B	470	110	-	-	-		10
77-32	180	9.7	-	-	-		0
77-33	110	15	-	1700	1700	8.3:1 total	0
77-34	12	4.1	-	66	66	7.0:1 total	0
77-35	25	7.0	-	440	440	6.25:1 total	0
77-36	9.2	4.2	-	120	120	5.85:1 total	0
77-37	160	11	-	-	-		0
77-38	12	4.5	-	210	210	6.35:1 total	0
77-39	28	7.5	-	-	-		0

TABLE 4: continued

77-40	27	3.0	-	-	-		0
77-41	25	4.7	-	-	-		0
77-42	22	8.2	-	-	-		0
77-43	87	17	-	-	-		0
77-44	3.4	4.3	-	-	-		0
77-45	81	11	-	-	-		0
77-46	56	5.7	-	-	-		0
77-47	11	5.4	-	-	-		0
77-48	50	1.2	-	-	-		0
77-49	49	12	-	-	-		0
77-50	19	3.7	-	-	-		0
77-51	1000	66	-	-	-		0
77-52	37	8.7	-	-	-		0
77-53	20	5.1	-	-	-		0
77-54	22	9.1	-	-	-		0
77-55	16	3.0	90	45	135	6.35:1 amph. 7:1 other 7:1 total	0
77-56	23	7.5	-	-	-		0
77-57	14	3.7	190	140	330	9.15:1 amph. 8.5:1 other 8.5:1 total	0
77-58	3	2.3	-	-	-		0
77-59	18	18	-	-	-		0
77-60	13	6.6	-	-	-		0
77-61	9.6	4.4	-	-	-		0
77-62	450	130	-	-	-		0

TABLE 4: continued

77-63	2000	750	4100	0	4100	13:1 total	0
77-64A	240	52	-	-	-		0
77-64B	200	55	-	-	-		10
77-65A	120	32	-	-	-		0
77-65B	300	35	-	-	-		4
77-66A	190	42	-	-	-		0
77-66B	380	55	-	-	-		9
77-67A	44	8.2	-	-	-		0
77-67B	31	3.7	-	-	-		3
77-68	12	3.6	-	-	-		0
77-69	10	6.3	-	170	170	4.85:1 total	0
77-70A	29	12	-	430	430	8.2:1 total	0
77-70B	91	13	-	-	-		7
77-71	no data						
77-72	no data						
77-73	39	7.8	-	310	310	6.5:1 total	0
77-74A	90	17	-	-	-		0
77-74B	73	17	-	-	-		12
77-74C	41	15	-	-	-		24
77-75A	32	6.9	-	1500	1500	9:1 total	0
77-75B	57	13	-	-	-		12
77-75C	55	18	-	-	-		24
77-76	57	23	-	-	-		0
77-77	no data						
77-78	8.2	2.4	-	49	49	5.5:1 total	0

TABLE 4: continued

77-79	27	8.4	-	-	-			0
77-80A	4.8	2.7	-	48	48	8:1	total	0
77-80B	17	3.2	-	-	-			8
77-81A	12	3.6	-	-	-			0
77-81B	2.2	2.0	-	16	16	6:1	total	2
77-82A	6.1	2.5	-	-	-			0
77-82B	7.7	8.8	-	-	-			1
77-83A	8.7	2.7	-	-	-			0
77-83B	37	4.7	-	-	-			4
77-84A	11	6.3	-	110	110	6.5:1	total	0
77-84B	19	3.4	-	-	-			10
77-85A	11	9.5	-	-	-			0
77-85B	58	44	-	-	-			10
77-86A	66	14	-	-	-			0
77-86B	32	8.8	-	-	-			10
77-87A	82	35	-	1100	1100	7:1	total	0
77-87B	20	8.6	-	-	-			10
77-88	92	10	-	-	-			0
77-89A	160	61	-	-	-			0
77-89B	160	58	-	-	-			12
77-89C	210	57	-	-	-			24
77-90	6.5	5.5	-	190	190	7.6:1	total	0
77-91	no data							
77-92	4.8	2.2	-	450	450	6.95:1	total	0
77-93	no data							

TABLE 4: continued

77-94	no data						
77-95	no data						
77-96	280	35	2100	2600	4700	7.1:1 amph. 6.4:1 other 6.65:1 total	0
77-97	no data						
77-98	no data						
77-99	no data						
77-100A	840	160	-	-	-		0
77-100B	950	220	-	-	-		8
77-101A	740	160	-	-	-		0
77-101B	850	470	-	-	-		8
77-101C	1200	440	-	-	-		16
77-102	1000	350	-	-	-		0
77-103	1600	130	-	-	-		0
77-104A	1500	84	-	-	-		0
77-104B	1100	290	-	-	-		10
77-104C	1900	160	-	-	-		20
77-104D	2100	260	-	-	-		24
77-105A	1100	190	-	-	-		0
77-105B	1600	170	-	-	-		6
77-106	740	130	-	-	-		0
77-107	86	11	-	-	-		0
77-108	72	13	-	-	-		0
77-109	850	74	-	-	-		0
77-110	26	4.9	-	-	-		0

TABLE 4: continued

77-111	39	5.1	-	-	-	0
77-112	49	8.0	-	-	-	0
77-113	28	13	-	-	-	0

TABLE 5: ENERGY DISPERSIVE X-RAY FLUORESCENCE ANALYSES OF AMPHIBOLES IN WATER SAMPLES

SAMPLE 77-12

Probable Amphibole	SiO_2	Al_2O_3	FeO	MgO	CaO	Na_2O	K_2O	TiO_2	MnO	P_2O_5	S	Cl	Cr_2O_3
Grunerite	45.96	.04	40.62	10.65	.22	0	0	0	2.16	.19	0	.16	0
"	48.29	.07	36.66	11.92	.09	1.25	0	.01	1.33	.27	0	.11	0
"	42.57	.02	44.45	11.41	0	.43	.01	.01	.96	.02	.13	0	0
Riebeckite	47.90	.40	35.25	11.22	0	2.53	0	.11	1.54	.32	.73	0	0
Cummingtonite	50.64	.22	29.43	17.72	.07	1.19	0	0	.27	.22	.24	0	0
Mn-Cummingtonite	52.93	.61	13.89	23.30	.22	.86	0	.01	7.63	.54	0	0	0
Anthophyllite	49.67	.53	17.35	21.55	.26	4.72	0	.07	4.95	.73	.17	0	0

SAMPLE 77-13 B

Mn-Cummingtonite	52.50	.50	12.70	21.51	.94	.60	.40	.04	9.73	.51	.31	.24	0
Anthophyllite	53.59	.10	16.31	23.34	.52	.80	.06	.03	4.65	.33	.04	.24	0

SAMPLE 77-14 B

Anthophyllite	52.85	.34	18.55	21.24	.77	1.39	.62	0	3.10	0	.08	1.60	0
"	56.66	0	17.81	23.89	0	.95	0	0	.44	0	0	.25	0
Hornblende	42.25	6.23	32.83	10.33	7.41	0	.49	0	.37	0	.09	0	0
Grunerite	49.72	.13	35.76	.27	.84	3.21	4.27	0	1.71	.29	.15	3.53	.14

Table 5 continued

Probable Amphibole	SiO_2	Al_2O_3	FeO	MgO	CaO	Na_2O	K_2O	TiO_2	MnO	P_2O_5	S	Cl	Cr_2O_3
SAMPLE 77-15 C													
Grunerite	48.78	.16	44.36	4.80	.24	.66	.03	0	.84	.13	0	0	0
Anthophyllite	55.21	.16	15.34	22.46	.19	.64	.19	.30	5.29	.19	0	0	.02
"	54.98	0	18.37	19.45	.19	.41	.23	.57	2.75	0	0	0	2.26
"	60.63	1.31	9.37	22.63	.09	.79	.21	.01	4.36	.10	.08	.16	.30
"	58.01	.54	10.73	25.01	.34	1.72	.24	0	3.21	.06	0	0	0
SAMPLE 77-19													
Grunerite	47.74	1.55	40.20	3.61	0	.01	1.12	.44	5.32	0	0	0	0
SAMPLE 77-30													
Actinolite	58.24	3.80	18.37	6.85	10.49	.97	1.10	.18	0	0	0	0	0
SAMPLE 77-31B													
Riebeckite	39.79	.99	47.06	0	0	6.71	2.06	0	0	0	.14	3.01	.24
SAMPLE 77-33													
Cummingtonite	48.95	.34	34.14	12.62	0	2.27	.15	0	.61	.55	.38	0	0

Table 5 continued

Probable Amphibole	SiO_2	Al_2O_3	FeO	MgO	CaO	Na_2O	K_2O	TiO_2	MnO	P_2O_5	S	Cl	Cr_2O_3
SAMPLE 77-38													
Grunerite	47.68	.54	45.73	3.71	.12	0	.45	0	.98	0	0	.58	.23
Anthophyllite	66.22	.13	7.10	26.55	0	0	0	0	0	0	0	0	0
SAMPLE 77-73A													
Cummingtonite	52.66	.92	14.37	18.68	.29	5.21	.02	0	6.43	.90	.38	.15	0
SAMPLE 77-98B													
Grunerite	51.35	.65	36.75	9.51	0	0	.55	0	.94	.05	0	.20	0
SAMPLE 77-104D													
Anthophyllite	60.81	.27	8.67	27.72	.19	1.75	0	0	.23	.08	0	0	.28
SAMPLE 77-105B													
Grunerite	43.11	0	53.17	2.64	.19	0	0	0	.89	0	0	0	0
"	45.26	0	47.16	5.29	.51	0	.03	.04	1.59	0	0	0	.12
Anthophyllite	62.91	0	9.41	25.40	.29	0	0	.10	1.49	0	.40	0	0

TABLE 6: X-RAY FLUORESCENCE ANALYSES OF TAILINGS, SEDIMENTS AND SOILS

SAMPLE	SiO_2	Al_2O_3	FeO	MgO	CaO	Na_2O	K_2O	TiO_2	MnO	P_2O_5
1-Top	43.76	12.13	20.20	1.76	2.44	2.40	1.41	0.32	15.30	0.29
1-Bot.	50.37	13.59	15.40	2.31	2.39	2.32	2.04	0.45	10.84	0.30
2-Top	49.12	5.02	37.12	1.96	1.24	0.95	0.92	0.23	3.07	0.38
2-Bot.	64.75	11.41	13.13	2.53	1.81	2.10	1.91	0.47	1.33	0.56
3	44.65	2.64	43.56	2.50	2.34	0.15	0.50	0.11	3.31	0.24
4	44.32	2.55	42.97	2.64	2.67	0.89	0.49	0.11	3.14	0.23
5	55.35	11.00	11.22	2.55	2.21	2.26	2.10	0.50	12.43	0.38
6	64.17	14.71	8.73	3.46	1.98	2.90	2.97	0.70	0.18	0.19
7-Bot.	69.10	10.35	10.15	2.20	1.80	2.16	1.67	0.44	1.87	0.26
8-Bot.	59.12	9.46	16.09	2.01	1.86	2.26	1.83	0.41	6.03	0.92
9-Bot.	54.35	10.13	11.83	1.95	1.88	2.05	2.00	0.42	15.01	0.39
10	65.44	13.32	9.75	2.34	2.36	2.91	2.52	0.47	0.52	0.36
11	66.29	12.69	9.18	2.28	2.29	2.73	2.48	0.45	1.22	0.39
12	68.15	12.43	9.06	2.26	2.12	2.56	2.22	0.49	0.42	0.29
14-Bot.	69.71	9.93	11.43	1.81	1.88	2.37	1.64	0.45	0.52	0.26
15	66.32	12.42	11.11	2.71	1.77	2.11	2.04	0.52	0.61	0.40
16	71.83	12.16	6.45	2.00	2.01	2.50	2.26	0.44	0.12	0.24
17-Top	69.89	11.81	8.59	1.87	1.87	2.48	2.23	0.45	0.29	0.52
18	64.65	14.25	10.00	2.23	2.00	2.70	2.60	0.50	0.68	0.40
19-Bot.	63.43	15.86	8.04	3.32	2.17	2.87	3.22	0.79	0.14	0.17
20-Bot.	63.99	9.21	8.54	1.76	1.64	1.70	1.71	0.37	10.69	0.39
21-Bot	63.66	9.38	14.86	1.65	1.71	1.71	1.67	0.40	4.03	1.24

TABLE 6: continued

22	68.26	9.10	14.96	1.20	1.72	2.65	1.54	0.35	0.12	0.09
23-Bot	70.74	10.36	10.36	1.48	1.63	2.60	1.65	0.34	0.63	0.20
24-Top	61.96	9.91	11.70	2.26	1.75	1.70	1.70	0.42	8.26	0.34
24-Mid.	51.39	8.83	8.15	1.84	1.79	1.54	1.74	0.40	24.05	0.28
24-Bot.	66.96	11.83	10.12	2.48	1.71	1.99	1.92	0.48	2.12	0.39
25-Bot.	59.36	10.00	15.48	2.00	1.82	2.21	1.64	0.41	6.64	0.45
26-Mid.	68.69	11.04	10.30	2.45	1.82	1.84	1.73	0.44	1.26	0.43
26-Bot.	56.62	9.68	8.86	2.06	1.80	1.89	1.72	0.41	16.56	0.38
27-Top	69.24	7.96	14.37	1.93	1.54	1.55	1.33	0.33	1.02	0.73
27-Bot.	77.96	8.83	5.64	2.11	1.48	1.72	1.44	0.35	0.17	0.31
28-Top	53.25	6.60	31.25	2.06	1.40	1.27	1.05	0.27	2.48	0.37
28-Bot	62.93	13.39	13.44	2.23	1.81	2.04	1.88	0.47	1.20	0.62
29-Bot	57.97	10.52	15.69	1.85	2.16	2.20	1.86	0.38	6.56	0.81
30	70.54	11.16	10.38	1.30	1.88	2.51	1.60	0.28	0.23	0.13
31-Top	50.69	5.40	34.67	2.26	1.42	0.77	0.90	0.24	3.28	0.36
31-Mid.	54.64	9.23	14.07	2.30	2.93	1.91	1.54	0.36	12.44	0.57
31-Bot	54.67	10.48	11.12	2.50	2.83	1.97	1.66	0.40	13.60	0.76
32	51.13	5.69	34.12	2.38	1.40	1.18	1.01	0.25	2.58	0.26
33-Top	42.66	3.12	45.19	2.48	2.76	0.22	0.59	0.10	2.71	0.19
33-Mid.	49.28	3.35	36.92	3.33	2.74	0.33	0.62	0.15	3.08	0.21
33-Bot.	55.92	0.13	23.76	2.61	1.90	0.81	1.54	0.44	2.39	0.49
34	44.96	2.59	41.89	3.21	4.09	0.21	0.53	0.09	2.26	0.17
35	52.48	1.38	36.23	3.04	5.15	0.23	0.39	0.06	0.96	0.09
38-Top	66.23	8.00	19.15	1.54	1.32	2.06	0.95	0.32	0.33	0.11
38-Bot.	72.27	9.08	11.73	1.61	1.53	2.13	1.04	0.38	0.14	0.10
39-Top	61.83	6.27	26.09	1.18	1.18	1.78	0.88	0.22	0.43	0.14
40-top	53.11	4.61	35.50	0.67	0.78	1.37	0.88	0.15	2.84	0.10

TABLE 6: continued

41	66.33	13.12	10.31	2.10	2.40	3.04	1.94	0.41	0.18	0.16
42	49.11	1.55	38.43	3.24	5.19	0.11	0.34	0.06	1.81	0.15
43-Bot.	61.36	0.45	31.89	2.02	3.17	0.30	0.23	0.04	0.46	0.08
49	70.35	11.63	9.00	1.61	1.86	2.89	1.96	0.36	0.25	0.08
50	68.55	13.15	8.39	1.83	2.76	2.92	1.74	0.41	0.16	0.10
52	63.43	11.29	15.56	1.90	2.66	2.77	1.53	0.58	0.20	0.09
53	68.78	11.60	10.72	1.71	2.49	2.66	1.39	0.41	0.15	0.09
54	58.86	8.12	24.50	1.89	2.52	1.79	1.02	0.74	0.44	0.13
55	65.23	6.16	23.56	0.94	0.88	1.01	0.99	0.30	0.91	0.02
56	69.22	10.03	14.59	0.73	1.47	1.94	1.56	0.20	0.17	0.10
57	57.20	5.15	33.13	1.04	0.87	1.03	0.84	0.24	0.45	0.04
TAILINGS	65.90	0.25	29.94	1.17	1.93	0.27	0.19	0.03	0.29	0.05

TABLE 7: ENERGY DISPERSIVE X-RAY FLUORESCENCE ANALYSES OF AMPHIBOLES IN SEDIMENTS AND SOILS (wt.% oxides)

Probable Amphibole	SiO_2	Al_2O_3	FeO	MgO	CaO	Na_2O	K_2O	TiO_2	MnO	P_2O_5	S	Cl	Cr_2O_3
SAMPLE 1 (Top)													
Grunerite	40.98	2.98	50.21	.53	.24	0	.44	.17	3.58	.18	.01	.42	.34
Gedrite	43.20	17.00	19.95	15.16	0	0	1.10	2.74	.06	0	0	0	.78
"	43.81	16.61	20.78	14.25	.08	0	3.64	.40	0	.08	0	0	.35
"	40.98	14.51	29.76	9.35	.87	1.82	1.11	.39	0	0	0	.29	.91
"	38.79	19.21	32.35	8.66	.21	.25	.05	.48	0	0	0	0	0
SAMPLE 1 (Bottom)													
Anthophyllite	58.74	1.66	13.64	23.83	.20	.88	.43	.01	.32	.28	0	0	0
Gedrite	49.21	13.40	26.69	8.58	1.67	0	0	.30	0	0	0	.16	0
"	40.41	15.40	29.40	10.34	.40	0	3.64	.04	.28	0	0	.8	0
SAMPLE 3													
Grunerite	60.20	1.20	37.09	0	.15	0	.07	0	1.04	.06	0	.01	.19
"	42.08	.98	42.57	1.24	2.04	.04	.06	.10	10.36	.01	.02	.00	.52
Anthophyllite	62.39	.97	11.22	21.74	0	2.91	0	.01	.25	.03	.01	.13	.34
Cummingtonite	44.46	6.75	24.71	19.32	.78	1.38	.40	0	.53	0	.09	.03	1.55
Gedrite	36.82	9.73	35.08	10.34	2.25	.35	2.66	.18	1.48	0	.04	.29	.80

Table 7 continued

SAMPLE 4

Probable Amphibole	SiO_2	Al_2O_3	FeO	MgO	CaO	Na_2O	K_2O	TiO_2	MnO	P_2O_5	S	Cl	Cr_2O_3
Grunerite	48.50	5.47	44.97	.15	0	0	0	.12	.46	0	.04	.12	.16
Anthophyllite	57.21	.05	13.66	25.98	.19	1.34	.03	0	1.22	.18	.14	0	0
"	61.17	.45	9.18	23.90	0	1.89	0	0	3.41	0	0	0	0
Grunerite	59.10	1.48	38.68	.44	0	0	0	0	.30	0	0	0	0
Cummingtonite	60.97	.40	27.15	10.29	0	0	.33	0	.63	.05	0	0	.18
"	48.57	3.84	32.35	12.92	.22	0	.79	.06	.11	.12	0	1.04	0
Gedrite	36.17	16.72	28.25	16.29	0	0	2.58	0	0	0	0	0	0

SAMPLE 5

Gedrite	37.67	16.47	28.96	12.95	.01	0	2.02	.29	.93	0	.06	.59	.05
"	37.75	15.15	27.99	19.11	0	0	0	0	0	0	0	0	0

SAMPLE 9 (Bottom)

Grunerite	55.97	4.92	35.33	.17	.16	0	1.06	.10	0	.36	.82	.47	.64
Gedrite	41.03	15.57	24.04	15.04	.21	0	3.50	.62	0	0	0	0	0

Table 7 continued

Probable Amphibole	SiO_2	Al_2O_3	FeO	MgO	CaO	Na_2O	K_2O	TiO_2	MnO	P_2O_5	S	Cl	Cr_2O_3
SAMPLE 11													
Grunerite	46.99	1.43	43.37	0	2.37	.60	1.62	.12	1.91	.28	.98	0	.34
Cummingtonite	42.64	7.70	32.61	6.87	1.63	.45	1.21	0	3.37	.08	3.00	0	.42
Gedrite	38.29	14.05	27.54	11.58	.75	0	3.66	1.19	2.43	0	.48	.03	0
SAMPLE 14 (Bottom)													
Grunerite	58.62	4.56	34.88	.24	.46	0	.13	.04	.55	.13	.24	0	.15
"	51.14	5.43	41.11	0	.18	0	.22	0	.74	.38	.54	.26	0
Gedrite	49.44	15.84	25.89	8.80	0	.01	0	0	0	0	0	0	0
SAMPLE 16													
Gedrite	40.39	12.49	34.89	12.12	0	0	0	0	.10	0	0	0	.07
"	50.99	10.18	28.81	8.91	.17	.17	.59	0	0	0	0	0	.18
SAMPLE 20 (Bottom)													
Gedrite	39.68	14.64	29.37	12.83	.50	0	1.03	.06	1.03	.13	.08	.10	.56
"	41.26	16.11	17.19	19.05	.24	.67	3.10	.24	.92	0	.09	.11	1.01
"	42.55	23.84	22.49	10.21	.50	0	.35	.05	0	0	0	0	0
Cummingtonite	48.30	7.33	33.90	7.96	.21	0	.71	.07	1.42	.01	0	0	.07
Grunerite	38.68	1.62	54.28	.08	.34	0	.75	.07	3.44	.15	0	.24	.35

Table 7 continued

SAMPLE 31 (Top)

Probable Amphibole	SiO_2	Al_2O_3	FeO	MgO	CaO	Na_2O	K_2O	TiO_2	MnO	P_2O_5	S	Cl	Cr_2O_3
Anthophyllite	57.07	.39	18.97	17.83	.20	.65	.02	.07	3.89	.18	.09	.15	.48
"	60.54	.35	7.43	30.90	0	.[illegible]	.27	0	.16	[illegible]	.08	0	0
"	54.74	[illegible]5	[illegible].40	29.20	0	.01		0	0	0	0	0	0
"	57.35	[illegible]	9.36	16 28	.01	.50	[illegible]	0	5.9[illegible]	.10	0	.04	.26
"	48.52	[illegible].03	21.5[illegible]	[illegible].45	.18	.72	[illegible]	[illegible]	.24	.0[illegible]	0	.[illegible]7	.05
"	57. 7	[illegible]	11.[illegible]	23.4[illegible]	0	1.[illegible]	.02	0	5.24	.07	.18	.0[illegible]	.22
"	[illegible]	[illegible]	15.9[illegible]	22.[illegible]	[illegible]3	90	0	[illegible]	.[illegible]4	.[illegible]7	0	[illegible]	0
"	[illegible].09		10.[illegible]	27.05	0	0	0	[illegible]	1.54	0	0	[illegible]	0
"	55.96	.07	[illegible]	[illegible]	[illegible]	[illegible]	0	[illegible]	4.72	0	0	0	0
"	56	0	1[illegible].22	[illegible].[illegible]3	[illegible]	.8[illegible]	0	0	.76	0	[illegible]	[illegible]	0
"	65.77	0	[illegible]4.74	[illegible]8.[illegible]9	0	[illegible]	[illegible]	0	.18	0	0	0	0
"	56.[illegible]9	1.[illegible]7	22.95	[illegible]	0	1.[illegible]8	[illegible]	0	.17	[illegible]	0	[illegible]	.78
Gedrite	[illegible]4	[illegible]	16.6[illegible]	26.30	13.[illegible]	[illegible]	0	[illegible]3.8[illegible]	.0[illegible]	0	[illegible]	0	[illegible]
"	[illegible].2	9.91	[illegible].93	[illegible]2	0	.9[illegible]	[illegible]	0	0	[illegible]	0	0	0
"	0	1[illegible].44	[illegible]	14.[illegible]	.81	.11	[illegible].74	.03	.17	0	0	.03	[illegible]
"	44.91	[illegible]	31.[illegible]	8.[illegible]	.18	0	3[illegible].[illegible]3	[illegible]	0	0	0	0	0
Cummingtonite	[illegible].99	[illegible]	[illegible].[illegible]3	14.69	[illegible].99	1.01	0	0	[illegible].12	[illegible]	0	0	0
"	[illegible].8	.60	24.42	[illegible].[illegible]3	.25	[illegible]	1.26	.02	1.03	[illegible]06	0	0	0
"	[illegible].76	99	3[illegible].[illegible]	[illegible]3	.09	[illegible]	[illegible]3	.17	.20	.03	.04	[illegible]	.25
[illegible]rite	39.18	4.80	4[illegible]	1.02	1.13	[illegible]0	1.12	.1[illegible]	[illegible].9	[illegible]	.12	0	.32
"	[illegible]5.[illegible]3	[illegible]	[illegible]	[illegible]2	[illegible].53	0	0	0	0	.41	0	0	0	0
Actinolite	[illegible]	[illegible].[illegible]2	6.[illegible]	[illegible]9.[illegible]	11.08	.25	0	.09	[illegible]0	.21	.22	.36	.49
"	5[illegible].0	1.62	[illegible].[illegible]	13.[illegible]	8.[illegible]0	1.84	.38	0	.56	0	0	.22	1.[illegible]

Table 7 continued

Probable Amphibole	SiO_2	Al_2O_3	FeO	MgO	CaO	Na_2O	K_2O	TiO_2	MnO	P_2O_5	S	Cl	Cr_2O_3
SAMPLE 31 (Bottom)													
Gedrite	38.31	12.21	30.82	11.74	2.51	0	1.34	.36	2.16	0	.19	.15	.22
SAMPLE 33 (Top)													
Grunerite	47.24	0	40.22	9.31	0	0	0	0	3.05	0	.08	0	.10
"	42.53	5.38	39.06	10.36	.33	0	0	0	.21	0	0	0	2.13
"	39.74	.07	54.68	4.22	.32	0	0	0	.25	.44	0	0	.28
"	55.19	.18	40.24	.37	.45	0	.13	0	.20	.15	0	.27	2.82
Anthophyllite	57.06	.29	12.19	26.75	.12	.58	0	0	2.30	.29	0	.12	.30
SAMPLE 33 (Middle)													
Anthophyllite	62.22	.20	4.91	31.47	0	.78	0	0	.40	0	0	0	0
"	57.33	0	15.97	22.11	0	0	0	0	4.59	0	0	0	0
"	66.30	0	13.98	19.70	0	0	0	0	0	0	0	0	0
"	64.85	0	10.77	24.36	0	0	0	0	0	0	0	0	0
"	63.31	.19	12.97	22.97	0	.56	0	0	0	0	0	0	0
Gedrite	49.50	16.18	18.25	15.72	.28	0	0	.06	0	0	0	0	0

Table 7 continued

SAMPLE 33 (Bottom)

Probable Amphibole	SiO_2	Al_2O_3	FeO	MgO	CaO	Na_2O	K_2O	TiO_2	MnO	P_2O_5	S	Cl	Cr_2O_3
Anthophyllite	63.81	.40	3.55	31.91	0	.33	0	0	0	0	0	0	0
"	64.43	.09	4.30	30.49	0	0	0	0	.69	0	0	0	0
"	60.48	0	11.85	23.30	.33	0	0	0	4.03	0	0	0	0
"	58.22	.40	17.30	22.32	0	0	0	0	1.76	0	0	0	0
"	60.32	0	11.75	23.23	0	.63	0	0	4.08	0	0	0	0
"	61.64	.37	9.59	26.35	0	1.35	.06	.07	0	.14	0	.02	.41
"	61.62	.41	11.71	24.49	0	1.61	0	0	.02	.14	0	0	0
"	65.48	.35	5.40	28.76	0	0	0	0	0	0	0	0	0
"	56.52	0	9.73	22.45	0	0	0	0	3.29	0	0	0	0
"	64.45	0	6.98	28.19	0	.28	0	.09	0	0	0	0	0
Gedrite	39.17	15.30	26.70	15.63	.30	0	2.62	.29	0	0	0	0	0
"	47.08	14.10	17.60	16.61	0	0	5.61	0	0	0	0	0	0
"	51.29	11.39	21.86	11.50	0	0	3.95	0	0	0	0	0	0
Grunerite	55.57	0	40.43	3.99	0	0	0	0	0	0	0	0	0
"	49.56	.18	43.67	6.45	0	.14	0	0	0	0	0	0	0
	43.01	.50	47.46	6.05	.21	.45	0	.04	1.35	.24	.06	.08	.53
"	46.67	.10	45.95	5.47	.18	.08	0	.06	1.20	.06	.06	0	.16
"	48.92	.41	49.38	0	.06	0	0	0	1.18	.05	0	0	0
Hornblende	42.57	13.26	26.59	5.81	10.96	0	.40	.03	.08	0	0	.07	.22

Table 7 continued

SAMPLE 34

Probable Amphibole	SiO_2	Al_2O_3	FeO	MgO	CaO	Na_2O	K_2O	TiO_2	MnO	P_2O_5	S	Cl	Cr_2O_3
Anthophyllite	48.98	0	24.75	23.06	.06	.59	0	0	2.55	0	0	0	0
"	60.35	.06	14.80	24.75	0	0	0	.03	0	0	0	0	0
"	57.97	.56	8.39	30.10	.08	1.49	0	0	1.41	0	0	0	0
"	58.75	.11	11.34	24.34	.24	.90	.09	.01	4.25	.05	0	0	.02
Grunerite	41.20	.94	55.57	.54	.10	0	.21	.12	.95	.15	.08	.03	.11
"	52.47	.12	24.85	9.60	.70	0	0	.03	12.17	.05	0	0	0

SAMPLE 35

Grunerite	56.70	.86	41.72	0	.06	.09	.03	.01	.32	.04	0	.04	.13
"	58.62	.64	38.91	0	1.02	0	.82	0	0	0	0	0	0
Anthophyllite	61.53	.29	16.15	20.23	.06	.40	0	0	.65	.35	0	0	.38
"	64.10	.08	5.05	30.00	0	.30	0	0	.05	.15	0	.15	.11
"	60.20	.12	14.94	18.66	.18	0	0	0	5.31	.07	0	0	.52
"	59.38	.06	11.29	27.61	.02	0	0	.03	.65	.13	.13	.49	.19
"	54.68	.04	27.63	15.40	0	0	0	0	2.24	0	0	0	0
Riebeckite	43.28	1.09	43.67	.44	.17	7.76	.01	.05	2.71	.04	.14	0	.63

Table 7 continued

SAMPLE 38 (Top)

Probable Amphibole	SiO_2	Al_2O_3	FeO	MgO	CaO	Na_2O	K_2O	TiO_2	MnO	P_2O_5	S	Cl	Cr_2O_3
Anthophyllite	57.30	.26	16.19	21.49	0	.32	0	0	3.87	.20	0	0	.37
"	60.87	.08	9.40	28.31	0	.91	0	0	.13	.30	0	0	0
"	65.29	.34	10.62	20.64	0	2.17	0	0	.11	.10	.03	0	.70
"	62.10	.23	9.26	27.72	0	.42	0	0	0	.27	0	0	0
"	64.53	.12	18.22	16.44	0	.69	0	0	0	0	0	0	0
"	57.94	0	22.97	16.66	0	.79	0	0	1.64	0	0	0	0
Grunerite	58.37	1.86	37.91	.26	.80	0	.25	0	0	.41	.14	0	0
"	41.97	5.80	46.52	0	.93	0	.16	0	3.92	0	0	.31	.39
"	48.99	0	38.14	11.57	0	0	.59	0	.30	.11	0	0	.30
"	49.01	0	38.13	11.57	0	0	.59	0	.30	.11	0	0	.30
"	47.13	.05	44.53	7.80	0	0	0	0	.19	.13	.06	.10	0
"	49.56	0	39.39	10.09	0	0	0	.04	0	.20	0	.08	.64
"	51.04	.24	42.17	5.71	0	0	0	0	.25	.20	0	.39	0
"	51.74	.05	41.11	6.26	0	0	.03	0	0	.20	.36	.05	.20
Cummingtonite	60.57	.12	31.84	7.47	0	0	0	0	0	0	0	0	0
"	59.33	0	29.49	11.16	0	.01	0	0	0	0	0	0	0
"	56.33	.55	27.31	11.57	0	0	0	0	3.54	0	0	0	0
Riebeckite	50.23	3.28	40.51	.53	.20	3.32	.03	.18	.92	.45	0	0	.36
"	47.52	.40	37.79	11.29	0	2.74	.05	0	.21	0	0	0	0

Table 7 continued

Probable Amphibole	SiO_2	Al_2O_3	FeO	MgO	CaO	Na_2O	K_2O	TiO_2	MnO	P_2O_5	S	Cl	Cr_2O_3
SAMPLE 38 (Bottom)													
Actinolite	54.96	.58	9.08	21.76	12.10	.97	0	.07	.09	.13	0	0	.28
"	58.87	.28	8.30	20.09	11.94	.44	0	.09	0	0	0	0	0
Gedrite	42.08	15.51	24.84	12.75	1.66	0	2.88	.28	0	0	0	0	0
"	41.60	16.02	20.19	18.19	1.90	0	2.10	0	0	0	0	0	0
"	38.58	13.05	36.02	8.69	.60	0	2.30	.27	0	0	0	.09	.39
"	39.07	11.60	26.02	21.18	1.08	0	.71	0	0	0	0	.34	0
"	38.81	12.68	35.70	11.76	.64	0	.56	.24	0	0	.12	0	0
SAMPLE 39 (Bottom)													
Anthophyllite	62.38	1.73	11.44	24.19	.08	.17	0	0	0	0	0	0	0
Gedrite	36.69	12.77	27.02	19.34	.18	.36	0	0	.63	0	0	0	0
"	41.28	14.46	19.92	17.66	1.75	.84	2.36	.56	.16	0	0	.32	.70
Grunerite	42.53	.06	39.44	9.82	0	0	0	.01	.39	.16	0	.02	.56
"	48.97	.17	39.75	9.05	.07	.28	.15	0	.94	.08	.01	0	.54
"	45.30	5.09	46.38	.32	.52	1.22	.87	0	.03	.13	0	.14	0
SAMPLE 42													
Anthophyllite	52.60	1.22	26.55	15.49	.16	.43	0	.03	2.83	.10	.06	.11	.42
Hornblende	37.98	11.35	17.43	18.13	14.10	.44	0	0	.57	0	0	0	0
Grunerite	53.28	0	36.85	8.96	.47	0	0	0	.44	0	0	0	0

Table 7 continued

Probable Amphibole	SiO_2	Al_2O_3	FeO	MgO	CaO	Na_2O	K_2O	TiO_2	MnO	P_2O_5	S	Cl	Cr_2O_3
SAMPLE 50													
Grunerite	47.46	.23	43.07	7.74	.27	.48	0	.06	.11	.10	.09	.24	.14
"	45.66	1.03	44.92	7.17	.49	0	.17	0	.12	.15	0	.30	0
"	47.63	.18	41.38	8.98	.27	.48	.06	.09	.63	.06	.09	0	.15
Tremolite	62.55	.09	7.03	21.75	8.57	0	0	0	0	0	0	0	0
"	64.60	.12	2.04	23.09	9.77	.37	0	0	0	0	0	0	0
Actinolite	57.73	.25	9.79	21.27	9.27	.74	.14	.11	0	.11	.14	.05	.40
SAMPLE 51													
Actinolite	57.98	.99	10.27	17.81	10.84	.71	.29	.02	.27	.24	.30	.11	.16
"	59.58	.17	10.86	18.60	9.61	.77	0	0	.22	.19	0	0	0
Anthophyllite	61.09	0	20.75	16.76	.17	.92	.15	0	.05	.11	0	0	0
Grunerite	52.63	0	39.97	6.74	.25	0	0	0	.40	0	0	0	0
"	47.84	.20	37.68	9.73	2.62	0	.98	0	.80	0	0	0	.15
SAMPLE 52													
Grunerite	49.21	.03	36.12	13.52	0	0	.35	0	.34	.11	0	.08	.25
"	42.34	3.43	49.99	1.76	.03	0	.09	.06	1.98	.16	0	.14	0
"	46.41	.98	47.62	4.65	0	0	.07	0	.03	.08	.16	0	0
"	43.81	0	48.93	7.25	0	0	0	0	0	0	0	0	0
Actinolite	56.68	2.48	13.14	16.65	10.44	.26	.14	.02	0	.03	0	.15	0
"	56.74	.15	22.73	10.56	9.81	0	0	0	0	0	0	0	0
Hornblende	50.08	10.86	18.21	11.10	9.09	.58	0	0	0	0	.07	0	0

Table 7 continued

Probable Amphibole	SiO_2	Al_2O_3	FeO	MgO	CaO	Na_2O	K_2O	TiO_2	MnO	P_2O_5	S	Cl	Cr_2O_3
SAMPLE 53													
Grunerite	48.30	.56	42.96	6.82	1.15	0	0	0	0	.14	0	.07	0
"	47.31	.72	43.83	7.46	.03	.38	0	.05	0	.07	0	0	.15
"	47.10	0.71	43.60	5.79	.11	.20	1.10	.02	.31	.13	.17	.15	.30
"	44.40	1.38	47.38	4.48	.12	0	.77	0	.33	.24	.02	.34	.54
"	46.60	2.29	39.99	9.25	.14	.72	.36	0	.12	.25	.02	.11	.15
Actinolite	53.20	.09	24.67	11.12	8.83	.40	.79	0	.12	.13	.52	0	.13
SAMPLE 54													
Grunerite	45.32	.37	46.97	5.81	.42	.11	.34	.01	.36	.25	0	.03	0
"	48.27	.18	40.24	10.07	.03	.23	.36	0	.15	0	0	0	.47
"	58.54	.19	29.30	9.80	1.50	.23	0	0	.20	0	0	0	.12
"	58.48	.09	34.98	5.37	.10	0	0	0	.77	.08	0	0	.12
SAMPLE 55													
Actinolite	53.62	0	20.28	14.72	9.41	0	0	0	0	0	0	1.67	.29
Grunerite	47.98	0	51.37	.57	0	0	.07	0	0	0	0	0	0
"	52.90	0	45.03	2.06	0	0	0	0	0	0	0	0	0
"	53.05	.40	37.33	9.22	0	0	0	0	0	0	0	0	0
SAMPLE 56													
Cummingtonite	54.13	0	30.98	13.55	0	.29	0	0	0	.09	0	.06	.88

Table 7 continued

SAMPLE 57

Probable Amphibole	SiO_2	Al_2O_3	FeO	MgO	CaO	Na_2O	K_2O	TiO_2	MnO	P_2O_5	S	Cl	Cr_2O_3
Grunerite	54.86	2.02	42.58	0	.37	0	.08	0	0	.08	0	0	0
"	50.24	.48	46.63	0	.07	0	0	0	0	0	0	0	2.56

SAMPLE 58

Grunerite	47.83	.29	47.39	3.21	0	0	.44	0	.84	0	0	0	0

TABLE 8: ANALYTICAL DATA FOR MINERALS IN ROCK SPECIMENS

L-1 (anthophyllite)

ELECTRON MICROPROBE

	Wt.%	No. of ions on basis of 23 O	Wt.%	No. of ions on basis of 23 O
SiO_2	57.90	7.742	56.27	7.791
TiO_2	0	.0	0	0
Al_2O_3	0.73	.114	0	0
FeO	3.59	.401	10.92	1.264
MnO	6.60	.747	6.23	..730
MgO	30.86	6.150	25.49	5.259
CaO	0.31	.045	1.10	.163
Na_2O	0	0	0	0
K_2O	0	0	0	0

ENERGY DISPERSIVE X-RAY SPECTROSCOPY

	Wt.%		Wt.%
SiO_2	55.8 61.0	TiO_2	0.1 0
Al_2O_3	0.1 0.3	MnO	3.7 7.9
FeO	18.0 20.5	P_2O_5	0.8 0.8
MgO	17.5 18.3	S	0 0
CaO	0.6 0.5	Cl	0.1 0
Na_2O	2.1 0.6	Cr_2O_3	1.2 0.1
K_2O	0.2 0		

L-4 (grunerite)

ENERGY DISPERSIVE X-RAY SPECTROSCOPY - average of 25 analyses

	Wt.%		Wt.%
SiO_2	47.6	TiO_2	tr.
Al_2O_3	0.3	MnO	0.4
FeO	42.8	P_2O_5	<0.1
MgO	8.1	S	-
CaO	0.2	Cl	-
Na_2O	tr.	Cr_2O_3	tr.
K_2O	tr.		

An additional 16 analyses gave the following element/Si ratios:

Fe/Si	0.750
Mg/Si	0.133
Ca/Si	0.006
Mn/Si	0.008

X-RAY FLUORESCENCE SPECTROSCOPY

	Wt.%		Wt.%
SiO_2	52.32	Na_2O	0
Al_2O_3	1.76	K_2O	0.05
Fe_2O_3	32.22	TiO_2	0.04
MgO	12.90	MnO	0.70
CaO	0	P_2O_5	0.01

L-6 (grunerite)

ELECTRON MICROPROBE

	Wt.%	No. of ions on basis of 23 O	Wt.%	No. of ions on basis of 23 O
SiO_2	50.70	7.876	50.38	7.825
TiO_2	0	0	0	0
Al_2O_3	0	0	0	0
FeO	40.65	5.280	39.89	5.183
MnO	0.36	.048	0.54	.072
MgO	8.29	1.921	8.67	2.007
CaO	0	0	0.52	.087
Na_2O	0	0	0	0
K_2O	0	0	0	0
SiO_2	50.22	7.805	50.65	7.867
TiO_2	0	0	0	0
Al_2O_3	0	0	0	0
FeO	40.21	5.225	40.40	5.249
MnO	0.35	.045	0.39	.053
MgO	8.95	2.073	8.31	1.925
CaO	0.29	.048	0.23	.039
Na_2O	0	0	0	0
K_2O	0	0	0	0
SiO_2	50.50	7.845	50.15	7.804
TiO_2	0	0	0	0
Al_2O_3	0	0	0	0
FeO	40.21	5.223	40.38	5.225
MnO	0.45	.060	0.44	.057
MgO	8.56	1.983	8.79	2.038
CaO	0.27	.044	0.25	.042
Na_2O	0	0	0	0
K_2O	0	0	0	0

L-6 (grunerite) continued

	Wt.%	No. of ions on basis of 23 O	Wt. %	No. of ions on basis of 23 O
SiO_2	50.22	7.823	47.94	7.581
TiO_2	0	0	0	0
Al_2O_3	0	0	0	0
FeO	40.86	5.323	40.77	5.391
MnO	0.41	.055	0.52	.070
MgO	8.51	1.975	8.35	1.968
CaO	0	0	2.41	.410
Na_2O	0	0	0	0
K_2O	0	0	0	0
SiO_2	50.32	7.846	50.52	7.824
TiO_2	0	0	0	0
Al_2O_3	0	0	0	0
FeO	40.97	5.342	39.56	5.123
MnO	0.41	.055	0.41	.055
MgO	8.05	1.871	9.22	2.128
CaO	0.23	.038	0.28	.047
Ka_2O	0	0	0	0
K_2O	0	0	0	0
SiO_2	50.25	7.824		
TiO_2	0	0		
Al_2O_3	0	0		
FeO	40.63	5.291		
MnO	0.37	.049		
MgO	8.45	1.962		
CaO	0.29	.049		
Ka_2O	0	0		
K_2O	0	0		

L-6 (grunerite) continued

X-RAY POWDER DIFFRACTION

Intensity	hkl	d(obs.)	d(calc.)	d(obs.-calc.)
8	0 2 0	9.1650	9.1490	.0160
58	1 1 0	8.3066	8.3224	-.0159
58	-1 1 0	8.3066	8.3224	-.0159
4	1 3 0	5.0964	5.1077	-.0112
12	0 4 0	4.5870	4.5745	.0125
14	2 2 0	4.1616	4.1612	.0004
14	-2 2 0	4.1616	4.1612	.0004
5	-1 3 1	3.8667	3.8691	-.0024
7	1 3 1	3.4662	3.4580	.0082
58	2 4 0	3.2666	3.2687	-.0021
58	-2 4 0	3.2666	3.2687	-.0021
72	3 1 0	3.0685	3.0708	-.0023
72	-3 1 0	3.0685	3.0708	-.0023
31	1 5 1	2.7631	2.7585	.0046
16	0 6 1	2.6329	2.6315	.0014
5	2 6 0	2.5495	2.5538	-.0043
5	-2 6 0	2.5495	2.5538	-.0043
5	3 5 0	2.3738	2.3720	.0018
5	-3 5 0	2.3738	2.3720	.0018
7	1 7 1	2.2220	2.2190	.0030
12	2 6 1	2.1936	2.1978	-.0042
4	3 5 1	2.0424	2.0419	.0005
27	4 6 1	1.6625	1.6637	-.0012
11	4 8 0	1.6367	1.6344	.0023
10	6 0 0	1.5547	1.5575	-.0028
100	0 12 0	1.5291	1.5248	.0043
5	3 11 0	1.4670	1.4673	-.0003
5	-3 11 0	1.4670	1.4673	-.0003

L-6 (grunerite) continued

20	-6	6	1	1.[illegible]	1.4[illegible]6	-.0005
8	-2	12	2	1.3022	1.[illegible]	.0000
6	4	12	0	1.2780	1.2769	
6	8	0	0	1.1692	1.[illegible]1	.0011
8	1	17	1	1.[illegible]	1.0426	.012

CELL CONSTANTS

a_o = 9.54[illegible] ± [illegible] Å
b_o = 18.298 ± [illegible] Å
c_o = 5.320 ± 0.[illegible] Å
β = 101.81 ± 0.[illegible] deg
V = [illegible]09.62 ± 2.[illegible] Å³
a sin β = 9.345 Å

L-7 (grunerite)

X-RAY POWDER DIFFRACTION

Intensity	hkl	d(obs.)	d(calc.)	d(obs.-calc.)
43	1 1 0	8.3066	8.3289	-.0223
43	-1 1 0	8.3066	8.3289	-.0223
12	2 0 0	4.6707	4.6771	-.0064
14	2 2 0	4.1713	4.1644	.0068
14	-2 2 0	4.1713	4.1644	.0068
7	-1 3 1	3.8750	3.8847	-.0097
12	1 3 1	3.4796	3.4778	.0018
33	2 4 0	3.2666	3.2702	-.0036
33	-2 4 0	3.2666	3.2702	-.0036
100	3 1 0	3.0737	3.0738	-.0001
100	-3 1 0	3.0737	3.0738	-.0001
31	2 2 1	3.0178	3.0119	.0059
24	1 5 1	2.7631	2.7685	-.0053
19	0 6 1	2.6367	2.6380	-.0013
7	2 6 0	2.5530	2.5545	-.0014
7	-2 6 0	2.5530	2.5545	-.0014
33	2 6 1	2.2064	2.2042	.0022
7	-4 0 2	1.9569	1.9543	.0026
12	4 6 1	1.6667	1.6681	-.0014
12	-6 6 1	1.4060	1.4060	-.0000
7	4 12 0	1.2787	1.2772	.0015
10	-5 11 2	1.1864	1.1870	-.0006
7	8 0 0	1.1692	1.1693	-.0001

CELL CONSTANTS

a_o = 9.551 ± 0.0037 Å

b_o = 18.297 ± 0.0100 Å

c_o = 5.369 ± 0.0076 Å

β = 101.65 ±0.059 deg.

V = 918.98 ±0.53 $Å^3$

$a \sin \beta$ = 9.354 Å

L-7 (grunerite) continued

ENERGY DISPERSIVE X-RAY SPECTROSCOPY - average of 31 analyses

	Wt.%		Wt.%
SiO_2	46.6	K_2O	<0.1
Al_2O_3	tr.	TiO_2	<0.1
FeO	43.9	MnO	0.4
MgO	7.1	P_2O_5	0.6
CaO	0.9	S	<0.1
Na_2O	0.1	Cl	<0.1

L-8 (grunerite)

ELECTRON MICROPROBE

	Wt.%	No. of ions on basis of 23 0	Wt.%	No. of ions on basis of 23 0
SiO_2	50.44	7.836	51.60	7.926
TiO_2	0	0	0	0
Al_2O_3	0	0	0	0
FeO	40.55	5.269	38.85	4.991
MnO	0.27	.035	0.30	.039
MgO	8.74	2.024	9.25	2.117
CaO	0	0	0	0
Na_2O	0	0	0	0
K_2O	0	0	0	0

L-8 (grunerite) continued

	Wt.%	No. of ions on basis of 23 0	Wt.%	No. of ions on basis of 23 0
SiO_2	51.30	7.898	50.69	7.856
TiO_2	0	0	0	0
Al_2O_3	0	0	0	0
FeO	39.41	5.074	40.49	5.247
MnO	0	0	0	0
MgO	9.28	2.130	8.84	2.130
CaO	0	0	0	0
Na_2O	0	0	0	0
K_2O	0	0	0	0

SiO_2	50.87	7.863
TiO_2	0	0
Al_2O_3	0	0
FeO	39.85	5.152
MnO	0	0
MgO	9.01	2.076
CaO	0.28	.047
Na_2O	0	0
K_2O	0	0

L-9 (grunerite)

ELECTRON MICROPROBE

	Wt.%	No. of ions on basis of 23 O	Wt.%	No. of ions on basis of 23 O
SiO_2	51.04	7.809	50.78	7.828
TiO_2	0	0	0	0
Al_2O_3	0	0	0	0
FeO	36.11	4.620	37.93	4.888
MnO	0.86	.111	0.74	.098
MgO	10.66	2.431	9.57	2.200
CaO	1.33	.291	0.96	.159
Na_2O	0	0	0	0
K_2O	0	0	0	0
SiO_2	51.87	7.901	50.30	7.722
TiO_2	0	0	0	0
Al_2O_3	0	0	0	0
FeO	36.43	4.642	36.93	4.742
MnO	0.65	.084	0.72	.093
MgO	10.47	2.378	11.43	2.617
CaO	0.57	.093	0.62	.102
Na_2O	0	0	0	0
K_2O	0	0	0	0
SiO_2	50.93	7.879		
TiO_2	0	0		
Al_2O_3	0	0		
FeO	39.12	5.062		
MnO	0.71	.092		
MgO	8.53	1.968		
CaO	0.72	.120		
Na_2O	0	0		
K_2O	0	0		

L-9 (actinolite)

ELECTRON MICROPROBE

	Wt.%	No. of ions on basis of 23 O	Wt.%	No. of ions on basis of 23 O
SiO_2	53.34	7.892	53.06	7.853
TiO_2	0	0	0	0
Al_2O_3	0	0	0	0
FeO	23.91	2.959	23.96	2.965
MnO	0.34	.043	0	0
MgO	10.65	2.348	11.02	2.430
CaO	11.76	1.865	11.97	1.898
Na_2O	0	0	0	0
K_2O	0	0	0	0
SiO_2	52.00	7.802	53.43	7.866
TiO_2	0	0	0	0
Al_2O_3	0	0	0	0
FeO	25.67	3.221	22.90	2.818
MnO	0.28	.035	0	0
MgO	9.43	2.109	11.64	2.552
CaO	12.63	2.031	12.03	1.897
Na_2O	0	0	0	0
K_2O	0	0	0	0

L-9 (actinolite) continued

X-RAY POWDER DIFFRACTION

Intensity	hkl	d(obs.)	d(calc.)	d(obs.-calc.)
8	0 2 0	9.0712	9.0871	-.0159
86	1 1 0	8.4249	8.4708	-.0459
86	-1 1 0	8.4249	8.4708	-.0459
6	0 4 0	4.5521	4.5435	.0085
6	2 2 0	4.2302	4.2354	-.0052
6	-2 2 0	4.2302	4.2354	-.0052
10	0 4 1	3.4012	3.4014	-.0001
10	1 5 0	3.4012	3.3982	.0030
22	2 4 0	3.2962	3.2955	.0007
22	-2 4 0	3.2962	3.2955	.0007
100	3 1 0	3.1371	3.1433	-.0062
100	-3 1 0	3.1371	3.1433	-.0062
8	-1 5 1	2.9544	2.9626	-.0082
8	2 2 1	2.9544	2.9480	.0064
7	3 3 0	2.8182	2.8236	-.0054
30	1 5 1	2.7263	2.7191	.0072
7	0 6 1	2.6033	2.6083	-.0051
11	3 5 0	2.3982	2.3982	.0000
17	-4 2 1	2.3411	2.3440	-.0029
16	2 6 1	2.1759	2.1721	.0037
12	2 8 0	2.0556	2.0524	.0033
24	3 5 1	2.0187	2.0251	-.0064
9	5 1 0	1.9065	1.9043	.0022
19	4 6 1	1.6584	1.6571	.0013
6	-6 2 1	I.6274	1.6246	.0027
6	1 11 0	1.6274	1.6281	-.0008
10	6 0 0	1.5951	1.5957	-.0006

L-9 (actinolite) continued

CELL CONSTANTS

a_o = 9.920 ± 0.0067 Å
b_o = 18.174 ± 0.0140 Å
c_o = 5.316 ± 0.0161 Å
β = 105.18 ± 0.123 deg.
V = 924.98 ± 2.80 $Å^3$

ENERGY DISPERSIVE X-RAY SPECTROSCOPY - average of 41 analyses

	Wt.%		Wt.%
SiO_2	51.9	MgO	11.3
Al_2O_3	0	CaO	9.8
FeO	25.1		

L-10 (grunerite)

X-RAY POWDER DIFFRACTION

Intensity	hkl	d(obs.)	d(calc.)	d(obs.-calc.)
100	1 1 0	8.4651	8.3302	.1349
100	-1 1 0	8.4651	8.3302	.1349
3	1 3 0	5.1257	5.1117	.0140
9	2 0 0	4.7075	4.6771	.0304
7	0 4 0	4.5988	4.5777	.0211
18	2 2 0	4.1907	4.1651	.0256
18	-2 2 0	4.1907	4.1651	.0256
5	-1 3 1	3.8917	3.8772	.0145
7	1 3 1	3.4729	3.4685	.0044
31	2 4 0	3.2784	3.2715	.0069
31	-2 4 0	3.2784	3.2715	.0069
70	3 1 0	3.0789	3.0738	.0050
70	-3 1 0	3.0789	3.0738	.0050
8	2 2 1	3.0128	3.0043	.0086
28	1 5 1	2.7715	2.7645	.0069

L-10 (grunerite) continued

12	0	6	1	2.6367	2.6359	.0007
7	-2	0	2	2.5149	2.5101	.0048
4	3	5	0	2.3769	2.3741	.0028
4	-3	5	0	2.3769	2.3741	.0028
9	-3	5	1	2.3009	2.2998	.0011
9	-4	2	1	2.2485	2.2466	.0020
7	1	7	1	2.2220	2.2226	-.0006
19	2	6	1	2.2012	2.2020	-.0008
8	3	5	1	2.0446	2.0461	-.0014
4	-4	0	2	1.9509	1.9512	-.0003
8	6	0	0	1.5583	1.5590	-.0007
16	-6	6	1	1.4060	1.4064	-.0005
4	5	1	2	1.3876	1.3896	-.0020
8	-2	12	2	1.3029	1.3039	-.0010
7	4	12	0	1.2772	1.2779	-.0007
7	-4	12	0	1.2772	1.2779	-.0007
6	-9	1	2	1.0390	1.0395	-.0005
3	-8	6	3	1.0161	1.0161	-.0001

CELL CONSTANTS

a_o = 9.553 ± 0.0047 Å
b_o = 18.311 ± 0.0128 Å
c_o = 5.342 ± 0.0078 Å
β = 101.72 ± 0.059 deg.
V = 914.98 ± 1.34 $Å^3$
a sin β = 9.354 Å

ENERGY DISPERSIVE X-RAY SPECTROSCOPY - average of 7 analyses

	Wt.%		Wt.%
SiO_2	49.8	K_2O	tr.
Al_2O_3	0.8	TiO_2	tr.
FeO	38.0	MnO	0.3
MgO	9.4	P_2O_5	tr.
CaO	0.2	S	tr.
Na_2O	0.8	Cl	0
		Cr_2O_3	tr.

L-13 (grunerite)

X-RAY POWDER DIFFRACTION

Intensity	hkl	d(obs.)	d(calc.)	d(obs.-calc.)
45	1 1 0	8.4249	8.3331	.0918
45	-1 1 0	8.4249	8.3331	.0918
9	0 4 0	4.5988	4.5803	.0185
9	2 2 0	4.1810	4.1666	.0144
9	-2 2 0	4.1810	4.1666	.0144
5	1 3 1	3.4729	3.4712	.0017
14	2 4 0	3.2784	3.2729	.0055
14	-2 4 0	3.2784	3.2729	.0055
100	3 1 0	3.0789	3.0748	.0041
100	-3 1 0	3.0789	3.0748	.0041
7	2 2 1	3.0029	3.0063	-.0034
8	1 5 1	2.7715	2.7665	.0050
6	0 6 1	2.6367	2.6377	-.0011
3	-2 0 2	2.5149	2.5121	.0028
4	-3 5 1	2.3009	2.3008	.0001
2	1 7 1	2.2273	2.2241	.0032
5	4 6 1	1.6653	1.6676	-.0023
2	4 8 0	1.6380	1.6365	.0015
6	6 0 0	1.5583	1.5595	-.0012
4	-6 6 1	1.4060	1.4069	-.0009
6	-2 12 2	1.3037	1.3047	-.0010
2	4 12 0	1.2780	1.2785	-.0006

CELL CONSTANTS

a_o = 9.557 ± 0.0068 Å
b_o = 18.321 ± 0.0137 Å
c_o = 5.347 ± 0.0093 Å
β = 101.71 ± 0.111 deg.
V = 916.63 ± 1.59 $Å^3$
a sin β = 9.357 Å

L-13 (grunerite) continued

ENERGY DISPERSIVE X-RAY SPECTROSCOPY

	Wt.%		Wt.%
SiO_2	54.2	K_2O	0.4
Al_2O_3	2.8	TiO_2	0.1
FeO	35.1	MnO	0.2
MgO	7.2	S	0
CaO	0	Cl	0
Na_2O	0	Cr_2O_3	0.2

An additional 61 analyses gave the following element/Si ratios:

Fe/Si	0.746
Mg/Si	0.191

L-17 (tremolite)

X-RAY POWDER DIFFRACTION

Intensity	hkl	d(obs.)	d(calc.)	d(obs.-calc.)
7	0 2 0	9.0712	9.0309	.0403
46	1 1 0	8.3851	8.4133	-.0282
46	-1 1 0	8.3851	8.4133	-.0282
11	0 0 1	5.0819	5.1070	-.0251
11	1 3 0	5.0819	5.0866	-.0046
3	-1 1 1	4.8742	4.8763	-.0022
7	2 0 0	4.7450	4.7539	-.0089
4	0 4 0	4.5063	4.5155	-.0092
1	0 2 1	4.4394	4.4454	-.0061
2	2 2 0	4.2104	4.2066	.0037
2	-2 2 0	4.2104	4.2066	.0037
1	-2 0 1	4.0221	4.0238	-.0018

L-17 (tremolite) continued

4	-1	3	1	3.8750	3.8756	-.0006
10	1	3	1	3.3822	3.3824	-.0002
19	2	4	0	3.2725	3.2740	-.0015
19	-2	4	0	3.2725	3.2740	-.0015
100	3	1	0	3.1210	3.1215	-.0005
100	-3	1	0	3.1210	3.1215	-.0005
3	-3	1	1	3.0228	3.0189	.0039
12	2	2	1	2.9402	2.9402	.0001
12	-1	5	1	2.9402	2.9409	-.0007
13	3	3	0	2.8053	2.8044	.0009
7	-3	3	1	2.7303	2.7293	.0011
20	1	5	1	2.7063	2.7071	-.0009
6	0	6	1	2.5923	2.5933	-.0010
3	0	0	2	2.5495	2.5435	-.0040
5	-2	0	2	2.5321	2.5322	-.0001
2	-2	6	1	2.4106	2.4104	.0002
5	3	5	0	2.3829	2.3823	.0006
13	-3	5	1	2.3353	2.3358	-.0005
9	-4	2	1	2.3208	2.3191	.0018
3	-1	7	1	2.2981	2.2991	-.0010
2	-2	4	2	2.2090	2.2086	.0004
1	1	7	1	2.1809	2.1821	-.0012
7	2	6	1	2.1609	2.1628	-.0019
2	-1	5	2	2.1317	2.1309	.0009
2	2	0	2	2.0406	2.0443	.0003
7	3	5	1	2.0166	2.0171	-.0005
5	3	7	0	2.0018	2.0010	.0008
1	-3	7	1	1.9729	1.9731	-.0002
4	-4	2	4	1.9629	1.9638	-.0009
4	1	9	0	1.9629	1.9636	-.0007
3	4	2	1	1.9255	1.9272	-.0016
23	5	1	0	1.8898	1.8911	-.0013

L-17 (tremolite) continued

3	-4	6	1	1.8733	1.8764	-.0031
3	-1	9	1	1.8661	1.8657	.0004
2	2	4	2	1.8625	1.8624	.0001
1	-1	7	2	1.8448	1.8449	-.0001
1	-4	4	2	1.8378	1.8377	.0001
2	-5	1	2	1.7445	1.7438	.0007
1	-5	5	1	1.7142	1.7163	-.0021
1	-3	7	2	1.7142	1.7134	.0008
1	0	10	1	1.7039	1.7028	.0010
2	-1	3	3	1.6836	1.6844	-.0007
2	-3	1	3	1.6808	1.6808	-.0000
2	0	2	3	1.6737	1.6729	.0008
12	4	6	1	1.6502	1.6499	.0003
10	4	8	0	1.6367	1.6370	-.0003
4	1	11	0	1.6182	1.6180	.0002
8	6	0	0	1.5851	1.5846	.0005
3	6	2	0	1.5607	1.5608	-.0001
5	4	0	2	1.5559	1.5548	.0011
3	-6	0	2	1.5314	1.5310	.0004
2	1	9	2	1.5189	1.5187	.0001
4	-2	6	3	1.5122	1.5124	-.0002
5	0	12	0	1.5044	1.5052	-.0007
2	2	2	3	1.4681	1.4679	.0001
2	3	7	2	1.4650	1.4655	-.0005
2	3	11	0	1.4578	1.4579	-.0001
3	-6	4	2	1.4507	1.4499	.0008
39	4	10	0	1.4387	1.4381	.0006
22	-6	6	1	1.4367	1.4367	-.0000
1	-5	3	3	1.4250	1.4242	.0008
2	-5	9	1	1.3985	1.3987	-.0002
2	6	2	1	1.3985	1.3985	.0001
3	5	1	2	1.3645	1.3645	.0000

L-17 (tremolite) continued

4	7	1	0	1.3550	1.3544	.0006
3	1	11	2	1.3407	1.3409	-.0002
3	-3	11	2	1.3357	1.3347	.0010
3	5	3	2	1.3340	1.3343	-.0003
3	2	6	3	1.3340	1.3337	.0003
2	-1	9	3	1.3211	1.3209	.0002
6	-7	5	1	1.3092	1.3084	.0007
4	-1	1	4	1.3068	1.3064	.0004
3	0	12	2	1.2968	1.2967	.0001
5	-2	12	2	1.2937	1.2938	-.0001
4	-1	3	4	1.2802	1.2799	.0003
3	0	0	4	1.2765	1.2768	-.0002
3	-3	3	4	1.2736	1.2745	-.0009
2	-4	0	4	1.2678	1.2661	.0017
1	-4	4	4	1.2191	1.2191	-.0000
2	-5	11	2	1.1980	1.1981	-.0000
1	7	9	0	1.1240	1.1248	-.0008
1	5	13	0	1.1225	1.1218	.0007
1	-7	1	4	1.0739	1.0740	-.0001
4	5	11	2	1.0511	1.0512	-.0001
8	-2	2	5	1.0477	1.0478	-.0001
8	7	11	0	1.0477	1.0466	.0011
4	-8	6	3	1.0452	1.0463	-.0011
2	1	17	1	1.0281	1.0283	-.0002
3	6	6	3	.9799	.9801	-.0001

CELL CONSTANTS

a_o = 9.827 ± 0.0013 Å

b_o = 18.062 ± 0.0025 Å

c_o = 5.279 ± 0.0006 Å

β = 104.65 ± 0.011 deg.

V = 906.47 ± 0.10 $Å^3$

L-17 (tremolite) continued

ENERGY DISPERSIVE X-RAY SPECTROSCOPY - average of 38 analyses

	Wt.%		Wt.%
SiO_2	60.5	TiO_2	tr.
Al_2O_3	0.3	MnO	tr.
FeO	0.5	P_2O_5	< 0.1
MgO	23.8	S	tr.
CaO	13.7	Cl	tr.
Na_2O	0.8	H_2O	0.2
K_2O	tr		

L-22 (grunerite)

ELECTRON MICROPROBE

	Wt.%	No. of ions on basis of 23 O	Wt.%	No. of ions on basis of
SiO_2	51.[illegible]	8.010	50.[illegible]	.853
TiO_2	0	0	0	
Al_2O_3	0	0	0	
FeO	41.2[illegible]	5.377	[illegible].51	.434
MnO	0.42	.056	0.[illegible]	.049
MgO	6.2[illegible]	1 442	[illegible]	[illegible]. 01
CaO	0.63	[illegible]	[illegible] 65	[illegible]
Na_2O	0	0		
K_2O	0	0	0	0

L-22A (grunerite) continued

	Wt.%	No of ions on basis of 23 O	Wt.%	No. of ions on basis of 23 O
SiO_2	49.62	7.818	49.24	7.784
TiO_2	0	0	0	0
Al_2O_3	0	0	0	0
FeO	42.93	5.658	42.94	5.677
MnO	0	0	0.36	.049
MgO	6.79	1.596	6.72	1.581
CaO	0.64	.109	0.72	.124
Na_2O	0	0	0	0
K_2O	0	0	0	0
SiO_2	50.03	7.874	49.36	7.735
TiO_2	0	0	0	0
Al_2O_3	0	0	1.47	.272
FeO	42.60	5.606	41.52	5.442
MnO	0.38	.051	0.53	.070
MgO	6.33	1.485	6.37	1.488
CaO	0.65	.109	0.73	.122
Na_2O	0	0	0	0
K_2O	0	0	0	0
SiO_2	51.75	8.042		
TiO_2	0	0		
Al_2O_3	0	0		
FeO	40.85	5.309		
MnO	0.63	.082		
MgO	6.06	1.404		
CaO	0.73	.121		
Na_2O	0	0		
K_2O	0	0		

L-22A (grunerite) continued

X-RAY POWDER DIFFRACTION

Intensity	hkl	d(obs.)	d(calc.)	d(obs.-calc.)
59	1 1 0	8.4249	8.3239	.1010
59	-1 1 0	8.4249	8.3239	.1010
2	2 0 0	4.6829	4.6741	.0089
8	2 2 0	4.1616	4.1619	-.0003
8	-2 2 0	4.1616	4.1619	-.0003
2	-1 3 1	3.8833	3.8763	.0070
2	1 3 1	3.4530	3.4576	-.0045
16	2 4 0	3.2784	3.2685	.0099
16	-2 4 0	3.2784	3.2685	.0099
100	3 1 0	3.0789	3.0718	.0071
100	-3 1 0	3.0789	3.0718	.0071
3	2 2 1	2.9980	2.9937	.0043
6	0 6 1	2.6329	2.6318	.0011
3	-2 0 2	2.5115	2.5111	.0004
2	3 5 0	2.3738	2.3720	.0018
2	-3 5 0	2.3738	2.3720	.0018
2	1 7 1	2.2220	2.2182	.0038
6	2 6 1	2.1936	2.1966	-.0031
3	3 5 1	2.0403	2.0407	-.0005
2	-4 0 2	1.9549	1.9547	.0001
2	5 3 0	1.7874	1.7875	-.0001
2	-5 3 0	1.7874	1.7875	-.0001
6	4 8 0	1.6340	1.6343	-.0003
4	6 0 0	1.5571	1.5580	-.0009
2	3 11 0	1.4670	1.4669	.0001
2	-3 11 0	1.4670	1.4669	.0001

L-22A (grunerite) continued

2	-2 12 2	1.3022	1.3029	-.0008
2	8 0 0	1.1680	1.1685	-.0005
2	7 13 0	.9685	.9686	-.0001
2	-7 13 0	.9685	.9686	-.0001

CELL CONSTANTS

a_o	= 9.558	± 0.0043	Å	
b_o	= 18.289	± 0.0080	Å	
c_o	= 5.333	± 0.0065	Å	
β	= 102.03	± 0.087	deg.	
V	= 911.76	± 1.11	$Å^3$	
a sin β	= 9.348		Å	

ENERGY DISPERSIVE X-RAY SPECTROSCOPY - average of 24 analyses

	Wt.%		Wt.%
SiO_2	46.8	TiO_2	0
Al_2O_3	0.2	MnO	0.3
FeO	44.9	P_2O_5	0
MgO	6.8	S	0
CaO	0.6	Cl	0
Na_2O	0.1	Cr_2O_3	0.2
K_2O	0		

X-RAY FLUORESCENCE SPECTROSCOPY

	Wt.%		Wt.%
SiO_2	49.27	Na_2O	0.24
Al_2O_3	1.51	K_2O	0.47
FeO	37.42	TiO_2	0.08
MgO	7.47	MnO	0.64
CaO	2.76	P_2O_5	0.14

L-22A (Hedenbergite)

ELECTRON MICROPROBE

	Wt.%	No. of ions on basis of 23 O	Wt.%	No. of ions on basis of 23 O
SiO_2	47.81	1.939	46.03	1.886
TiO_2	0	0	0	0
Al_2O_3	0	0	1.41	.068
FeO	23.31	.791	25.24	.865
MnO	0.36	.012	.32	.011
MgO	4.68	.282	3.64	.222
CaO	23.84	1.037	23.37	1.027
Na_2O	0	0	0	0
K_2O	0	0	0	0

SiO_2	49.49	1.983
TiO_2	0	0
Al_2O_3	0	0
FeO	22.70	.760
MnO	0	0
MgO	4.73	.282
CaO	23.09	.991
Na_2O	0	0
K_2O	0	0

L-22B (grunerite)

ELECTRON MICROPROBE

	Wt.%	No. of ions on basis of 23 O	Wt.%	No. of ions on basis of 23 O
SiO_2	50.51	7.916	50.10	7.814
TiO_2	0	0	0	0
Al_2O_3	0	0	0	0
FeO	41.88	5.490	40.44	5.274
MnO	0.58	.077	0.59	.078
MgO	6.39	1.494	8.21	1.906
CaO	0.63	.107	0.68	.114
Na_2O	0	0	0	0
K_2O	0	0	0	0
SiO_2	50.46	7.904	50.93	7.944
TiO_2	0	0	0	0
Al_2O_3	0	0	0	0
FeO	41.68	5.461	41.07	5.358
MnO	0.56	.075	0.67	.089
MgO	6.57	1.533	6.73	1.566
CaO	0.73	.122	0.58	.098
Na_2O	0	0	0	0
K_2O	0	0	0	0
SiO_2	50.38	7.885	50.99	7.941
TiO_2	0	0	0	0
Al_2O_3	0	0	0	0
FeO	41.46	5.426	40.89	5.327
MnO	0.57	.076	0.44	.058
MgO	6.96	1.622	6.94	1.609
CaO	0.64	.106	0.74	.124
Na_2O	0	0	0	0
K_2O	0	0	0	0

L-22B (grunerite) continued

	Wt.%	No. of ions on basis of 23 O	Wt.%	No. of ions on basis of 23 O
SiO_2	50.19	7.873	50.28	7.892
TiO_2	0	0	0	0
Al_2O_3	0	0	0	0
FeO	41.92	5.499	42.14	5.531
MnO	0.55	.073	0.47	.062
MgO	6.82	1.593	6.49	1.518
CaO	0.53	.089	0.63	.105
Na_2O	0	0	0	0
K_2O	0	0	0	0

ENERGY DISPERSIVE X-RAY SPECTROSCOPY

	Wt.%		Wt.%
SiO_2	46.5 51.2	TiO_2	0 0
Al_2O_3	0.6 0.2	MnO	0.9 0.5
FeO	40.2 38.9	P_2O_5	tr. 0
MgO	7.0 8.8	S	0 0
CaO	4.7 0	Cl	tr. 0.2
Na_2O	0 0.2	Cr_2O_3	0.1 0.1
K_2O	0 0		

L-22B (actinolite)

X-RAY POWDER DIFFRACTION

Intensity	hkl	d(obs.)	d(calc.)	d(obs.-calc)
100	1 1 0	8.4651	8.4354	.0297
100	-1 1 0	8.4651	8.4354	.0297
2	-1 1 1	4.9009	4.8942	.0066
83	3 1 0	3.1425	3.1327	.0099
83	-3 1 0	3.1425	3.1327	.0099
20	1 5 1	2.7223	2.7242	-.0019
6	0 6 1	2.6069	2.5998	.0071
3	-2 0 2	2.5425	2.5425	.0000
6	3 5 0	2.3921	2.3860	.0061
9	1 1 2	2.3470	2.3402	.0068
4	-4 2 1	2.3151	2.3138	.0013
9	2 6 1	2.1759	2.1764	-.0005
7	3 5 1	2.0316	2.0334	-.0018
3	1 5 2	1.9770	1.9751	.0019
6	4 6 1	1.6598	1.6617	-.0019
10	5 5 1	1.5123	1.5131	-.0009
11	-6 4 2	1.4457	1.4461	-.0004
4	2 10 2	1.3628	1.3621	.0007
2	-1 9 3	1.3291	1.3282	.0010
2	7 5 1	1.1786	1.1788	-.0003
2	5 11 2	1.0584	1.0589	-.0005
4	0 10 4	1.0511	1.0515	-.0004
6	-4 10 4	1.0390	1.0391	-.0002
3	6 6 3	.9927	.9925	.0001
3	-4 6 5	.9867	.9869	-.0001

L-22B (actinolite) continued

CELL CONSTANTS

a_o	= 9.827	±	0.0042	Å
b_o	= 18.057	±	0.0033	Å
c_o	= 5.327	±	0.0090	Å
β	= 103.77	±	0.070	deg.
V	= 918.09	±	1.55	$Å^3$

ENERGY DISPERSIVE X-RAY SPECTROSCOPY - average of 64 analyses

	Wt.%		Wt.%
SiO_2	53.3	TiO_2	tr.
Al_2O_3	0.5	MnO	0.2
FeO	25.1	P_2O_5	0.1
MgO	9.6	S	tr.
CaO	10.4	Cl	tr.
Na_2O	0.3	Cr_2O_3	0.1
K_2O	tr.		

L-25 (grunerite)

ELECTRON MICROPROBE

	Wt.%	No. of ions on basis of 23 O	Wt.%	No. of ions on basis of 23 O
SiO_2	50.86	7.823	50.92	7.798
TiO_2	0	0	0	0
Al_2O_3	0	0	0	0
FeO	37.66	4.844	36.09	4.622
MnO	0.70	.091	0.85	.111
MgO	9.96	2.284	10.81	2.466
CaO	0.82	.134	1.15	.189
Na_2O	0	0	0	0
K_2O	0	0	0.17	.034

L-25 (grunerite) continued

	Wt.%	No. of ions on basis of 23 O	Wt.%	No. of ions on basis of 23 O
SiO_2	50.95	7.810	50.90	7.815
TiO_2	0	0	0	0
Al_2O_3	0	0	0	0
FeO	36.72	4.707	37.15	4.771
MnO	0.96	.125	0.99	.129
MgO	10.62	2.428	10.36	2.371
CaO	0.73	.120	0.60	.099
Na_2O	0	0	0	0
K_2O	0	0	0	0
SiO_2	51.29	7.858	50.70	7.807
TiO_2	0	0	0	0
Al_2O_3	0	0	0	0
FeO	37.16	4.762	37.37	4.813
MnO	0.80	.104	1.15	.150
MgO	10.18	2.324	9.97	2.288
CaO	0.57	.093	0.81	.134
Na_2O	0	0	0	0
K_2O	0	0	0	0

L-25 (grunerite) continued

X-RAY POWDER DIFFRACTION

Intensity	hkl	d(obs.)	d(calc.)	d(obs.-calc.)
11	0 2 0	9.1178	9.1569	-.0391
100	1 1 0	8.3066	8.3255	-.0190
100	-1 1 0	8.3066	8.3255	-.0190
5	1 3 0	5.1257	5.1111	.0145
7	2 0 0	4.6829	4.6736	.0093
7	0 4 0	4.5752	4.5785	-.0032
21	2 2 0	4.1424	4.1628	-.0203
21	-2 2 0	4.1424	4.1628	-.0203
4	-1 3 1	3.9001	3.8806	.0195
9	1 3 1	3.4530	3.4602	-.0071
36	2 4 0	3.2725	3.2706	.0019
36	-2 4 0	3.2725	3.2706	.0019
61	3 1 0	3.0737	3.0716	.0021
61	-3 1 0	3.0737	3.0716	.0021
9	2 2 1	2.9931	2.9946	-.0015
26	1 5 1	2.7715	2.7605	.0110
15	0 6 1	2.6329	2.6351	-.0021
6	2 6 0	2.5565	2.5556	.0010
6	-2 6 0	2.5565	2.5556	.0010
6	-2 0 2	2.5149	2.5136	.0014
6	-3 5 1	2.3009	2.3029	-.0021
13	2 6 1	2.1987	2.1984	.0003
4	3 5 1	2.0403	2.0416	-.0014
4	1 5 2	2.0018	2.0006	.0011
7	-4 0 2	1.9569	1.9560	.0009
3	5 3 0	1.7874	1.7875	-.0001
3	-5 3 0	1.7874	1.7875	-.0001
23	4 6 1	1.6639	1.6635	.0005

L-25 (grunerite) continued

11	4	8	0	1.6367	1.6353	.0014
3	-1	5	3	1.5989	1.6003	-.0014
6	6	0	0	1.5583	1.5579	.0004
4	3	11	0	1.4660	1.4684	-.0024
4	-3	11	0	1.4660	1.4684	-.0024
77	-6	6	1	1.4050	1.4076	-.0026
11	5	1	2	1.3849	1.3848	.0000
8	-2	12	2	1.3037	1.3045	-.0008
7	4	12	0	1.2772	1.2778	-.0005
4	8	0	0	1.1686	1.1684	.0002
11	1	17	1	1.0448	1.0435	.0012
11	-9	1	2	1.0418	1.0410	.0008
4	-8	6	3	1.0180	1.0182	-.0002

CELL CONSTANTS

a_o = 9.558 ± 0.0029 Å

b_o = 18.314 ± 0.0069 Å

c_o = 5.339 ± 0.0043 Å

β = 102.056 ± 0.043 deg.

V = 913.92 ± 0.39 Å^3

$d \sin \beta$ = 9.347 Å

L-25 (grunerite) continued

ENERGY DISPERSIVE X-RAY SPECTROSCOPY - average of 60 analyses

	Wt.%		Wt.%
SiO_2	49.2	TiO_2	tr.
Al_2O_3	0.3	MnO	0.8
FeO	40.7	P_2O_5	0.1
MgO	7.4	S	tr.
CaO	0.9	Cl	tr.
Na_2O	0.1	Cr_2O_3	0.2
K_2O	tr.		

L-25 (actinolite)

ENERGY DISPERSIVE X-RAY SPECTROSCOPY - average of 42 analyses

	Wt.%		Wt.%
SiO_2	51.5	TiO_2	0
Al_2O_3	0.3	MnO	0.3
FeO	29.7	P_2O_5	0.1
MgO	8.6	S	0
CaO	9.0	Cl	0
Na_2O	0.1	Cr_2O_3	0.3
K_2O	0		

L-26 (grunerite)

ELECTRON MICROPROBE

	Wt.%	No. of ions on basis of 23 O	Wt.%	No. of ions on basis of 23 O
SiO_2	50.76	7.961	50.84	7.945
TiO_2	0	0	0	0
Al_2O_3	0	0	0	0
FeO	43.19	5.666	42.11	5.504
MnO	0	0	0.38	.050
MgO	6.04	1.412	6.67	1.566
CaO	0	0	0	0
Na_2O	0	0	0	0
K_2O	0	0	0	0
SiO_2	50.10	7.846	50.57	7.930
TiO_2	0	0	0	0
Al_2O_3	0	0	0	0
FeO	42.04	5.505	42.56	5.581
MnO	0.34	.044	0.30	.040
MgO	7.54	1.758	6.31	1.475
CaO	0	0	0.26	.044
Na_2O	0	0	0	0
K_2O	0	0	0	0
SiO_2	50.47	7.895		
TiO_2	0	0		
Al_2O_3	0	0		
FeO	42.11	5.509		
MnO	0.30	.040		
MgO	7.12	1.661		
CaO	0	0		
Na_2O	0	0		
K_2O	0	0		

L-29A (grunerite

ELECTRON MICROPROBE

	Wt.%	No. of ions on basis of 23 O	Wt.%	No. of ions on basis of 23 O
SiO_2	50.06	7.787	50.[illegible]	7.[illegible]
TiO_2	0	0	0	0
Al_2O_3	0		0	0
FeO	40.57	5.279	[illegible]	5.326
MnO	[illegible]	0	0.35	.045
MgO	9.03	2.094	[illegible]	2.116
CaO	0.32	.054	0	0
Na_2O	0	0		
K_2O	0	0	0	0
SiO_2	52.11	7.983	[illegible].89	
TiO_2	0	0	0	0
Al_2O_3	0	0	0	0
FeO	38.75	[illegible].965	[illegible] 72	5.[illegible]32
MnO	0	0	0	
MgO	8.86	2.022	9.[illegible]	2.[illegible]2
CaO	[illegible].[illegible]0	[illegible]47	[illegible] 0	.[illegible] 0
Na_2O	0	0	0	
K_2O	0	0	0	0
SiO_2	49.83	7.782	53.00	8.[illegible]
TiO_2	0	0	0	
Al_2O_3	0			0
FeO	41.19	[illegible]	36.01	[illegible]7[illegible]
MnO	0.30	.040	0	0
MgO	8.68	2.018	9.[illegible]	[illegible].212
CaO	0	0	0.3[illegible]	[illegible] 0
Na_2O	0	0		
K_2O	0	0	[illegible]	0

L-29 A (grunerite) continued

X-RAY POWDER DIFFRACTION

Intensity	hkl	d(obs.)	d(calc.)	d(obs.-calc.)
84	1 1 0	8.3851	8.3305	.0546
84	-1 1 0	8.3851	8.3305	.0546
13	2 0 0	4.6829	4.6758	.0072
37	2 2 0	4.1616	4.1652	-.0036
37	-2 2 0	4.1616	4.1652	-.0036
8	-1 3 1	3.8833	3.8733	.0100
11	1 3 1	3.4596	3.4620	-.0024
50	2 4 0	3.2843	3.2732	.0112
50	-2 4 0	3.2843	3.2732	.0112
100	3 1 0	3.0737	3.0731	.0006
100	-3 1 0	3.0737	3.0731	.0006
8	2 2 1	2.9980	2.9981	-.0001
79	1 5 1	2.7631	2.7625	.0006
18	0 6 1	2.6367	2.6358	.0009
18	-2 0 2	2.5047	2.5037	.0010
18	2 6 1	2.1987	2.2008	-.0022
11	3 5 1	2.0446	2.0443	.0004
37	4 6 1	1.6653	1.6656	-.0003
16	6 0 0	1.5583	1.5586	-.0003
40	-6 6 1	1.4060	1.4068	-.0009
63	5 1 2	1.3867	1.3867	.0000
11	-2 12 2	1.3037	1.3042	-.0005

CELL CONSTANTS

a_o = 9.553 ± 0.0048 Å

b_o = 18.334 ± 0.0128 Å

c_o = 5.323 ± 0.0061 Å

β = 101.79 ± 0.059 deg.

V = 912.59 ± 1.05 $Å^3$

$a \sin \beta$ = 9.352 Å

L-29A(grunerite) continued

ENERGY DISPERSIVE X-RAY SPECTROSCOPY - average of 39 analyses

	Wt.%		Wt.%
SiO_2	44.0	TiO_2	0
Al_2O_3	tr.	MnO	0.1
FeO	47.2	P_2O_5	1.1
MgO	6.2	S	0
CaO	0.1	Cl	0
Na_2O	tr.	Cr_2O_3	0.7
K_2O	0		

L-29A (eulite)

ELECTRON MICROPROBE

	Wt.%	No. of ions on basis of 6 O
SiO_2	56.25	2.158
TiO_2	0	0
Al_2O_3	0	0
FeO	32.26	1.035
MnO	0.33	.011
MgO	11.16	.638
CaO	0	0
Na_2O	0	0
K_2O	0	0

L-29B (grunerite)

ENERGY DISPERSIVE X-RAY SPECTROSCOPY - average of 30 analyses

	Wt.%		Wt.%
SiO_2	45.8	TiO_2	0
Al_2O_3	0.3	MnO	tr.
FeO	47.2	P_2O_5	tr.
MgO	6.0	S	0
CaO	tr.	Cl	0
Na_2O	0	Cr_2O_3	0.3
K_2O	0		

L-29C (grunerite)

ELECTRON MICROPROBE

	Wt.%	No. of ions on basis of 23 O	Wt.%	No. of ions on basis of 23 O
SiO_2	47.06	7.529	46.44	7.465
TiO_2	0	0	0	0
Al_2O_3	0	0	0	0
FeO	44.45	5.947	44.72	6.013
MnO	0.30	.041	0.43	.059
MgO	8.19	1.953	8.17	1.959
CaO	0	0	0.22	0.38
Na_2O	0	0	0	0
K_2O	0	0	0	0

L-29C (grunerite) continued

	Wt.%	No. of ions on basis of 23 O
SiO_2	46.55	7.468
TiO_2	0	0
Al_2O_3	0	0
FeO	44.46	5.964
MnO	0.33	.045
MgO	8.41	2.010
CaO	0.26	.045
Na_2O	0	0
K_2O	0	0

L-29C (ankerite)

ELECTRON MICROPROBE

	Wt.%	No. of ions on basis of 6 O
FeO	36.36	1.757
MnO	0.89	.043
MgO	13.07	1.124
CaO	49.68	3.075

L-32 (anthophyllite)

ELECTRON MICROPROBE

	Wt.%	No. of ions on basis of 23 O	Wt.%	No. of ions on basis of 23 O
SiO_2	49.81	6.705	57.09	7.733
TiO_2	0	0	0	0
Al_2O_3	15.63	2.481	0.72	.115
FeO	11.76	1.325	12.43	1.408
MnO	0	0	0.24	.027
MgO	22.24	4.463	28.97	5.847
CaO	0.55	.079	0.55	.080
Na_2O	0	0	0	0
K_2O	0	0	0	0
SiO_2	57.28	7.744	58.53	7.893
TiO_2	0	0	0	0
Al_2O_3	0	0	0	0
FeO	13.12	1.490	12.35	1.393
MnO	0	0	0.23	.026
MgO	29.16	5.898	28.63	5.755
CaO	0.44	.064	0.27	.039
Na_2O	0	0	0	0
K_2O	0	0	0	0
SiO_2	57.09	7.714	57.25	7.778
TiO_2	0	0	0	0
Al_2O_3	0.60	.095	0	0
FeO	12.04	1.360	13.07	1.485
MnO	0	0	0.24	.027
MgO	29.76	5.994	28.90	5.852
CaO	0.52	.075	0.55	.080
Na_2O	0	0	0	0
K_2O	0	0	0	0

L-32 (anthophyllite) continued

SiO_2	58.26	7.869	57.84	7.847
TiO_2	0	0	0	0
Al_2O_3	0	0	0	0
FeO	12.37	1.397	13.39	1.520
MnO	0.36	.041	0	0
MgO	28.71	5.779	28.28	5.716
CaO	0.31	.045	0.48	.070
Na_2O	0	0	0	0
K_2O	0	0	0	0
SiO_2	57.29	7.793	57.44	7.746
TiO_2	0	0	0	0
Al_2O_3	0	0	0.94	.149
FeO	13.72	1.561	11.51	1.298
MnO	0	0	0.40	.045
MgO	28.63	5.802	29.19	5.867
CaO	0.35	.051	0.51	.074
Na_2O	0	0	0	0
K_2O	0	0	0	0

X-RAY POWDER DIFFRACTION

Intensity	hkl	d(obs.)	d(calc.)	d(obs.-calc.)
8	0 2 0	9.0712	9.0267	.0445
42	2 1 0	8.2295	8.2580	-.0285
7	2 3 0	5.0390	5.0502	-.0112
10	0 4 0	4.5063	4.5133	-.0070
14	4 2 0	4.1329	4.1290	.0039
5	2 2 1	4.0860	4.0915	-.0055
37	4 4 0	3.2375	3.2364	.0012
100	6 1 0	3.0531	3.0510	.0022
7	5 2 1	2.8801	2.8794	.0007

L-32 (anthophyllite) continued

8	2	5	1	2.8400	2.8379	.0021
20	6	3	0	2.7549	2.7527	.0022
7	1	6	1	2.5851	2.887	-.0036
10	4	8	0	2.0316	2.0297	.0019
7	2	8	1	2.0251	2.0252	-.0001
5	6	6	1	1.9976	1.9973	.0003
7	7	0	2	1.8697	1.8715	-.0018
17	10	1	0	1.8448	1.8476	-.0027
13	9	5	1	1.6966	1.6967	-.0001
12	2	11	0	1.6156	1.6162	-.0006
12	0	5	3	1.5826	1.5821	.0005
10	12	1	2	1.3324	1.3316	.0008
10	12	6	1	1.3324	1.3318	.0006
7	0	9	3	1.3227	1.3230	-.0003
7	14	1	0	1.3227	1.3231	-.0004
9	8	9	2	1.3163	1.3159	.0004

CELL CONSTANTS

a_o = 18.573 ± 0.0105 Å
b_o = 18.053 ± 0.0149 Å
c_o = 5.280 ± 0.0059 Å
V = 1770.49 ± 1.46 $Å^3$

ENERGY DISPERSIVE X-RAY SPECTROSCOPY - average of 23 analyses

	Wt.%		Wt.%
SiO_2	56.0	TiO_2	0
Al_2O_3	0.4	MnO	0.3
FeO	16.6	P_2O_5	0.8
MgO	23.5	S	0
CaO	0.2	Cl	0
Na_2O	tr.	Cr_2O_3	0.6
K_2O	0		

L-45 (grunerite)

X-RAY POWDER DIFFRACTION

Intensity	hkl			d(obs.)	d(calc.)	d(obs.-calc.)
13	0	2	0	9.2126	9.1442	.0684
69	1	1	0	8.3066	8.3235	-.0169
69	-1	1	0	8.3066	8.3235	-.0169
15	2	0	0	4.6586	4.6739	-.0153
7	0	4	0	4.5637	4.5721	-.0085
18	2	2	0	4.1616	4.1617	-.0001
18	-2	2	0	4.1616	4.1617	-.0001
4	-1	3	1	3.8750	3.8762	-.0012
7	1	3	1	3.4596	3.4595	.0001
56	2	4	0	3.2608	3.2683	-.0076
56	-2	4	0	3.2608	3.2683	-.0076
100	3	1	0	3.0685	3.0716	-.0031
100	-3	1	0	3.0685	3.0716	-.0031
29	2	2	1	2.9882	2.9956	-.0074
46	1	5	1	2.7631	2.7588	.0044
65	0	6	1	2.6292	2.6322	-.0030
8	-2	0	2	2.5115	2.5111	.0005
10	3	5	0	2.3708	2.3719	-.0011
10	-3	5	0	2.3708	2.3719	-.0011
14	-3	5	1	2.2981	2.3005	-.0024
7	-4	2	1	2.2459	2.2486	-.0027
14	1	7	1	2.2194	2.2187	.0007
29	2	6	1	2.1987	2.1974	.0013
7	3	5	1	2.0403	2.0415	-.0012
6	1	5	2	2.0018	2.0000	.0018
7	-4	0	2	1.9549	1.9539	.0010
22	4	6	1	1.6639	1.6633	.0006
3	-1	5	3	1.5976	1.5992	-.0016

L-45 (grunerite) continued

7	6	0	0	1.5571	1.5580	-.0009
4	3	11	0	1.4681	1.4668	.0012
4	-3	11	0	1.4681	1.4668	.0012
19	-6	6	1	1.4069	1.4067	.0002
6	5	1	2	1.3867	1.3856	.0011
7	-2	12	2	1.3022	1.3028	-.0007
7	4	12	0	1.2772	1.2766	.0007
11	1	17	1	1.0418	1.0422	-.0003
4	-8	6	3	1.0176	1.0172	.0004

CELL CONSTANTS

a_o	= 9.555	± 0.0029	Å
b_o	= 18.288	± 0.0048	Å
c_o	= 5.336	± 0.0030	Å
β	= 101.97	± 0.032	deg.
V	= 912.17	± 0.51	$Å^3$
a sin β	= 9.348		Å

L-46 (grunerite)

ELECTRON MICROPROBE

	Wt.%	No. of ions on basis of 23 O	Wt.%	No. of ions on basis of 23 O
SiO_2	52.80	7.968	52.67	7.963
TiO_2	0	0	0	0
Al_2O_3	0	0	0	0
FeO	35.99	4.542	36.29	4.588
MnO	0	0	0	0
MgO	11.21	2.522	11.04	2.486
CaO	0	0	0	0
Na_2O	0	0	0	0
K_2O	0	0	0	0
SiO_2	53.08	7.998	53.37	8.040
TiO_2	0	0	0	0
Al_2O_3	0	0	0	0
FeO	35.56	4.481	35.78	4.507
MnO	0	0	0	0
MgO	10.91	2.451	10.49	2.357
CaO	0.45	.072	0.36	.057
Na_2O	0	0	0	0
K_2O	0	0	0	0

L-46 (ankerite)

ELECTRON MICROPROBE

	Wt.%	Wt.%
FeO	32.11	31.57
MgO	16.70	15.22
CaO	51.17	53.18

L-47A (grunerite)

ELECTRON MICROPROBE

	Wt.%	No. of ions on basis of 23 O	Wt.%	No. of ions on basis of 23 O
SiO_2	50.91	7.820	51.43	7.861
TiO_2	0	0	0	0
Al_2O_3	0	0	0	0
FeO	38.42	4.936	37.73	4.824
MnO	0	0	0	0
MgO	10.39	2.377	10.58	2.412
CaO	0.29	.048	0.26	.041
Na_2O	0	0	0	0
K_2O	0	0	0	0
SiO_2	52.62	7.987	52.41	7.985
TiO_2	0.49	.056	0	0
Al_2O_3	0	0	0	0
FeO	37.21	4.724	37.87	4.826
MnO	0	0	0	0
MgO	9.68	2.191	9.71	2.204
CaO	0	0	0	0
Na_2O	0	0	0	0
K_2O	0	0	0	0
SiO_2	51.59	7.920	51.98	7.933
TiO_2	0	0	0	0
Al_2O_3	0	0	0	0
FeO	39.01	5.008	37.95	4.845
MnO	0	0	0	0
MgO	9.40	2.151	10.06	2.288
CaO	0	0	0	0
Na_2O	0	0	0	0
K_2O	0	0	0	0

L-47A (grunerite) continued

X-RAY POWDER DIFFRACTION

Intensity	hkl	d(obs.)	d(calc.)	d(obs.-calc.)
40	1 1 0	8.3456	8.3263	.0193
40	-1 1 0	8.3456	8.3263	.0193
3	1 3 0	5.0964	5.1040	-.0075
4	0 4 0	4.5637	4.5679	-.0042
16	2 2 0	4.1520	4.1632	-.0112
16	-2 2 0	4.1520	3.1632	-.0112
3	-1 3 1	3.8667	3.8729	-.0063
7	1 3 1	3.4596	3.4549	.0047
24	2 4 0	3.2666	3.2679	-.0013
24	-2 4 0	3.2666	3.2679	-.0013
100	3 1 0	3.0634	3.0736	-.0102
100	-3 1 0	3.0634	3.0736	-.0102
9	2 2 1	2.9931	2.9929	.0002
26	1 5 1	2.7590	2.7555	.0035
12	0 6 1	2.6292	2.6291	.0000
8	2 6 0	2.5530	2.5520	.0010
8	-2 6 0	2.5530	2.5520	.0010
6	-2 0 2	2.5047	2.5091	-.0044
3	3 5 0	2.3738	2.3719	.0019
3	-3 5 0	2.3738	2.3719	.0019
13	2 6 1	2.1961	2.1953	.0008
13	3 5 1	2.0403	2.0402	.0000
3	1 5 2	1.9997	1.9970	.0027
42	-4 0 2	1.9509	1.9545	-.0036
2	5 3 0	1.7906	1.7883	.0023
2	-5 3 0	1.7906	1.7883	.0023
12	4 6 1	1.6639	1.6626	.0013
14	4 8 0	1.6340	1.6339	.0001
51	6 0 0	1.5571	1.5590	-.0019
3	3 11 0	1.4670	1.4660	.0010
3	-3 11 0	1.4670	1.4660	.0010

L-47A (grunerite) continued

13	-6	6	1	1.4069	1.4075	-.0006
9	5	1	2	1.3840	1.3846	-.0007
9	-2	12	2	1.3014	1.3017	-.0003
14	4	12	0	1.2758	1.2760	-.0002
3	5	11	2	1.0654	1.0654	.0000
9	1	17	1	1.0406	1.0412	-.0006
3	-8	6	3	1.0184	1.0177	.0006

CELL CONSTANTS

a_o	= 9.564	± 0.0033	Å	
b_o	= 18.272	± 0.0055	Å	
c_o	= 5.327	± 0.0042	Å	
β	= 102.03	± 0.034	deg.	
V	= 910.52	± 0.72	$Å^3$	
a sin β	= 9.354		Å	

L-47B (grunerite)

ELECTRON MICROPROBE

	Wt.%	No. of ions on basis of 23	Wt.%	No. of ions on basis of 23
SiO_2	51.60	7.[illegible]	52.14	7.9[illegible]
TiO_2	0	0	[illegible]	[illegible]
Al_2O_3	0	[illegible]	[illegible]	[illegible]
FeO	35.39	4.507	[illegible]	[illegible]
MnO	0.38	.049	[illegible]	[illegible]
MgO	10.56	2.396	[illegible]	2.408
CaO	2.05	.335	[illegible]	.119
Na_2O	0	0	[illegible]	[illegible]
K_2O	0	0	[illegible]	[illegible]
SiO_2	52.34	7.9[illegible]	[illegible]	7.9[illegible]
TiO_2	0	[illegible]	[illegible]	[illegible]
Al_2O_3	0	[illegible]	[illegible]	[illegible]
FeO	35.[illegible]	4.5[illegible]	[illegible]	[illegible]
MnO	0.46	.060	[illegible]	043
MgO	10.63	2.401	[illegible]	[illegible]
CaO	1.06	[illegible]	[illegible]	.137
Na_2O	0	[illegible]	[illegible]	[illegible]
K_2O	0	0	[illegible]	[illegible]
SiO_2	51.82	7.896	[illegible]4	7.960
TiO_2	0	0	[illegible]	[illegible]
Al_2O_3	0	0	[illegible]	[illegible]
FeO	36.63	4.668	35.72	4.526
MnO	0.43	.055	0.53	[illegible]
MgO	10.49	2.382	10.48	2.367
CaO	0.63	.102	0.74	.120
Na_2O	0	0	0	[illegible]
K_2O	0	0	0	[illegible]

L-47B (grunerite) continued

X-RAY POWDER DIFFRACTION

Intensity	hkl	d(obs.)	d(calc.)	d (obs.-calc.)
98	1 1 0	8.3456	8.3177	.0279
98	-1 1 0	8.3456	8.3177	.0279
6	1 3 0	5.1404	5.1029	,0375
18	2 0 0	4.6707	4.6705	.0002
15	0 4 0	4.5753	4.5692	.0061
26	2 2 0	4.1713	4.1589	.0124
26	-2 2 0	4.1713	4.1589	.0124
6	-1 3 1	3.8750	3.8749	.0001
15	1 3 1	3.4662	3.4579	.0084
100	2 4 0	3.2666	3.2662	.0005
100	-2 4 0	3.2666	3.2662	.0005
78	3 1 0	3.0685	3.0695	-.0009
78	-3 1 0	3.0685	3.0695	-.0009
16	2 2 1	2.9931	2.9939	-.0008
53	1 5 1	2.7631	2.7573	.0058
42	0 6 1	2.6367	2.6308	.0059
6	2 6 0	2.5530	2.5515	.0015
6	-2 6 0	2.5530	2.5515	.0015
7	-2 0 2	2.5115	2.5107	.0008
7	3 5 0	2.3708	2.3703	.0005
7	-3 5 0	2.3708	2.3703	.0005
27	-3 5 1	2.3009	2.2993	.0016
24	-4 2 1	2.2459	2.2474	-.0015
7	1 7 1	2.2194	2.2174	.0020
46	2 6 1	2.1961	2.1960	.0001
15	3 5 1	2.0424	2.0402	.0022
7	-4 0 2	1.9529	1.9533	-.0004

L-47B (grunerite) continued

29	4	6	1	1.6625	1.5522	.0003
20	4	8	0	1.6340	1.6331	.0009
13	6	0	0	1.5571	1.5568	.0003
20	0	12	0	1.5234	1.5231	.0003
16	-2	6	3	1.5200	1.5198	.0002
35	-6	6	1	1.4060	1.4058	.0001
7	5	1	2	1.3831	1.3847	-.0017
16	-2	12	2	1.3022	1.3022	-.0001
7	4	12	0	1.2750	1.2557	-.0007
7	-5	11	2	1.1858	1.1864	-.0006
22	1	17	1	1.0410	1.0415	-.0005

CELL CONSTANTS

a_o	= 9.549	± 0.0035	Å	
b_o	= 18.277	± 0.0047	Å	
c_o	= 5.335	± 0.0034	Å	
β	= 101.98	± 0.039	deg.	
V	= 910.82	± 0.58	$Å^3$	
a sin β	= 9.341		Å	

L-48 (grunerite)

X-RAY POWDER DIFFRACTION

Intensity	hkl	d(obs.)	d(calc.)	d(obs.-calc.)
18	0 2 0	9.2126	9.1498	.0628
99	1 1 0	8.3614	8.3201	.0412
99	-1 1 0	8.3614	8.3201	.0412
6	1 3 0	5.1257	5.1074	.0183
8	2 0 0	4.6829	4.6707	.0122
13	0 4 0	5.5870	4.5749	.0121
18	2 2 0	4.1616	4.1601	.0016
18	-2 2 0	4.1616	4.1601	.0016
8	1 3 1	3.4596	3.4619	-.0023
42	2 4 0	3.2725	3.2683	.0042
42	-2 4 0	3.2725	3.2683	.0042
100	3 1 0	3.0737	3.0697	.0040
100	-3 1 0	3.0737	3.0697	.0040
12	2 2 1	2.9980	2.9963	.0018
35	1 5 1	2.7673	2.7606	.0067
16	0 6 1	2.6329	2.6343	-.0013
5	2 6 0	2.5530	2.5537	-.0007
5	-2 6 0	2.5530	2.5537	-.0007
14	-2 0 2	2.5115	2.5138	-.0023
9	-3 5 1	2.3009	2.3009	.0000
6	1 7 1	2.2194	2.2201	-.0007
17	2 6 1	2.1987	2.1982	.0005
6	3 5 1	2.0446	2.0417	.0029
5	-4 0 2	1.9589	1.9546	.0043
6	5 1 0	1.8554	1.8586	-.0032
6	-5 1 0	1.8554	1.8586	-.0032
5	-4 6 1	1.8466	1.8460	.0006
3	5 3 0	1.7874	1.7864	.0010
3	-5 3 0	1.7874	1.7864	.0010

L-48 (grunerite) continued

20	4	8	0	1.6367	1.6341	.0025
16	6	0	0	1.5559	1.5569	-.0010
19	0	12	0	1.5245	1.5250	-.0004
12	-2	6	3	1.5211	1.5219	-.0007
3	3	11	0	1.4670	1.4673	-.0003
3	-3	11	0	1.4670	1.4673	-.0003
21	-6	6	1	1.4060	1.4063	-.0003
6	-2	12	2	1.3029	1.3038	-.0009
6	4	12	0	1.2765	1.2769	-.0003
4	8	0	0	1.1674	1.1677	-.0003

CELL CONSTANTS

a_o	= 9.549	±	0.0031	Å
b_o	= 18.300	±	0.0062	Å
c_o	= 5.343	±	0.0042	Å
β	= 101.98	±	0.064	deg.
V	= 913.33	±	0.72	$Å^3$
a sin β	= 9.341			Å

L-51A (grunerite)

ELECTRON MICROPROBE

	Wt.%	No. of ions on basis of 23 O	Wt.%	No. of ions on basis of 23 O
SiO_2	52.64	7.979	52.87	8.001
TiO_2	0	0	0	0
Al_2O_3	0	0	0	0
FeO	36.92	4.680	36.20	4.583
MnO	0	0	0.54	070
MgO	10.46	2.362	10.39	2.344
CaO	0	0	0	0
Na_2O	0	0	0	0
K_2O	0	0	0	0

X-RAY POWDER DIFFRACTION

Intensity	hkl	d(obs.)	D(calc.)	d(obs.-calc.)
3	0 2 0	9.1650	9.1427	.0223
28	1 1 0	8.3066	8.3228	-.0163
28	-1 1 0	8.3066	8.3228	-.0163
1	1 3 0	5.1110	5.1056	.0054
1	-1 1 1	4.8478	4.8381	.0097
2	2 0 0	4.6707	4.6736	-.0029
4	0 4 0	4.5753	4.5713	.0040
9	2 2 0	4.1616	4.1614	.0002
9	-2 2 0	4.1616	4.1614	.0002
3	1 3 1	3.4530	3.4554	-.0023
13	2 4 0	3.2608	3.2680	-.0072
13	-2 4 0	3.2608	3.2680	-.0072
100	3 1 0	3.0685	3.0715	-.0029
100	-3 1 0	3.0685	3.0715	-.0029

L-51A (grunerite) continued

3	2	2	1	2.9882	2.9922	-.0040
13	1	5	1	2.7631	2.7565	.0066
3	0	6	1	2.6292	2.6306	-.0014
2	2	6	0	2.5565	2.5528	.0037
2	-2	6	0	2.5565	2.5528	.0037
2	-2	0	2	2.5081	2.5084	-.0003
2	3	5	0	2.3708	2.3717	-.0009
2	-3	5	0	2.3708	2.3717	-.0009
4	-3	5	1	2.3009	2.3005	.0004
2	-4	2	1	2.2459	2.2489	-.0031
2	1	7	1	2.2168	2.2174	-.0006
10	2	6	1	2.1961	2.1958	.0003
2	3	5	1	2.0403	2.0401	.0002
2	-4	0	2	1.9549	1.9534	.0014
4	4	6	1	1.6625	1.6624	.0001
3	6	0	0	1.5571	1.5579	-.0008
2	3	11	0	1.4670	1.4666	.0004
2	-3	11	0	1.4670	1.4666	.0004
7	-6	6	1	1.4060	1.4069	-.0009
2	5	1	2	1.3840	1.3841	-.0001
2	-2	12	2	1.3022	1.3023	-.0002
3	3	12	0	1.2772	1.2764	.0009
1	8	0	0	1.1692	1.1684	.0008
1	5	11	2	1.0654	1.0654	-.0000
4	1	17	1	1.0414	1.0419	-.0005
3	7	13	0	.9685	.9684	.0000
3	-7	13	0	.9685	.9684	.0000

CELL CONSTANTS

a_o = 9.557 ± 0.0022 Å

b_o = 18.285 ± 0.0035 Å

c_o = 5.327 ± 0.0033 Å

β = 102.02 ± 0.031 deg.

V = 910.46 ± 0.56 $Å^3$

a sin β = 9.347 Å

L-53 (grunerite)

ELECTRON MICROPROBE

	Wt.%	No. of ions on basis of 23 O	Wt.%	No. of ions on basis of 23 O
SiO_2	51.29	7.718	47.53	7.169
TiO_2	0	0	0	0
Al_2O_3	4.70	.832	9.92	1.764
FeO	36.16	4.551	35.95	4.534
MnO	0	0	0	0
MgO	7.87	1.764	6.59	1.483
CaO	0	0	0	0
Na_2O	0	0	0	0
K_2O	0	0	0	0
SiO_2	47.81	7.272	47.19	7.199
TiO_2	0	0	0	0
Al_2O_3	8.35	1.498	8.20	1.475
FeO	37.49	4.770	37.62	4.800
MnO	0	0	0	0
MgO	6.35	1.438	6.99	1.591
CaO	0	0	0	0
Na_2O	0	0	0	0
K_2O	0	0	0	0
SiO_2	47.46	7.240		
TiO_2	0	0		
Al_2O_3	7.68	1.381		
FeO	37.60	4.797		
MnO	0	0		
MgO	7.27	1.652		
CaO	0	0		
Na_2O	0	0		
K_2O	0	0		

L-53 (grunerite) continued

X-RAY POWDER DIFFRACTION

Intensity	hkl	d(obs.)	d(calc.)	d(obs.-calc.)
56	1 1 0	8.3851	8.3325	.0525
56	-1 1 0	8.3851	8.3325	.0525
9	-1 1 1	4.8478	4.8452	.0026
9	2 0 0	4.6952	4.6759	.0193
6	0 4 0	4.5988	4.5885	.0103
12	2 2 0	4.1810	4.1663	.0147
12	-2 2 0	4.1810	4.1663	.0147
8	-1 3 1	3.8917	3.8823	.0094
30	2 4 0	3.2725	3.2750	-.0025
30	-2 4 0	3.2725	3.2750	-.0025
100	3 1 0	3.0737	3.0733	.0004
100	-3 1 0	3.0737	3.0733	.0004
21	1 5 1	2.7673	2.7665	.0008
14	0 6 1	2.6442	2.6401	.0041
5	-2 0 2	2.5115	2.5117	-.0002
7	-3 5 1	2.2981	2.3032	-.0052
6	1 7 1	2.2273	2.2255	.0017
7	3 5 1	2.0403	2.0458	-.0055
7	-4 0 2	1.9529	1.9533	-.0004
11	4 6 1	1.6667	1.6666	.0001
8	4 8 0	1.6393	1.6375	.0018
11	0 12 0	1.5279	1.5295	-.0015
12	-6 6 1	1.4069	1.4077	-.0007
13	5 1 2	1.3876	1.3877	-.0001
7	-2 12 2	1.3068	1.3063	.0005

L-53 (grunerite) continued

CELL CONSTANTS

a_o	= 9.556	±	0.0064	Å
b_o	= 18.354	±	0.0103	Å
c_o	= 5.341	±	0.0065	Å
β	= 101.86	±	0.061	deg.
V	= 916.76	±	1.12	$Å^3$
a sin β	= 9.352			Å

ENERGY DISPERSIVE X-RAY SPECTROSCOPY - average of 20 analyses

	Wt.%		Wt.%
SiO_2	49.5	TiO_2	0
Al_2O_3	tr.	MnO	tr.
FeO	42.7	P_2O_5	0.1
MgO	7.4	S	0
CaO	0	Cl	0
Na_2O	0	Cr_2O_3	tr.
K_2O	0		

L-53 (siderite)

ELECTRON MICROPROBE

	Wt.%	Wt.%
FeO	85.92	86.69
MnO	1.74	1.41
MgO	11.69	10.94
CaO	0.65	0.96

L-54 (grunerite)

ENERGY DISPERSIVE X-RAY SPECTROSCOPY - average of 7 analyses

	Wt.%		Wt.%
SiO_2	52.6	TiO_2	0
Al_2O_3	0.5	MnO	0
FeO	36.8	P_2O_5	0
MgO	9.3	S	0
CaO	tr.	Cl	0
Na_2O	tr.	Cr_2O_3	0
K_2O	0		

L-55 (grunerite)

ELECTRON MICROPROBE

	Wt.%	No. of ions on basis of 23 O	Wt.%	No. of ions on basis of 23 O
SiO_2	51.53	7.848	53.07	8.062
TiO_2	0	0	0	0
Al_2O_3	0	0	0	0
FeO	36.43	4.640	37.30	4.738
MnO	0.37	.047	0	0
MgO	11.15	2.531	8.95	2.026
CaO	0.53	.086	0.68	.111
Na_2O	0	0	0	0
K_2O	0	0	0	0

L-55 (grunerite) continued

SiO_2	53.11	8.088	52.32	8.008
TiO_2	0	0	0	0
Al_2O_3	0	0	0	0
FeO	37.86	4.823	38.41	4.917
MnO	0	0	0	0
MgO	8.27	1.877	8.52	1.943
CaO	0.76	.124	0.76	.124
Na_2O	0	0	0	0
K_2O	0	0	0	0

SiO_2	52.89	8.061
TiO_2	0	0
Al_2O_3	0	0
FeO	37.92	4.833
MnO	0	0
MgO	8.48	1.928
CaO	0.71	.117
Na_2O	0	0
K_2O	0	0

X-RAY POWDER DIFFRACTION

Intensity	hkl	d(obs.)	d(calc.)	d(obs.-calc.)
50	1 1 0	8.3851	8.3274	.0577
50	-1 1 0	8.3851	8.3274	.0577
11	2 0 0	4.6829	4.6775	.0054
14	2 2 0	4.1713	4.1637	.0076
14	-2 2 0	4.1713	4.1637	.0076
3	-1 3 1	3.9086	3.8810	.0276
4	1 3 1	3.4729	3.4634	.0095
19	2 4 0	3.2784	3.2684	.0100
19	-2 4 0	3.2784	3.2684	.0100

L-55 (grunerite) continued

100	3	1	0	3.0789	3.0739	.0050
100	-3	1	0	3.0789	3.0739	.0050
6	2	2	1	3.0029	2.9993	.0036
6	0	6	1	2.6367	2.6325	.0041
2	2	6	0	2.5530	2.5524	. 006
2	-2	6	0	2.5530	2.5524	.0006
9	2	6	1	2.1987	2.1981	.0006
3	-4	0	2	1.9549	1.9576	-.0028
14	4	6	1	1.6639	1.6642	-.0003
13	-6	6	1	1.4060	1.4076	-.0016
3	-2	12	2	1.3037	1.3031	.0006
5	4	12	0	1.2772	1.2762	.0010
3	5	11	2	1.0658	1.0667	-.0009
5	1	17	1	1.0410	1.0416	-.0006

CELL CONSTANTS

a_o	= 9.564	± 0.0082	Å	
b_o	= 18.275	± 0.0097	Å	
c_o	= 5.351	± 0.0109	Å	
β	= 101.99	± 0.084	deg.	
V	= 914.82	± 1.86	$Å^3$	
a sin β	= 9.355		Å	

ENERGY DISPERSIVE X-RAY SPECTROSCOPY - average of 9 analyses

	Wt.%		Wt.%
SiO_2	48.4	TiO_2	0
Al_2O_3	0.4	MnO	0.1
FeO	41.4	P_2O_5	0
MgO	8.7	S	0
CaO	0.3	Cl	0
Na_2O	0.4	Cr_2O_3	0.1
K_2O	0		

L-55 (ankerite)

ELECTRON MICROPROBE

	Wt.%	Wt.%	Wt.%
FeO	37.79	40.33	40.44
MgO	13.67	15.70	14.61
CaO	48.54	43.97	44.95
MnO	0	0	0

ENERGY DISPERSIVE X-RAY SPECTROSCOPY

	Wt.%		Wt.%
SiO_2	1.2	TiO_2	0
Al_2O_3	0	MnO	1.0
FeO	39.5	P_2O_5	0
MgO	13.0	S	0
CaO	44.3	Cl	0.1
Na_2O	0.5	Cr_2O_3	0.5
K_2O	0		

L-56 (grunerite)

ELECTRON MICROPROBE

	Wt.%	No. of ions on basis of 23 O	Wt.	No. of ions on basis 23 O
SiO_2	53.17	7.959	52.56	7.92
TiO_2	0	0		
Al_2O_3	0	0	0	0
FeO	33.57	4.203	33.98	4.261
MnO	0.61	.076	0.45	.058
MgO	12.33	2.749	12.67	2.8[illegible]
CaO	0.33	.053	0.37	.060
Na_2O	0	0	0	0
K_2O	0	0	0	0
SiO_2	52.97	7.911	54.11	8.021
TiO_2	0	0	0	
Al_2O_3	0	0	0	
FeO	33.27	4.156	32.84	4.[illegible]
MnO	0.41	.052	0	0
MgO	13.35	2.970	13.06	2.886
CaO	0	0	0	0
Na_2O	0	0	0	0
K_2O	0	0	0	0
SiO_2	53.00	7.970	52.74	8.001
TiO_2	0	0	0	0
Al_2O_3	0	0	0	0
FeO	34.81	4.377	36.68	4.655
MnO	0.52	.066	0.50	.065
MgO	11.67	2.615	10.08	2.279
CaO	0	0	0	0
Na_2O	0	0	0	0
K_2O	0	0	0	0

L-56 (grunerite) continued

ENERGY DISPERSIVE X-RAY SPECTROSCOPY - average of 14 analyses

	Wt.%		Wt.%
SiO_2	50.0	TiO_2	0
Al_2O_3	0.2	MnO	0.1
FeO	39.5	P_2O_5	tr.
MgO	9.5	S	0
CaO	tr.	Cl	0
Na_2O	tr.	Cr_2O_3	0
K_2O	0		

L-56 (ankerite)

	Wt.%	Wt.%
FeO	24.49	26.66
MnO	1.64	1.20
MgO	20.52	20.31
CaO	53.35	51.85

L-57 (grunerite)

ELECTRON MICROPROBE

	Wt.%	No. of ions on basis of 23 O	Wt.%	No. of ions on basis of 23 O
SiO_2	50.85	7,747	49.87	7.633
TiO_2	0	0	0	0
Al_2O_3	5.17	.928	6.33	1.143
FeO	35.38	4.508	36.22	4.636
MnO	0.25	.033	0	0
MgO	5.76	1.309	4.94	1.126
CaO	0.22	.035	0	0
Na_2O	0	0	0	0
K_2O	2.37	.459	2.63	.515
SiO_2	51.17	7.786	52.21	7.888
TiO_2	0	0	0	0
Al_2O_3	5.26	.944	4.74	.843
FeO	35.74	4.548	35.15	4.442
MnO	0	0	0	0
MgO	5.28	1.195	5.86	1.319
CaO	0.30	.049	0	0
Na_2O	0	0	0	0
K_2O	2.25	.437	2.04	.393

L-57 (grunerite) continued

X-RAY POWDER DIFFRACTION

Intensity	hkl	d(obs.)	d(calc.)	d(obs.-calc.)
24	1 1 0	8.3851	8.3227	.0624
24	-1 1 0	8.3851	8.3227	.0624
9	2 2 0	4.1616	4.1614	.0003
9	-2 2 0	4.1616	4.1614	.0003
2	1 3 1	3.4729	3.4625	.0104
16	2 4 0	3.2666	3.2676	-.0010
16	-2 4 0	3.2666	3.2676	-.0010
100	3 1 0	3.0737	3.0716	.0021
100	-3 1 0	3.0737	3.0716	.0021
3	2 2 1	3.0079	2.9986	.0093
4	0 6 1	2.6367	2.6322	.0044
3	-2 0 2	2.5115	2.5125	-.0009
2	3 5 0	2.3708	2.3715	-.0006
2	-3 5 0	2.3708	2.3715	-.0006
6	2 6 1	2.1987	2.1981	.0006
2	3 5 1	2.0446	2.0424	.0022
2	-4 0 2	1.9549	1.9537	.0012
4	5 3 0	1.7890	1.7873	.0017
4	-5 3 0	1.7890	1.7873	.0017
4	4 8 0	1.6353	1.6338	.0015
11	6 0 0	1.5583	1.5580	.0003
2	3 11 0	1.4670	1.4663	.0007
2	-3 11 0	1.4670	1.4663	.0007
12	-6 6 1	1.4050	1.4062	-.0012
4	5 1 2	1.3858	1.3869	-.0012
4	-2 12 2	1.3022	1.3026	-.0005
3	4 12 0	1.2750	1.2762	-.0011
3	8 0 0	1.1680	1.1685	-.0005
3	5 11 2	1.0663	1.0666	-.0004

L-57 (grunerite) continued

CELL CONSTANTS

a_o	= 9.553	±	0.0035	Å
b_o	= 18.280	±	0.0075	Å
c_o	= 5.342	±	0.0052	Å
β	= 101.90	±	0.049	deg.
V	= 912.82	±	0.89	$Å^3$
a sin β	= 9.348			Å

ENERGY DISPERSIVE X-RAY SPECTROSCOPY - average of 8 analyses

	Wt.%		Wt.%
SiO_2	48.5	TiO_2	0
Al_2O_3	0.6	MnO	0.4
FeO	40.2	P_2O_5	0
MgO	9.4	S	0
CaO	tr.	Cl	0
Na_2O	0.6	Cr_2O_3	0.3
K_2O	0		

L-57 (ankerite)

	Wt.%
FeO	28.40
MnO	2.87
MgO	18.12
CaO	50.61

L-58 (grunerite)

ELECTRON MICROPROBE

	Wt.%	No. of ions on basis of 23 O	Wt.%	No. of ions on basis of 23 O
SiO_2	50.96	7.949	51.80	8.075
TiO_2	0	0	0	0
Al_2O_3	0	0	0	0
FeO	42.18	5.502	42.66	5.562
MnO	0	0	0	0
MgO	6.88	1.599	5.54	1.289
CaO	0	0	0	0
Na_2O	0	0	0	0
K_2O	0	0	0	0

SiO_2	51.10	7.992
TiO_2	0	0
Al_2O_3	0	0
FeO	42.02	5.473
MnO	0	0
MgO	6.64	1.542
CaO	0	0
Na_2O	0	0
K_2O	0	0

X-RAY POWDER DIFFRACTION

Intensity	hkl	d(obs.)	d(calc.)	d(obs.-calc.)
38	1 1 0	8.3456	8.3341	.0115
38	-1 1 0	8.3456	8.3341	.0115
11	2 0 0	4.6952	4.6781	.0171
13	2 2 0	4.1713	4.1670	.0043
13	-2 2 0	4.1713	4.1670	.0043

L-58 (grunerite) continued

27	2	4	0	3.2725	3.2743	-.0018
27	-2	4	0	3.2725	3.2743	-.0018
100	3	1	0	3.0737	3.0746	-.0009
100	-3	1	0	3.0737	3.0746	-.0009
4	2	2	1	3.0029	2.9963	.0067
19	1	5	1	2.7673	2.7617	.0056
9	0	6	1	2.6329	2.6357	-.0027
11	2	6	1	2.2012	2.2003	.0009
17	6	0	0	1.5595	1.5594	.0001
4	3	11	0	1.4702	1.4702	-.0000
4	-3	11	0	1.4702	1.4702	-.0000
12	-6	6	1	1.4069	1.4079	-.0010
12	5	1	2	1.3849	1.3859	-.0010
4	-2	12	2	1.3045	1.3044	.0000
4	8	0	0	1.1698	1.1695	.0002
4	-8	6	3	1.0168	1.0168	.0001

CELL CONSTANTS

a_o = 9.561 ± 0.0024 Å

b_o = [illegible] ± 0.0069 Å

c_o = [illegible] ± 0.0049 Å

β = 101.88 ± 0.031 deg.

V = [illegible] ± 0.84 $Å^3$

$a \sin \beta$ = [illegible] Å

L-58 (grunerite) continued

ENERGY DISPERSIVE X-RAY SPECTROSCOPY - average of 14 analyses

	Wt.%		Wt.%
SiO_2	46.3	TiO_2	tr.
Al_2O_3	0.5	MnO	tr.
FeO	46.7	P_2O_5	0
MgO	5.3	S	0
CaO	tr.	Cl	0
Na_2O	0.1	Cr_2O_3	0.2
K_2O	tr.		

L-59 (actinolite)

X-RAY POWDER DIFFRACTION

Intensity	hkl	d(obs.)	d(calc.)	d(obs.-calc.)
44	1 1 0	8.5057	8.4679	.0378
44	-1 1 0	8.5057	8.4679	.0378
7	2 2 0	4.2402	4.2339	.0062
7	-2 2 0	4.2402	4.2339	.0062
7	0 4 1	3.3949	3.3942	.0006
7	1 5 0	3.3949	3.3935	.0014
15	2 4 0	3.2962	3.2928	.0035
15	-2 4 0	3.2962	3.2928	.0035
100	3 1 0	3.1425	3.1432	-.0007
100	-3 1 0	3.1425	3.1432	-.0007
8	2 2 1	2.9497	2.9486	.0011
8	-1 5 1	2.9497	2.9548	-.0052
14	1 5 1	2.7223	2.7160	.006
16	0 6 1	2.6033	2.6034	-.0
11	4 0	2.398	2.3936	.0047

L-59. (actinolite) continued

10	-3	5	1	2.3441	2.3520	-.0079
14	2	6	1	2.1684	2.1708	-.0024
6	2	8	0	2.0490	2.0497	-.0007
9	3	5	1	2.0251	2.0250	.0001
8	5	1	0	1.9009	1.9043	-.0034
13	4	6	1	1.6584	1.6571	.0012
7	1	11	0	1.6260	1.6256	.0004
7	-6	2	1	1.6260	1.6223	.0038

CELL CONSTANTS

a_o	= 9.909	±	0.0073	Å
b_o	= 18.145	±	0.0151	Å
c_o	= 5.295	±	0.0170	Å
β	= 104.93	±	0.132	deg.
V	= 919.88	±	2.95	$Å^3$

ENERGY DISPERSIVE X-RAY SPECTROSCOPY - average of 11 analyses

	Wt.%		Wt.%
SiO_2	54.7	TiO_2	0
Al_2O_3	1.2	MnO	0.1
FeO	17.4	P_2O_5	tr.
MgO	14.4	S	tr.
CaO	11.0	Cl	0
Na_2O	0.8	Cr_2O_3	0.2
K_2O	0.1		

L-60 (magnesioriebeckite)

ELECTRON MICROPROBE

	Wt.%	No. of ions on basis of 23 O	Wt.%	No. of ions on basis of 23 O
SiO_2	56.70	8.196	56.35	8.167
TiO_2	0	0	0	0
Al_2O_3	0.53	.091	0	0
FeO	23.25	2.810	23.01	2.790
MnO	0	0	0	0
MgO	12.31	2.650	12.89	2.784
CaO	0	0	0.20	.032
Na_2O	7.21	2.022	7.55	2.122
K_2O	0	0	0	0
SiO_2	56.59	8.192	56.38	8.185
TiO_2	0	0	0	0
Al_2O_3	0.53	.090	0	0
FeO	23.37	2.829	23.64	2.870
MnO	0	0	0	0
MgO	12.06	2.600	12.51	2.707
CaO	0.28	.043	0.19	.031
Na_2O	7.18	2.016	7.26	2.043
K_2O	0	0	0	0
SiO_2	56.93	8.237	57.75	8.309
TiO_2	0	0	0	0
Al_2O_3	0	0	0	0
FeO	23.23	2.811	23.30	2.804
MnO	0	0	0	0
MgO	12.40	2.671	12.43	2.665
CaO	.23	.035	0.28	.043
Na_2O	7.05	1.9[illegible]	6.24	1.739
K_2O	0.17	.032	0	0

L-60 (magnesioriebeckite) continued

SiO_2	57.49	8.277	57.55	8.309
TiO_2	0	0	0	0
Al_2O_3	0	0	0	0
FeO	23.27	2.803	23.89	2.885
MnO	0	0	0	0
MgO	12.80	2.747	11.98	2.577
CaO	0	0	0	0
Na_2O	6.42	1.794	6.58	1.842
K_2O	0	0	0	0

ENERGY DISPERSIVE X-RAY SPECTROSCOPY - average of 20 analyses

	Wt.%		Wt.%
SiO_2	55.9	TiO_2	tr.
Al_2O_3	0.4	MnO	tr.
FeO	29.1	P_2O_5	tr.
MgO	7.7	S	tr.
CaO	tr.	Cl	tr.
Na_2O	6.3	Cr_2O_3	0.2
K_2O	tr.		

L-61 (grunerite)

ELECTRON MICROPROBE

	Wt.%	No. of ions on basis of 23 O	Wt.%	No. of ions on basis of 23 O
SiO_2	52.59	7.914	53.67	8.011
TiO_2	0	0	0	0
Al_2O_3	0	0	0	0
FeO	34.37	4.327	33.32	4.159
MnO	0.41	.103	0.78	.098
MgO	12.22	2.742	12.23	2.721
CaO	0	0	0	0
Na_2O	0	0	0	0
K_2O	0	0	0	0
SiO_2	53.11	7.987		
TiO_2	0	0		
Al_2O_3	0	0		
FeO	34.76	4.371		
MnO	0.64	.082		
MgO	11.48	2.573		
CaO	0	0		
Na_2O	0	0		
K_2O	0	0		

ENERGY DISPERSIVE X-RAY SPECTROSCOPY - average of 8 analyses

	Wt.%		Wt.%
SiO_2	49.5	TiO_2	0
Al_2O_3	0.4	MnO	0.4
FeO	40.4	P_2O_5	0
MgO	8.3	S	
CaO	0	Cl	0
Na_2O	0.4	Cr_2O_3	
K_2O	0		

L-62 (cummingtonite)

ELECTRON MICROPROBE

	Wt.%	No. of ions on basis of 23 O	Wt.%	No. of ions on basis of 23 O
SiO_2	52.57	7.541	55.15	8.048
TiO_2	0	0	0	0
Al_2O_3	5.84	.987	1.05	.181
FeO	25.75	3.089	29.80	3.637
MnO	0.45	.054	0.54	.066
MgO	15.41	3.294	13.47	2.929
CaO	0	0	0	0
Na_2O	0	0	0	0
K_2O	0	0	0	0
SiO_2	55.68	7.954	51.44	7.542
TiO_2	0	0	0	0
Al_2O_3	1.13	.191	3.41	.589
FeO	25.17	3.007	28.73	3.522
MnO	0.39	.047	0.55	.068
MgO	17.63	3.752	15.45	3.375
CaO	0	0	0.42	.067
Na_2O	0	0	0	0
K_2O	0	0	0	0

L-62 (cummingtonite) continued

X-RAY POWDER DIFFRACTION

Intensity	hkl	d(obs.)	d(calc.)	d(obs.-calc.)
58	1 1 0	8.3456	8.3071	.0385
58	-1 1 0	8.3456	8.3071	.0385
2	1 3 0	5.0819	5.0951	-.0132
7	2 0 0	4.6707	4.6651	.0056
4	0 4 0	4.5637	4.5616	.0021
15	2 2 0	4.1424	4.1536	-.0111
15	-2 2 0	4.1424	4.1536	-.0111
2	-1 3 1	3.8750	3.8690	.0060
5	1 3 1	3.4530	3.4554	-.0024
28	2 4 0	3.2608	3.2615	-.0007
28	-2 4 0	3.2608	3.2615	-.0007
100	3 1 0	3.0685	3.0658	.0027
100	-3 1 0	3.0685	3.0658	.0027
10	2 2 1	2.9931	2.9925	.0007
19	1 5 1	2.7549	2.7544	.0005
8	0 6 1	2.6254	2.6271	-.0017
3	2 6 0	2.5425	2.5476	-.0051
3	-2 6 0	2.5425	2.5476	-.0051
6	-2 0 2	2.5081	2.5072	.0009
2	3 5 0	2.3648	2.3671	-.0022
2	-3 5 0	2.3648	2.3671	-.0022
5	1 7	2.2142	2.2146	-.0004
12	2 6 1	2.1936	2.1[illegible]6	-.000[illegible]
6	3 5 1	2.0381	2.0[illegible]83	-.000[illegible]
[illegible]	-4 0 [illegible]	1.[illegible]	1.[illegible]98	-.00[illegible]
1	[illegible]	1.[illegible]9	[illegible]	[illegible]
6	4 8 0	1.[illegible]0	1.0308	.000[illegible]
[illegible]	[illegible] 5 [illegible]	.5976	1.[illegible]2	[illegible]
10	5 [illegible] 0	1.554[illegible]	1.555[illegible]	[illegible]

L-62 (cummingtonite) continued

4	3	11	0	1.4650	1.4636	.0014
4	-3	11	0	1.4650	1.4636	.0014
18	-6	6	1	1.4032	1.4036	-.0004
4	-2	12	2	1.2998	1.3001	-.0003
3	4	12	0	1.2743	1.2738	.0005
3	8	0	0	1.669	1.1663	.0006

CELL CONSTANTS

a_o	= 9.535	± 0.0029	Å	
b_o	= 18.247	± 0.0056	Å	
c_o	= 5.330	± 0.0030	Å	
β	= 101.90	± 0.050	deg.	
V	= 907.43	± 0.51	$Å^3$	
a sin β	= 9.330		Å	

ENERGY DISPERSIVE X-RAY SPECTROSCOPY - average of 18 analyses

	Wt.%		Wt.%
SiO_2	52.8	TiO_2	0
Al_2O_3	[illegible]	MnO	0.3
FeO	33.2	P_2O_5	0
MgO	12.0	S	0
CaO	tr	[illegible]	0
Na[illegible]O	.0	Cr_2O_3	0
K_2O	0		

L [illegible] (anker[illegible])

ELECTRON MICROPROBE

	At.	Wt.%
FeO	24.02	.46
MnO	1.[illegible]	[illegible]
[illegible]O	19.[illegible]8	21.[illegible]
CaO	55.2[illegible]	54.39

L-63 (grunerite)

X-RAY POWDER DIFFRACTION

Intensity	hkl	d(obs.)	d(calc.)	d(obs.-calc.)
3	0 2 0	9.2126	9.1476	.0650
43	1 1 0	8.3066	8.3247	-.0181
43	-1 1 0	8.3066	8.3247	-.0181
12	2 0 0	4.6707	4.6742	-.0035
9	2 2 0	4.1329	4.1623	-.0294
9	-2 2 0	4.1329	4.1623	-.0294
3	1 3 1	3.4662	3.4660	.0002
14	2 4 0	3.2666	3.2691	-.0025
14	-2 4 0	3.2666	3.2691	-.0025
100	3 1 0	3.0737	3.0719	.0018
100	-3 1 0	3.0737	3.0719	.0018
5	2 2 1	2.9980	3.0012	-.0031
14	1 5 1	2.7631	2.7625	.0007
4	0 6 1	2.6442	2.6346	.0096
3	-2 0 2	2.5115	2.5139	-.0024
3	-3 5 1	2.3009	2.3002	.0006
3	-4 2 1	2.2459	2.2476	-.0017
3	1 7 1	2.2299	2.2209	.0090
7	2 6 1	2.2012	2.1999	.0013
4	3 5 1	2.0446	2.0439	.0007
2	-4 0 2	1.9569	1.9538	.0030
2	5 3 0	1.7874	1.7876	-.0002
2	-5 3 0	1.7874	1.7876	-.0002
9	4 6 1	1.6653	1.6650	.0003
2	-1 5 3	1.6014	1.6022	-.0007
11	6 0 0	1.5583	1.5581	.0002

L-63 (grunerite) continued

13	-6 6 1	1.4060	1.4063	-.0004
3	5 1 2	1.3876	1.3880	-.0004
3	-2 12 2	1.3029	1.3036	-.0007
2	4 12 0	1.2772	1.2769	.0003
3	8 0 0	1.1692	1.1686	.0006
4	1 17 1	1.0423	1.0427	-.0004

CELL CONSTANTS

a_o	= 9.552	±	0.0042	Å
b_o	= 18.295	±	0.0080	Å
c_o	= 5.347	±	0.0049	Å
β	= 101.85	±	0.062	deg.
V	= 914.57	±	0.84	$Å^3$
a sin β	= 9.349			Å

ENERGY DISPERSIVE X-RAY SPECTROSCOPY - average of 16 analyses

	Wt.%		Wt.%
SiO_2	46.6	TiO_2	0
Al_2O_3	0.5	MnO	tr.
FeO	47.6	P_2O_5	0
MgO	4.7	S	0
CaO	0	Cl	0
Na_2O	tr.	Cr_2O_3	0.2
K_2O	0		

L-64 (actinolite)

Intensity	hkl	d(obs.)	d(calc.)	(d(obs.-calc.)
5	0 2 0	8.9793	9.0876	-.1083
55	1 1 0	8.4651	8.4599	.0052
55	-1 1 0	8.4651	8.4599	.0052
5	0 4 0	4.5521	4.5438	.0083
5	2 2 0	4.2302	4.2299	.0002
5	-2 2 0	4.2302	4.2299	.0002
5	0 4 1	3.3949	3.3932	.0016
5	1 5 0	3.3949	3.3976	-.0028
12	2 4 0	3.2903	3.2930	-.0028
12	-2 4 0	3.2903	3.2930	-.0028
100	3 1 0	3.1371	3.1383	-.0012
100	-3 1 0	3.1371	3.1283	-.0012
6	-1 5 1	2.9449	2.9517	-.0067
6	2 2 1	2.9449	2.9517	-.0061
9	3 3 0	2.8225	2.8200	.0026
13	1 5 1	2.7223	2.7186	.0037
3	0 6 1	2.6069	2.6047	.0022
5	3 5 0	2.3921	2.3960	-.0039
9	-3 5 1	2.3470	2.3452	.0018
7	2 6 1	2.1759	2.1734	.0025
2	2 8 0	2.0512	2.0519	-.0006
5	3 5 1	2.0251	2.0270	-.0019
11	5 1 0	1.9009	1.9012	-.0003
9	4 6 1	1.6598	1.6585	.0013
10	1 11 0	1.6287	1.6281	.0005
5	6 0 0	1.5939	1.5931	.0008

L-64 (actinolite) continued

CELL CONSTANTS

a_o	= 9.873	±	0.0070	Å
b_o	= 18.175	±	0.0096	Å
c_o	= 5.270	±	0.0118	Å
β	= 104.49	±	0.113	deg.
V	= 915.61	±	2.05	$Å^3$

ENERGY DISPERSIVE X-RAY SPECTROSCOPY - average of 11 analyses

	Wt.%		Wt.%
SiO_2	54.2	K_2O	0
Al_2O_3	0.3	TiO_2	0
FeO	24.4	MnO	0.4
MgO	9.7	S	0
CaO	10.3	Cl	0
Na_2O	0.3	Cr_2O_3	0.2